5-2018

Phospholipid membrane remodeling through exogenous fatty acid incorporation in certain bacterial species

Josh Herndon
University of Tennessee at Chattanooga, nmd773@mocs.utc.edu

Phospholipid membrane remodeling through exogenous fatty acid incorporation in certain bacterial species

Joshua Luke Herndon

Departmental Honors Thesis
The University of Tennessee at Chattanooga
Department of Chemistry and Physics

Examination Date: 04/02/2018

Steven J. Symes
Professor of Chemistry
Thesis Director

David K. Giles
Professor of Biology
Department Examiner

Kyle S. Knight
Professor of Chemistry
Department Examiner

Abstract

Phospholipid membrane remodeling through exogenous fatty acid incorporation in certain bacterial species

by Joshua Luke Herndon

Multi-drug resistant bacteria have become problematic in healthcare settings. Recent studies have documented the ability of some bacteria, such as *Vibrio* species, to assimilate exogenous fatty acids into their membrane phospholipids. Therefore, the current research was performed to determine whether the three virulent, multi-drug resistant bacteria *Acinetobacter baumannii, Klebsiella pneumoniae,* and *Escherichia coli* can remodel their cell membranes following exposure to a range of exogenous polyunsaturated fatty acids (PUFAs). Furthermore, we hypothesized that PUFAs would influence phenotypes associated with growth and virulence. Extracted phospholipids were examined by UPLC/MS analysis to confirm assimilation of exogenous PUFAs into the bacterial phospholipids. *A. baumanii*, *K. pneumoniae,* and *E. coli* were found to incorporate all exogenous PUFAs into their cell membranes, with the exception of docosahexaenoic acid (22:6) for *E. coli*. Membrane permeability assays were performed using Crystal violet (CV) and ethidium bromide (EtBr). Notably, *E. coli* samples exposed to 22:6 or arachidonic acid (20:4) took up approximately 35% or 60% more CV than the control sample, respectively. All PUFA-exposed *E. coli* samples demonstrated higher uptake of EtBr than the control sample, suggesting that every fatty acid tested increased membrane permeability. An assay for biofilm formation revealed that α-linolenic acid (18:3α), γ-linolenic acid (18:3γ), 20:4, and 22:6 significantly ($p < 0.002$) increased biofilm production in *E. coli*. Strikingly, 18:3 γ and 20:4 tripled biofilm formation when compared to the control sample. Similar phenotypic shifts were observed in *A. baumannii* and *K. pneumoniae*. Motility assays and minimum inhibitory concentration (MIC) assays using membrane-active cyclic peptide antibiotics were also performed. Taken together, the results of the experiments presented in this thesis suggest that exogenous PUFAs may be utilized in the future as combatants of multi-drug resistant bacteria in conjunction with antibiotics.

Acknowledgements

I want to thank Dr. Steve Symes for giving me the opportunity to participate in this research and for his outstanding performance as my thesis director and mentor over the course of the project. Dr. Symes was always thorough in his explanations, patient and helpful as I learned new things, willing to learn new things himself, and supportive of my academic growth through each step of the way. I also want to thank Dr. David Giles. Dr. Giles was a mentor to me over the course of this project as well and was instrumental in helping me understand the biological aspect of the research. Dr. Giles was also kind, patient, supportive, and trusting of me, and always answered my questions to the best of his ability with enthusiasm. Thank you, Dr. Symes and Dr. Giles! I feel truly fortunate to have had both of you as my mentors during this project. I would also like to thank the previous students that have participated in this research, notably Derek Anderson, for helping to lay the foundation that the research in this thesis was built upon. I want to thank the Grote Chemistry fund, the Westbrook Research Scholarship, and the National Science Foundation for the funding that made this research possible.

Contents

List of Figures and Tables

Figures:

Table:

Abbreviations

PUFA	**P**oly**u**nsaturated **F**atty **A**cid
PE	**P**hosphatidyl**e**thanolamine
PG	**P**hosphatidyl**g**lycerol
ESI	**E**lectro**s**pray **I**onization
MeOH	**M**ethanol
UPLC/MS	**U**ltra **P**erformance **L**iquid **C**hromatography/**M**ass **S**pectrometry
MDR	**M**ulti-**D**rug **R**esistant
LPS	**L**ipo**p**oly**s**accharide
KPC	***K****lebsiella* ***p****neumoniae* **C**arbapenemase
OD	**O**ptical **D**ensity
PBS	**P**hosphate **B**uffered **S**aline
m/z	**m**ass-to-charge ratio
CV	**C**rystal **V**iolet
EtBr	**Et**hidium **Br**omide
cAMP	**c**ationic **A**nti**m**icrobial **P**eptide
LIPID MAPS	**LIPID M**etabolites **a**nd **P**athways **S**trategy
XIC	E**x**tracted **I**on **C**hromatogram

I dedicate this thesis to my family, friends, and all those that have helped shape my life.

CHAPTER ONE

1. Introduction

1.1 Emergence of Multi-Drug Resistant Bacteria and Membrane Remodeling

Virulent, multi-drug resistant (MDR) bacteria have become more prevalent over the last few decades partially due to the selective pressure exerted by antibiotic use[1]. Non-MDR bacteria may acquire resistance genes via transformation or directly from MDR bacteria via bacterial conjugation[1], further increasing the number of MDR bacteria. MDR bacteria are especially problematic in environments consisting largely of immunocompromised individuals such as hospitals and are responsible for the increase in nosocomial infections.[2] The leading causes of nosocomial infections across the world are the ESKAPE pathogens (*Enterococcus faecium*, *Staphylococcus aureus*, *Klebsiella pneumoniae*, *Acinetobacter baumannii*, *Pseudomonas aeruginosa*, and *Enterobacter* species)[3]. Therefore, the rise of MDR bacteria is one of the most pervasive challenges in the healthcare industry[2] and has necessitated the development of novel treatments for MDR bacteria. Rather than attempt to synthesize new antibiotics or improve the efficiency of current ones, the focus of this research was on the manipulation of the phospholipid membranes of MDR bacteria via exposure to exogenous polyunsaturated fatty acids (PUFAs). Previous research has shown that some bacteria are capable of assimilating PUFAs into their phospholipid membranes rather than metabolizing them through β-oxidation[4]. This process is referred to as membrane remodeling and was first observed in *Escherichia coli*[5]. In gram-negative bacteria,

membrane remodeling is proposed to be carried out by FadL, an outer membrane transporter, by delivering exogenous fatty acids to the cytosolic face of the inner membrane and activating them to produce acyl-coenzyme A[5]. The assimilation process proceeds after the fatty acids have been converted to this form. Alterations of several phenotypes important to the virulence of MDR bacteria such as motility, biofilm formation, and antimicrobial resistance have been observed following membrane remodeling[6,7,8,9,10].

Three gram-negative, MDR bacteria were subjected to PUFA exposure and subsequent experimentation in this research: *Escherichia coli*, and two of the six ESKAPE pathogens, *Acinetobacter baumannii* and *Klebsiella pneumoniae*.

1.2 Fatty Acids and Phospholipids

Lipids may be broadly defined as hydrophobic molecules composed of carbon, hydrogen, and oxygen atoms. Carbon and hydrogen atoms greatly outnumber oxygen atoms in lipid molecules and as a result, they often feature long hydrocarbon chains. Fatty acids are characteristic lipid molecules that consist of a carboxyl group (COOH) and a hydrocarbon chain of the structural form $[(CH)_m(CH_2)_n(CH_3)]$, where m is the number of double bonds between two carbon atoms and n is the number of methylene groups. Written in standard notation, a fatty acid may be represented as a:b ($\Delta^{p_1, p_2, \cdots p_j}$), where a is the total number of carbon atoms in the fatty acid, b is the total number of double bonds between two carbon atoms, and ($\Delta^{p_1, p_2, \cdots, p_j}$) describes the location(s) of any double bond(s) relative to the carbonyl carbon atom. An example of this nomenclature as it pertains to the fatty acid arachidonic acid is 20:4 ($\Delta^{5, 8, 11, 14}$). Often, the ($\Delta^{p_1, p_2, \cdots p_j}$) term is omitted for simplicity. Fatty acids may be either saturated, monounsaturated, or

polyunsaturated, meaning they may possess no double bonds, one double bond, or more than one double bond, respectively. Unsaturated fatty acids that have two hydrocarbon chains on the same side of each double bond are known as *cis* isomers, whereas unsaturated fatty acids that have two hydrocarbon chains on opposite sides of each double bond are known as *trans* isomers. Some bacteria may convert *cis* fatty acids to *trans* fatty acids in response to toxic molecules or temperature, since *trans* isomers have an increased melting point and increase membrane rigidity[11]. Unsaturated fatty acids may either be ω-3 or ω-6 fatty acids, meaning that the last double bond along the hydrocarbon chain is either three carbons away from the terminal methyl group or six carbons away from the terminal methyl group, respectively.

The exogenous PUFAs used in this experiment were linoleic acid (18:2), α-linolenic acid (18:3-α), γ-linolenic acid (18:3-γ), dihomo-γ-linolenic acid (20:3), arachidonic acid (20:4), eicosapentaenoic acid (20:5), and docosahexaenoic acid (22:6). The structures of 18:2, 18:3-α, 18:3-γ, 20:3, 20:4, 20:5, and 22:6 are given in Figures 1.1, 1.2, 1.3, 1.4, 1.5, 1.6, and 1.7, respectively.

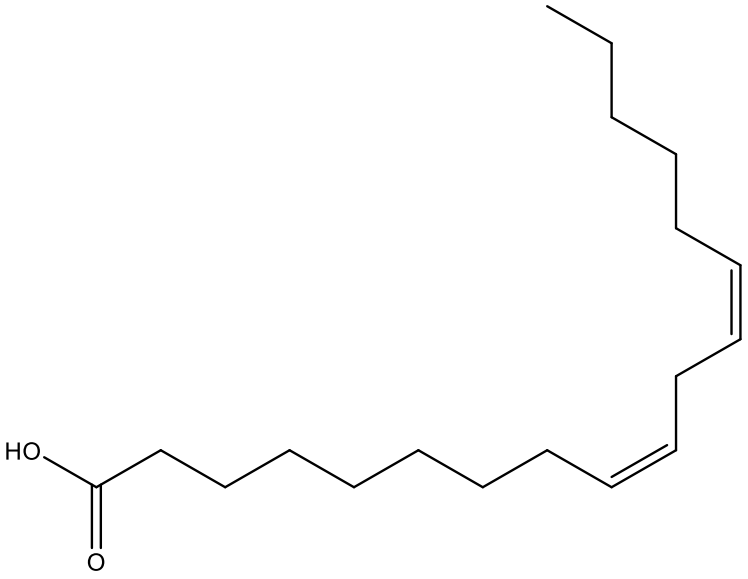

Figure 1.1: The structure of linoleic acid (18:2)

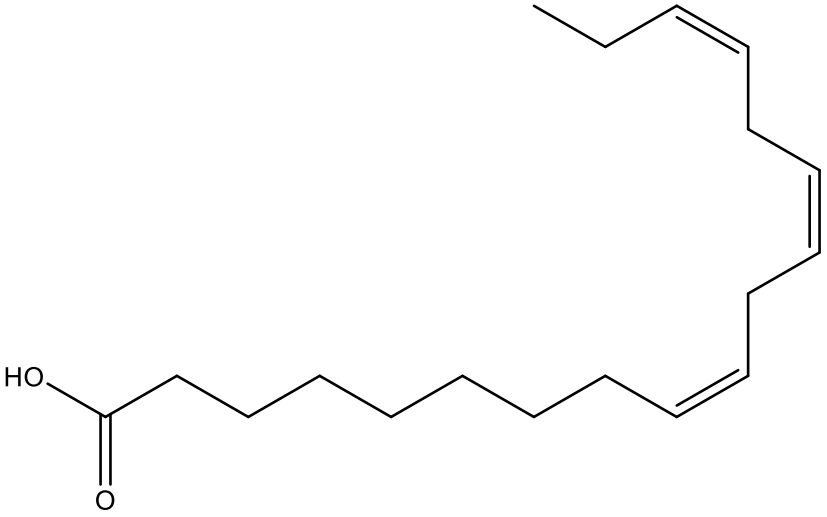

Figure 1.2: The structure of α-linolenic acid (18:3-α)

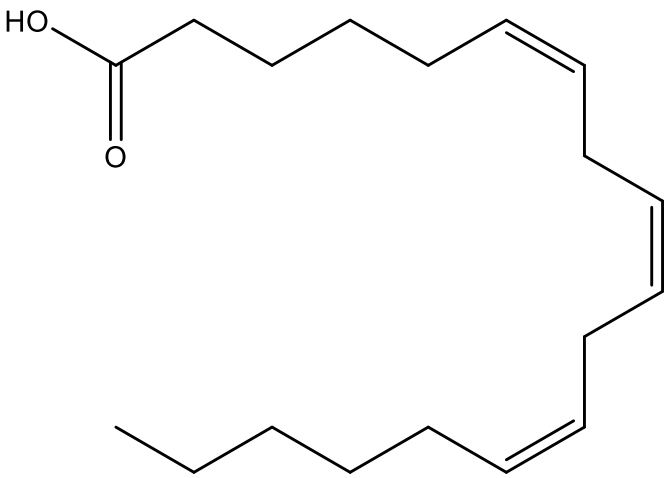

Figure 1.3: The structure of γ-linolenic acid (18:3-γ)

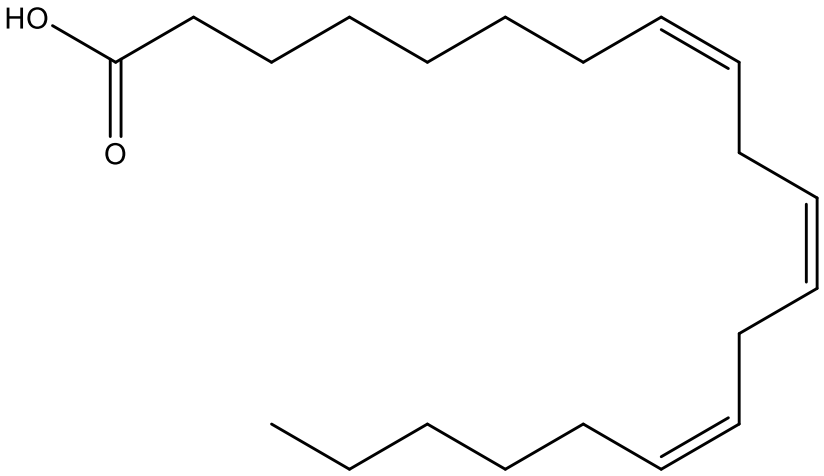

Figure 1.4: The structure of dihomo-γ-linolenic acid (20:3)

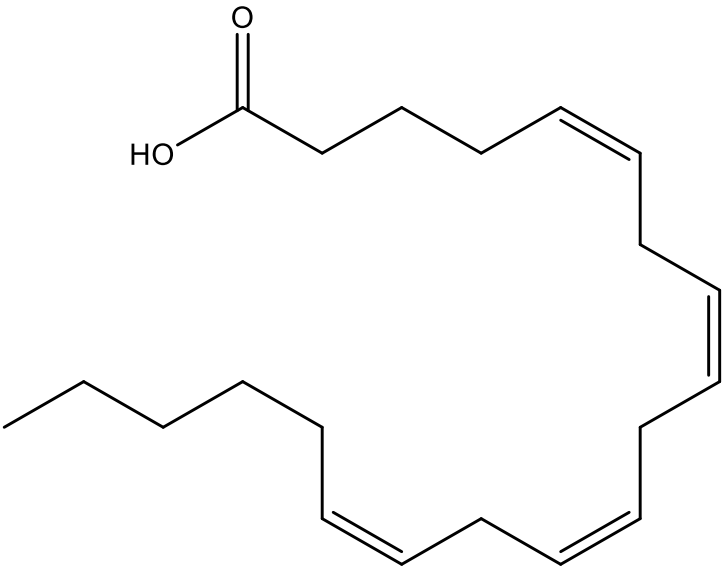

Figure 1.5: The structure of arachidonic acid (20:4)

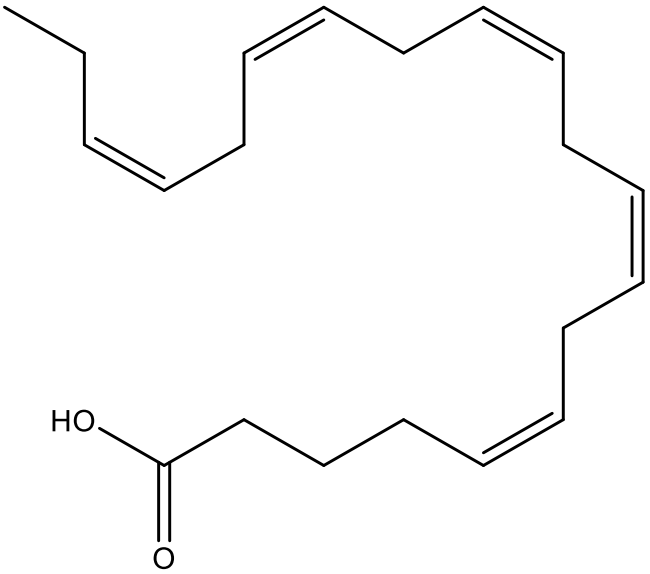

Figure 1.6: The structure of eicosapentaenoic acid (20:5)

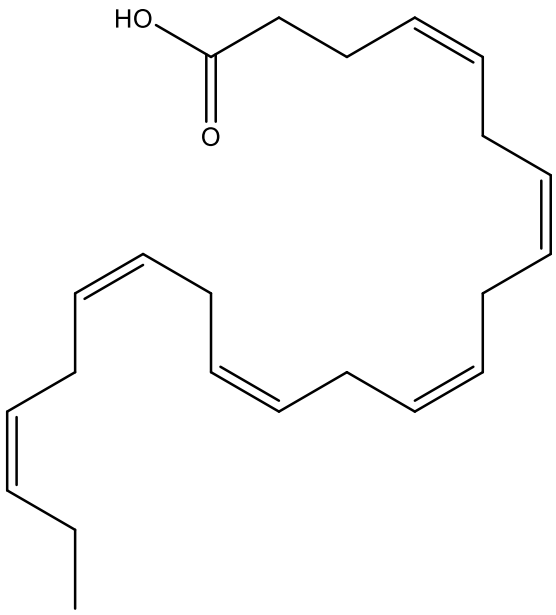

Figure 1.7: The structure of docosahexaenoic acid (22:6)

It should be noted that 18:3-α, 20:5, and 22:6 are ω-3 PUFAs, and 18:2, 18:3-γ, 20:3, and 20:4 are ω-6 PUFAs.

Phospholipids are more complex lipids than fatty acids and are essential for both prokaryotic and eukaryotic cellular function, since they are the major component of the cell membrane[12]. A diagram of a typical gram-negative cell membrane is presented in Figure 1.8.

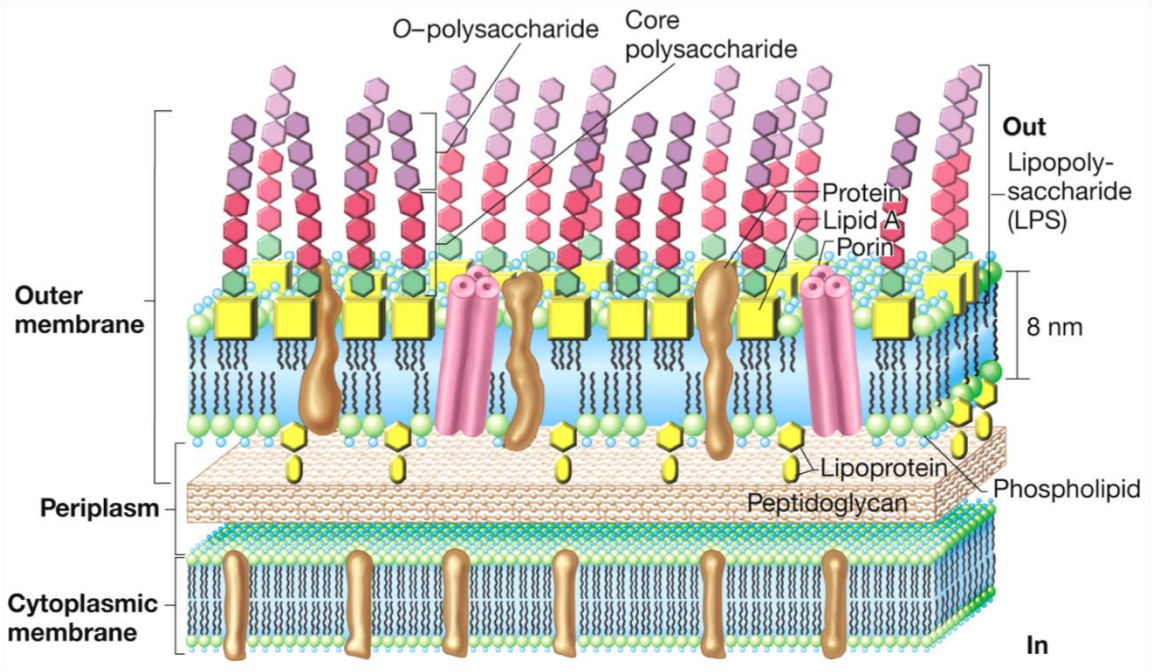

Figure 1.8: Diagram of a Gram-negative Cell Membrane[43]

Phospholipids are amphipathic molecules consisting of a polar head group, a phosphate group, a glycerol backbone, and two fatty acyl chains in the sn-1 and sn-2 positions. Examples of phospholipid structures are shown in Figures 1.9 and 1.10. The fatty acyl chains are derivatives of fatty acids that have been bonded to the glycerol backbone through a condensation reaction involving the carboxyl group of a fatty acid and one of the hydroxyl groups of the glycerol backbone. The final result is an ester linkage between the carbonyl carbon of the fatty acyl chain and an oxygen atom bonded to the glycerol backbone.

Phospholipids are categorized by their head groups. The two most abundant head groups for the phospholipids that form the cell membrane of gram-negative prokaryotes are ethanolamine and glycerol[13]. Phospholipids that have an ethanolamine head group are referred to as phosphatidylethanolamines (PEs) and those that have a glycerol head group

are referred to as phosphatidylglycerols (PGs). PEs were found to be more abundant than PGs in the gram-negative bacteria used in this experiment. Phospholipids with the same head group are said to be in the same "class" and may be distinguished from one another by their fatty acyl chains, which are often referred to as fatty acid tails. Conventional phospholipid nomenclature follows the format PX a_1:b_1/a_2:b_2, where PX is the abbreviation for the phospholipid class, a_1 is the total number of carbon atoms in the fatty acid tail in the sn-1 position, b_1 is the total number of double bonds along the fatty acid tail in the sn-1 position, a_2 is the total number of carbon atoms in the fatty acid tail in the sn-2 position, and b_2 is the total number of double bonds along the fatty acid tail in the sn-2 position. An example of phospholipid nomenclature is PE 16:0/18:1, which is a phosphatidylethanolamine phospholipid that has sixteen carbons and zero double bonds within the fatty acid tail in the sn-1 position, and eighteen carbons and one double bond within the fatty acid tail in the sn-2 position. Example structures of phosphatidylethanolamine and phosphatidylglycerol, the two most common phospholipids found within the cell membranes of gram-negative bacteria, are displayed in Figure 1.9 and Figure 1.10 respectively.

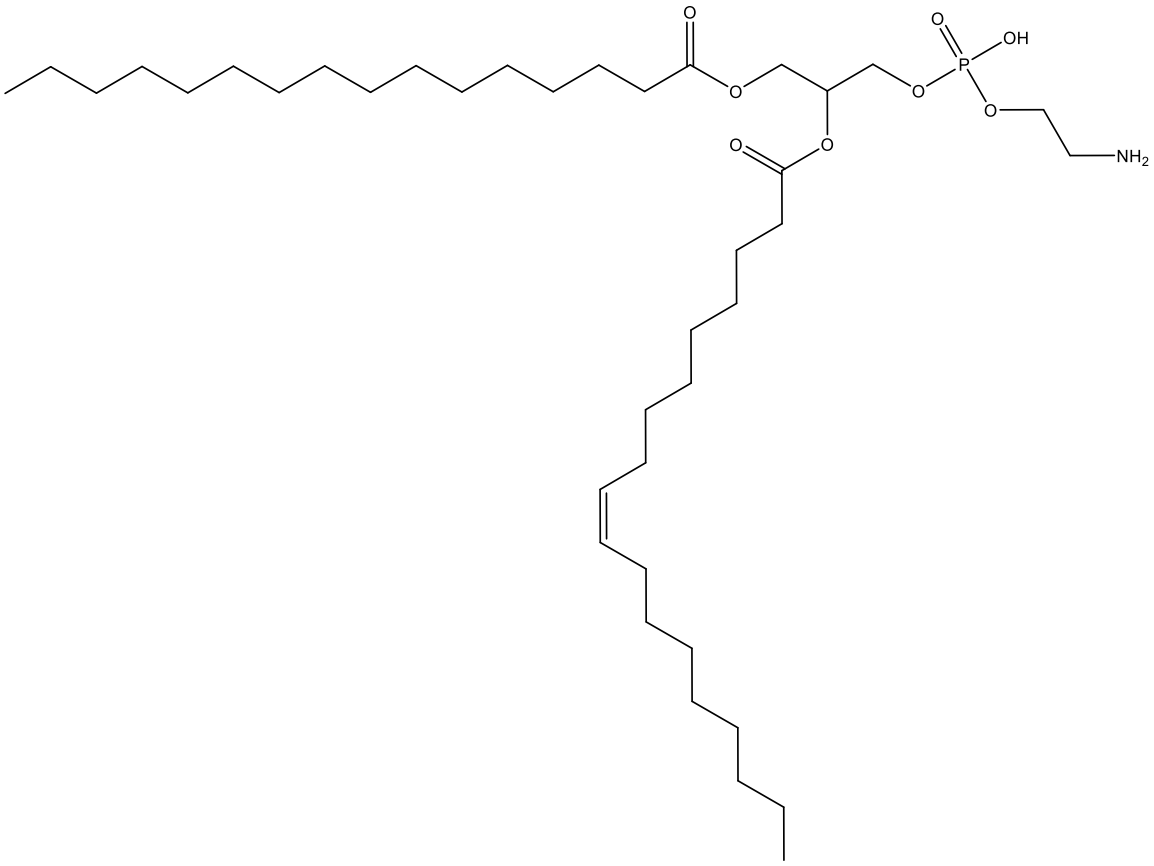

Figure 1.9: Phosphatidylethanolamine (PE) 16:0/18:1

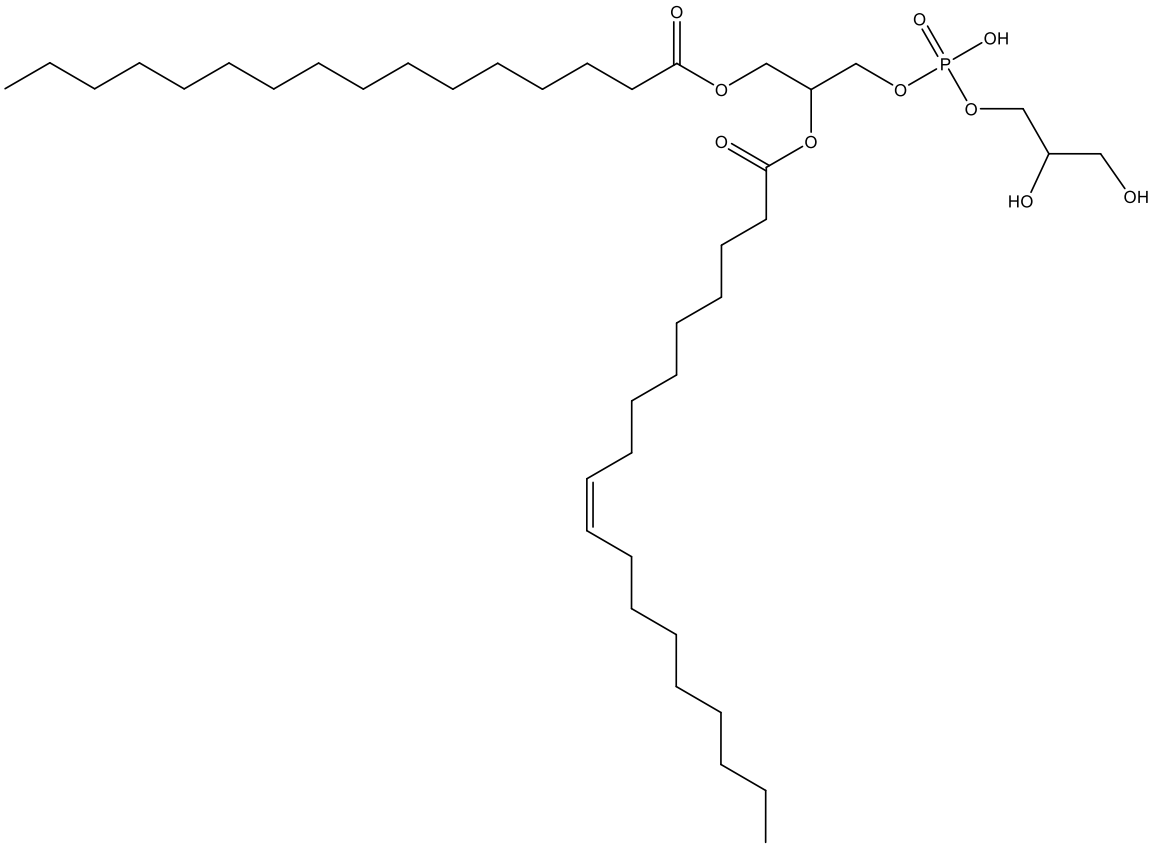

Figure 1.10: Phosphatidylglycerol (PG) 16:0/18:1

1.3 Gram-negative Bacteria and Cell Membranes

In 1884, biologist Christian Gram developed a staining method that allowed bacteria to be separated into two broad categories: bacteria that retained a violet dye (Gram-positive), and bacteria that did not retain the violet dye but instead retained a red dye (Gram-negative)[14]. Therefore, gram-positive bacteria appear purple and gram-negative bacteria appear red following the Gram staining. The distinction arises from morphological differences between the membranes of the two groups. Gram-positive bacteria possess a single phospholipid bilayer that is encapsulated by a thick mesh of

peptidoglycan layers, whereas gram-negative bacteria possess two lipid membranes separated by a thin layer of peptidoglycan in a space known as the periplasm[14]. The two lipid membranes are the inner membrane, which is composed of a phospholipid bilayer, and an outer membrane, composed of a lipid bilayer[14]. The outer membrane of Gram-negative bacteria is referred to as a lipid bilayer rather than a phospholipid bilayer because the inner leaflet of the outer membrane is composed of phospholipids, but the outer leaflet of the outer membrane is composed of glycolipids, particularly lipopolysaccharides[14,15]. The human immune system is sensitive to lipopolysaccharides since they are indicators of infection[14]. Despite the differences between the membranes of Gram-positive and Gram-negative bacteria, the general structure of a phospholipid bilayer is conserved between them. A phospholipid bilayer is composed of an inner leaflet and an outer leaflet, and the phospholipids that form each leaflet are arranged in a way such that the polar headgroups of the phospholipids face away from the opposing leaflet, and the hydrophobic fatty acid tails of the phospholipids face toward the opposing leaflet. This arrangement, along with integral proteins located within phospholipid bilayers, allows for the cell membrane to be semipermeable to molecules both inside and outside the cell.

Gram-negative bacteria were the focus of this research since they are generally more resistant to antimicrobial treatments and, as a consequence, may be considered more infectious than Gram-positive bacteria in some cases[14]. The increased resilience of Gram-negative bacteria may be attributed to the presence of lipopolysaccharides in the outer membrane and the periplasm[14]. The periplasm of Gram-negative bacteria is an aqueous environment located between the polar headgroups of the outer and inner membranes that

is an effective site for sequestering harmful enzymes like RNAse and alkaline phosphatase that degrade molecules essential for survival[14], and it is even considered to be an evolutionary precursor to eukaryotic lysozymes[14,16]. Some of the cellular functions that are carried out by membrane bound organelles in eukaryotes are performed by the inner membrane in Gram-negative bacteria[14]. Membrane proteins that are involved in energy production, lipid synthesis, and protein secretion in eukaryotes are mostly conserved in Gram-negative bacteria and are located within the inner membrane[14]. Thus, the inner membrane is essential for the survival of all Gram-negative bacteria. The majority of the fatty acid tails of the phospholipids in native Gram-negative bacteria are either saturated or monounsaturated and consist of sixteen or eighteen carbon atoms.

1.4 *Acinetobacter baumannii*

Acinetobacter baumannii is a MDR, Gram-negative bacteria that is listed as one of the ESKAPE pathogens[3]. Resistance to all existing antibiotic classes has been acquired among the species in the *Acinetobacter* genus[17]. Accordingly, *A. baumannii* is considered as one of the most difficult MDR Gram-negative bacteria to treat[18]. *A. baumannii* infection rates of hospitalized patients and individuals with compromised immune systems (nosocomial infections) have been increasing since the 1970s[18], and recent attention for the infectious bacteria was garnered following a surge in infection rates among wounded soldiers returning from Iraq[18,19]. Immunocompromised individuals receiving ventilation care are particularly susceptible to *A. baumannii* infection[20], and these infections have a high mortality rate[21].

Antimicrobial-inactivating enzymes and point mutations are two common mechanisms of resistance in *A. baumannii*[20,22]. *A. baumannii* has shown extensive resistance to carbapenems, which is a class of antibiotics that possess a β-lactam ring within their structure and include antibiotics such as penicillin and imipenem[20]. Resistance to carbapenems may be attributed to *A. baumannii*'s ability to synthesize class B metallo-β-lactamases that hydrolyze carbapenems[20,23]. Other antibiotics that work through different mechanisms of action such as polymyxins have been used in desperation, but *A. baumannii* has shown resistance to these antibiotics as well through phosphoethanolamine modification of Lipid A[24]. *A. baumannii*'s propensity for biofilm formation on a variety of common abiotic surfaces such as polystyrene and glass in hospital settings also contributes to its overall robustness and survivability[25].

1.5 *Klebsiella pneumoniae*

Klebsiella pneumoniae is also an MDR, Gram-negative bacteria listed as one of the ESKAPE pathogens[3]. To the surprise of some, *K. pneumoniae* can normally be found within the gastrointestinal reservoir of humans[26]. Harmful infections resulting in diseases such as pneumonia arise when *K. pneumoniae* is acquired through other means or when it penetrates the intestinal barrier; however, the mechanism by which it penetrates the intestinal barrier is not well understood[27]. *K. pneumoniae* recently acquired resistance to the carbapenem class of antibiotics via expression of the enzyme *Klebsiella pnuemoniae* carbapenemase (KPC) in 1996 and has since caused numerous hospital outbreaks in various parts of the world[28]. While other pathogenic Gram-negative bacteria have been shown to express KPCs, *K. pnuemoniae* is the most common species capable of expressing them[28].

K. pnuemoniae has been shown to form biofilms on polystyrene and other abiotic surfaces found within hospital settings[29]. Biofilm formation increases the difficulty of effectively treating *K. pneumoniae*, and previous research has even documented the inability of ampicillin to penetrate the biofilms of wild-type *K. pnuemoniae*[30].

1.6 *Escherichia coli*

Escherichia coli is a Gram-negative bacteria that is regarded as a model organism due to its hardiness, versatility, and ease of handling, and has consequently become one of the most well-understood organisms in the world[31]. Despite the extensive research conducted on *E. coli*, little to no attention has been given to its ability to remodel its membrane with exogenous fatty acids, even though it is the organism that was used to determine some of the mechanisms involved in membrane remodeling[5].

Most *E. coli* strains are harmless to humans and are even found within the intestines of humans and other mammals, but pathogenic strains of *E. coli* do exist[32]. Pathogenic *E. coli* strains may be separated into two broad categories: those that cause intestinal infections and those that cause extraintestinal infections[33]. Intestinal infections typically result in severe diarrhea, while extraintestinal infections may manifest as urinary tract infections, meningitis, and septicaemia[33]. Previous research has shown that some urinary tract isolates of *E. coli* displayed resistance to at least three of the following antibiotics: ampicillin, cephalothin, ciprofloxacin, nitrofurantoin, and trimethoprim-sulfamethoxazole, allowing the isolates to be considered multi-drug resistant[34]. Some *E. coli* strains have also demonstrated the ability to express β-lactamases[35] similar to *K. pneumoniae*.

The overall goals of this study were to determine if *A. baumannii*, *K. pneumoniae*, and *E. coli* are capable of assimilating exogenous PUFAs into the phospholipids of their cell membranes, and if so, to determine the impact that these modifications have on their virulence and survivability.

CHAPTER TWO

2. Materials and Methods

2.1 Bacteria Growth and Exogenous PUFA Supplementation

2.1.1 Growth Procedure

The following growth procedure was used for *Acinetobacter baumannii* ATCC17978 and *Klebsiella pneumoniae* ATCC13883:

Eight overnight cultures were aseptically prepared by transferring an isolated bacterial colony from an agar plate into a test tube containing G56 minimal medium [0.4 % glucose, 0.4 % casaminio acids (Fisher BioReagents), supplemented with 150 mM NaCl] near an open flame. On the following morning, seven cultures were supplemented with one of the seven PUFAs (see Ch. 1) at a final concentration of 300 µM while the eighth culture had no fatty acid supplemented and served as a control sample. All cultures were then grown to roughly OD_{600} = 0.9 in a Thermo Scientific MaxQ 4000 Benchtop Incubating/Refrigerating Shaker set to 200 RPM and 37.0 °C. Absorbance measurements were made using a Thermo Scientific Genesys 10S UV-Vis Spectrophotometer set to transmit light at a wavelength of 600 nm. A nearly identical growth procedure was used for *Escherichia coli* MG1655, with the only difference being that *E. coli* cultures were grown in M9 minimal media rather than G56 minimal media. For the sake of coherence, only the experimental conditions for the assays performed on *E. coli* will be delineated in the following sections.

2.1.2 Growth Curves

Two growth curves were performed for *E. coli*. One growth curve was performed by growing *E. coli* cultures within a Thermo Scientific MaxQ 4000 Benchtop Incubating/Refrigerating Shaker set to 200 RPM and 37.0 °C in CM9 or M9 minimal medium supplemented with or without glucose and one of the seven PUFAs or no PUFA. The latter growth curve is referred to as the sole carbon source growth curve. Both growth curves were conducted for a period of 12 hours, and absorbance measurements were made every hour at 600 nm with a Thermo Scientific Genesys 10S UV-Vis Spectrophotometer to monitor growth progress.

2.2 Lipid Extraction via Bligh and Dyer Method

Lipids were extracted from bacterial cultures by following the Bligh and Dyer method[36]. After growing cultures to roughly $OD_{600} = 0.9$, cells were pelleted in a Corning LSE Compact Centrifuge set to 4000 RPM for a duration of 10 minutes. The supernatant was discarded and the remaining cell pellet was washed with 5 mL of phosphate buffered saline (PBS), centrifuged, and the supernatant discarded. The cell pellets were resuspended in 5 mL of single-phase Bligh/Dyer mixture (1:2:0.8 chloroform:methanol:water), capped, vortexed, and allowed to sit in this state at room temperature for approximately 20 minutes. The purpose of this step was to lyse the cells, thereby allowing any cellular lipids to freely dissolve in the Bligh/Dyer mixture. These solutions were then centrifuged for 10 minutes in order to pellet undesirable cell fragments such as proteins and DNA. The nonpolar cell lipids dissolved in the

Bligh/Dyer supernatant were decanted into clean 10 mL tubes. A volume of 1.3 mL of chloroform and 1.3 mL of water were added to convert the single-phase Bligh/Dyer mixture into a two-phase Bligh/Dyer mixture, with an aqueous upper phase and an organic lower phase. Following another 10-minute centrifugation, the lower organic phase containing the cell lipids was removed via glass pipette and transferred into clean, fresh tubes. To ensure quantitative lipid extraction, the upper aqueous phase was extracted a second time with an additional 2.6 mL of chloroform to reestablish the two-phase Bligh/Dyer mixture. These solutions were centrifuged for 10 minutes and the lower, organic phases were again removed and pooled with their respective first extractions. For final purification, 5.2 mL of methanol and 4.68 mL of water were added to the pooled lower phases in order to re-establish a two-phase Bligh/Dyer mixture. These solutions were centrifuged for 10 minutes. Final, purified total lipid extracts were obtained by transferring the lower organic phases into clean test tubes. These total lipid extracts were dried under a stream of inert nitrogen gas administered by an Organomation N-EVAP 111. The dried lipid extracts were then capped and stored at -20 °C prior to UPLC/MS analysis.

2.3 Weighing of Dried Total Lipid Extracts

Empty Waters LCMS Certified Amber Screw-Top LC vials were obtained and weighed in triplicate on a Mettler Toledo XS205 DualRange Analytical Balance. The empty LC vial masses were averaged. Using a 2:1 chloroform:methanol solution, the dried lipid extracts were transferred to the pre-weighed LC vials and dried once more under a stream of inert N_2 gas. The dried lipid extract-LC vial systems were weighed on the analytical balance in triplicate and averaged. The masses of the total lipid extracts were obtained by

subtracting the average masses of the empty LC vials from the average masses of the dried lipid extract-LC vial systems. The dried lipid extracts were dissolved in 1 mL of 2:1 chloroform:methanol to form parent solutions. The masses of the lipid extracts were then used to calculate the volumes of parent solutions needed to form working solutions of particular concentrations (250 ppm for *A. baumannii*, 400 ppm for *K. pneumoniae* and *E. coli*). After creating the working solutions, both parent and working solutions were dried under a stream of inert N_2 gas and stored in a freezer. Table 2.1 provides the masses of the empty LC vials and the dried lipid extract-LC vial systems for the *E. coli* samples.

Table 2.1: Masses of *E. coli* Dried Lipid Extracts

E. coli Sample	Mass of LC vial (g)	Mass of Dried Lipid Extract-LC Vial System (g)	Average Mass of Dried Lipid Extract (mg)
Ec (-)	2.52613	2.52656	0.49
	2.52605	2.52653	
	2.52599	2.52654	
Ec 18:2	2.56071	2.56137	0.69
	2.56067	2.56136	
	2.56065	2.56138	
Ec 18:3-α	2.59827	2.59884	0.63
	2.59817	2.59884	
	2.59818	2.59882	
Ec 18:3-γ	2.58428	2.58487	0.60
	2.58423	2.58485	
	2.58424	2.58484	
Ec 20:3	2.52597	2.52647	0.53
	2.52590	2.52644	
	2.52591	2.52645	
Ec 20:4	2.54023	2.54088	0.65
	2.54024	2.54087	
	2.54020	2.54086	
Ec 20:5	2.55075	2.55134	0.59
	2.55072	2.55132	
	2.55075	2.55134	
Ec 22:6	2.57079	2.57146	0.68
	2.57074	2.57145	
	2.57076	2.57143	

2.4 Ultra Performance Liquid Chromatography Tandem Mass Spectrometry

Solvents A1 and B1 were used as the mobile phase for the liquid chromatography instrument. Solvent A1 was 30:70 25 mM ammonium acetate:MeOH, pH 6.7, and solvent B1 was pure MeOH. All solvents used were Optima grade (Fischer Scientific). The working solutions were placed within the Sample Manager of a Waters Acquity UPLC system to undergo reversed-phase chromatography gradient elution. During the analysis of a single sample, the automated syringe within the Sample Manager withdrew 25 µL of the sample and passed it through a sample loop that allowed for 5 µL of the sample to be injected onto the column. The mobile phase consisted of the aforementioned solvents A1 and B1, and was subjected to the following gradient: 50:50 A1:B1 held constant for 2 minutes, a linear increase of solvent B1 over the course of 8 minutes, ultimately reaching 100 % B1 at the 10 minute mark, followed by a rapid decrease in B1 over the course of 0.3 minutes, resulting in the reestablishment of 50:50 A1:B1 by 10.3 minutes, which was held constant for an additional 0.7 minutes for a total run time of 11 minutes. The column used was an Acquity BEH C8 column (2.1 x 100 mm, 1.7 µm particles). The chromatographically separated analyte molecules of the sample were then eluted into a QuattroTM micro API quadrupole mass spectrometer and ionized via electrospray ionization in the negative mode (ESI -) with a capillary of voltage 1.5 kV. The sample was desolvated using inert 350 °C nitrogen gas flowing at a rate of 600 L/h to induce a Coulombic explosion. The ionized analyte molecules were brought into the quadrupole mass spectrometer through a 50 V cone and a series of RF lenses. A photomultiplier tube (PMT) was used as the detector for the instrument. Scans were made from 200 m/z to

1500 m/z within quadrupole 1 (Q1). The scan time was 0.5 seconds with an interscan time delay of 0.01 seconds. Resultant chromatograms and mass spectra were analyzed using the MassLynx V4.1 software.

2.5 Assays

2.5.1 Motility Assay

For *E. coli*, a swimming motility assay was carried out in quadruplicate by adhering to the following protocol[37,6]: Motility assay plate solutions were prepared with 10 g L^{-1} tryptone, 10 g L^{-1} NaCl, 0.35 % agar, and 300 µM of one of the seven PUFAs. These solutions were autoclaved at 121 °C for 15 minutes and then cooled in a 50 °C water bath for approximately 15 minutes. The plates were partitioned into four quadrants so that each plate could be inoculated in quadruplicate after allowing sufficient time for the plates to dry. An overnight culture was grown to roughly OD_{600} 0.9 in M9 minimal media. The culture was pelleted, washed with PBS, and resuspended in 1 mL of PBS to OD_{600} 6.24. Cultures were then diluted in deionized water to OD_{600} 1.0. A volume of 2 µL of the culture grown in the M9 media was injected into the center of each quadrant of each motility assay plate. The plates were then incubated at 30 °C for a period of 12 hours. The motility of the *E. coli* bacteria in each plate was assessed following this incubation period by measuring the diameter of the motility halo in each quadrant, averaging these values, and calculating the standard deviations. Statistical analysis was carried out by using student's t-test (paired, two-tailed, $p < 0.01$).

2.5.2 Permeability Assays

Two different permeability assays were carried out to determine the effects of phospholipid remodeling on membrane permeability in *E. coli* by following previously established procedures[6,26]. The first assay was a crystal violet (CV) uptake assay. Eight separate *E. coli* cultures were grown to roughly OD_{600} 0.9 in the presence or absence of one of the seven PUFAs at a concentration of 300 μM within M9 minimal media supplemented with 2 % casamino acids. The cultures were pelleted, washed with PBS, and resuspended in 5 mL of PBS to OD 0.4. The hydrophobic compound CV was added to each of the cell cultures at a concentration of 5 mg/mL. Measurements were made in five-minute intervals (for a total of 20 minutes) by pelleting 1 mL of cell culture via centrifugation, decanting the supernatant, and collecting absorbance readings of the supernatant with a Thermo Scientific Genesys 10S UV-Vis Spectrophotometer set to transmit light at a wavelength of 590 nm. Microsoft Excel was used to determine the percentage of CV that was taken up by each culture since the spectrophotometric measurements effectively provided the percentage of CV that was not taken up by each culture.

The other permeability assay performed was an ethidium bromide (EtBr) uptake assay. Growth conditions for this assay were nearly identical to the growth conditions used for the CV uptake assay. The cultures were pelleted, washed with PBS, and resuspended in 5 mL of PBS to OD_{600} 0.7. Ethidium bromide was added to each cell culture at a concentration of 5 mg/mL. Measurements were made in five-minute intervals (for a total of 20 minutes) by pelleting 1 mL of cell culture via centrifugation, decanting the supernatant, and collecting fluorimetric readings by using an excitation wavelength of

530 nm and a detection wavelength of 585 nm. A Varian Cary Eclipse Fluorescence Spectrophotometer with a 20-nm excitation slit was used for this assay.

For both the CV uptake assay and the EtBr uptake assay, statistical significance was determined by a student's t-test (paired, 2-tailed, $p < 0.002$) after performing three biological replicates.

2.5.3 Antimicrobial Peptide Susceptibility Assay

A previously established protocol[6,26] was used to determine the effect that PUFA exposure has on antimicrobial peptide susceptibility in *E. coli.* Cultures were grown to roughly OD_{600} 0.9 in M9 minimal medium either in the presence of one of the seven PUFAs at a concentration of 300 µM or in the absence of PUFAs. Following centrifugation, the cultures were washed with M9 minimal medium and resuspended at an OD_{600} 0.1. A volume of 170 µL of each E. coli culture was added to the wells of a 96-well microtiter plate and supplemented with either 300 µM of one of the seven PUFAs or no PUFAs. A volume of 30 µL of a two-fold concentration of each antimicrobial peptide (polymyxin B and colistin) was added to the wells for a total volume of 200 µL per well. Following an incubation period of 24 hours at 37 °C, absorbance measurements were made at 600 nm using a Biotek Synergy microplate reader. Two experiments were performed in triplicate for both antimicrobial peptides.

2.5.4 Biofilm Formation Assay

The effect of PUFA exposure on biofilm formation in *E. coli* was assessed by using a previously established protocol[38]. Overnight *E. coli* cultures were grown in LB broth and transferred to 96-well microtiter plates containing CM9 (M9 minimal medium

supplemented with casamino acids) and either one of the seven PUFAs at a concentration of 300 µM or, in the case of the control samples, no PUFAs. The plates were incubated at 37 °C for 24 hours. After this incubation period, planktonic cells were removed and the plates were washed with deionized water in triplicate. A volume of 125 µL of 3 % crystal violet solution was added to each well, and the plates were incubated at room temperature for a period of 15 minutes. Following this incubation period, the plates were washed with deionized water in triplicate and dried for approximately 3 hours. After inspecting the plates to ensure sufficient dryness, 125 µL of a 30 % acetic acid solution was added to each well and the plates were incubated for 15 minutes. The dissolved crystal violet was transferred to a fresh 96-well microtiter plate, and absorbance measurements were made for each well at 550 nm using a Biotek Synergy microplate reader. The assay was carried out in octuplet and statistical analysis was performed using student's t-test (paired, 2-tailed, $p < 0.002$).

CHAPTER THREE

3. Results

3.1 Overview

One purpose of this experiment was to determine the effect that exogenous polyunsaturated fatty acid (PUFA) exposure has on phenotypes important to the virulence and survivability of the Gram-negative bacteria *Acinetobacter baumannii, Klebsiella pneumoniae,* and *Escherichia coli*. UPLC/MS analysis confirmed that all three of the Gram-negative bacteria can undergo membrane remodeling, which is the alteration of the phospholipid membrane profile with exogenously supplied fatty acids. With this confirmation, a series of biological assays were conducted to determine how membrane remodeling with either linoleic acid (18:2), alpha-linolenic acid (18:3-α), gamma-linolenic acid (18:3-γ), dihomo-γ-linolenic acid (20:3), arachidonic acid (20:4), eicosapentaenoic acid (20:5), or docosahexaenoic acid (22:6) affects motility, permeability, antimicrobial peptide susceptibility, and biofilm formation in the bacteria.

The total lipid extracts of each bacterial sample were assessed via UPLC/MS analysis to confirm that exogenous PUFA incorporation had occurred. Reversed-phase gradient elution was utilized using a BEH C8 column with the conditions described in Section 2.4. The sample that was not grown in the presence of 300 μM of a given fatty acid was used as a control to verify that the exogenous PUFAs 18:2, 18:3-α, 18:3-γ, 20:3, 20:4, 20:5, and 22:6 are not constituents of the native phospholipid species.

Since the UPLC/MS analysis was carried out in the negative mode following electrospray ionization (ESI-), $[M-H]^-$ ions were detected and analyzed in the various mass spectra using the MassLynx software. $[M-H]^-$ ions are formed via a single deprotonation. Fatty acyl chain cone fragment ions ($[R_xCO_2]^-$) aided in the identification of parent phospholipid ions since they represent the loss of a fatty acyl chain from either the sn-1 position or sn-2 position of the glycerol backbone as the phospholipids passed through the high voltage cone of the quadrupole mass spectrometer. Phospholipids were identified with the aid of the LIPID Metabolites and Pathways Strategy (LIPID MAPS)[39] database and the fatty acyl chain cone fragments generated by the high voltage cone of the mass spectrometer. In the negative ionization mode, singly-charged PG phospholipids possess an odd m/z value and singly-charged PE phospholipids possess an even m/z value.

Although biological assays were conducted on each of the gram-negative bacteria, only the data for the assays conducted on *E. coli* will be presented in this chapter for the sake of simplicity. The results of the assays performed on *A. baumannii* and *K. pneumoniae* will be discussed in Chapter 4.

3.2 *Acinetobacter baumannii* Results

3.2.1 *Acinetobacter baumannii* Mass Spectra and Chromatograms

The complete chromatogram of the *A. baumannii* control sample is given by Figure 3.1. "1" represents the free fatty acid region in the chromatogram and "2" represents the phospholipid region of the chromatogram. The two distinct regions arise from the drastic polarity differences between free fatty acids and phospholipids and the specific LC gradient that was used. It is important to note that within the phospholipid region itself,

phosphatidylglycerols elute from the column sooner than phosphatidylethanolamines since they are the more polar phospholipid type between the two. The phospholipid region of the *A. baumannii* control sample chromatogram is given in Figure 3.2, and the mass spectra of specific chromatogram peaks in the phospholipid region are given in Figure 3.3 and Figure 3.4.

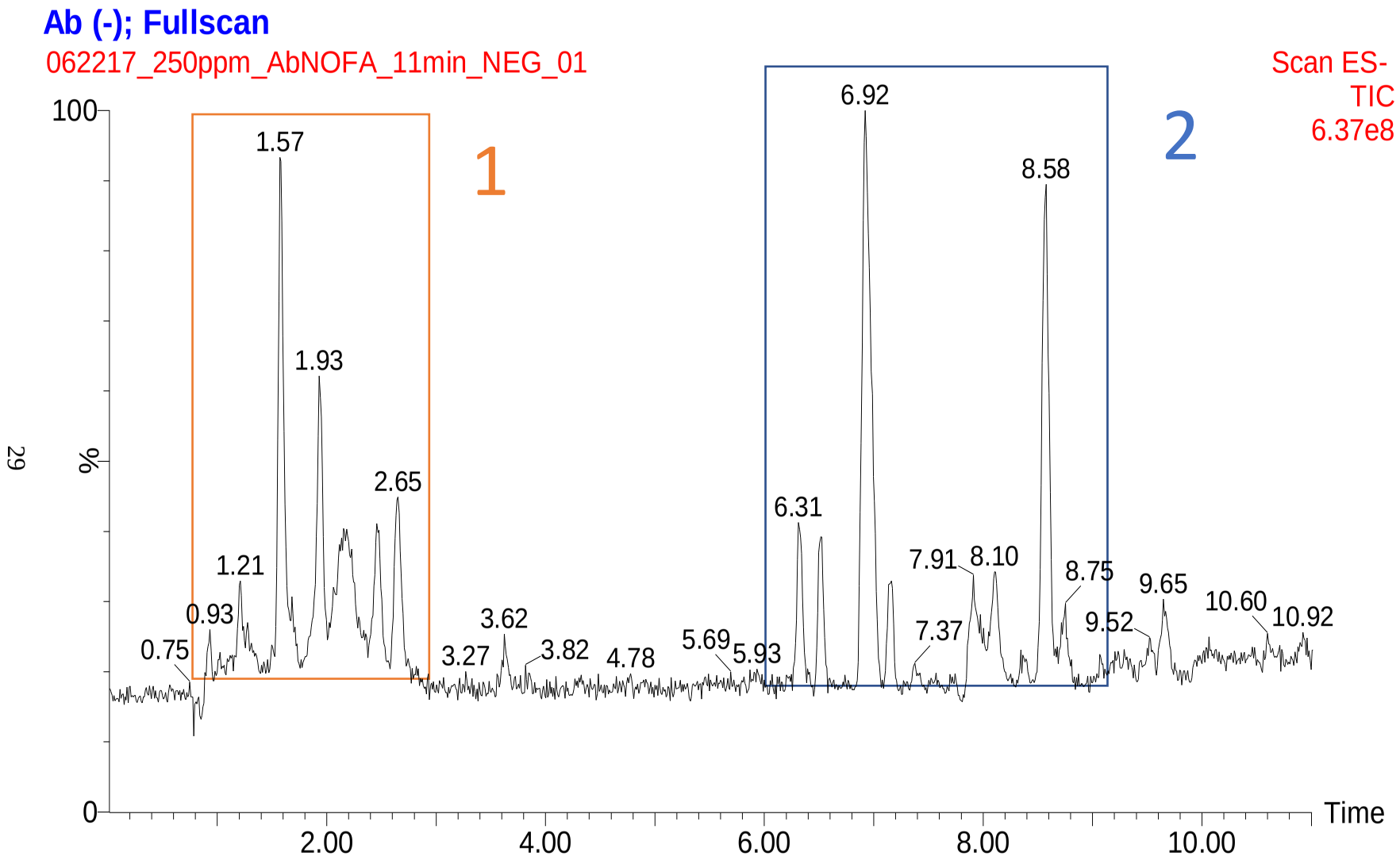

Figure 3.1: The complete chromatogram of the *A. baumannii* control sample

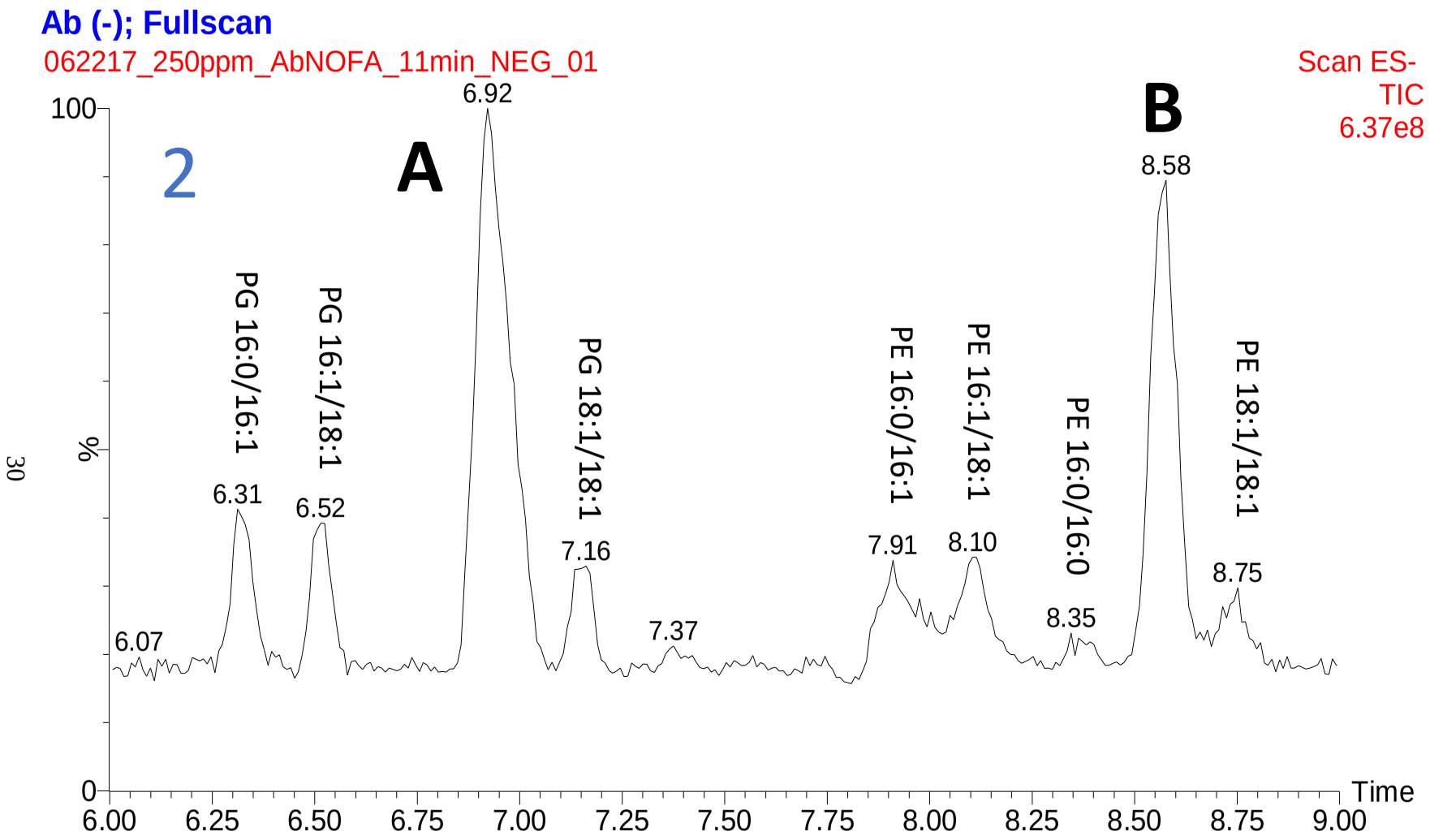

Figure 3.2: The phospholipid region of the chromatogram of the *A. baumannii* control sample

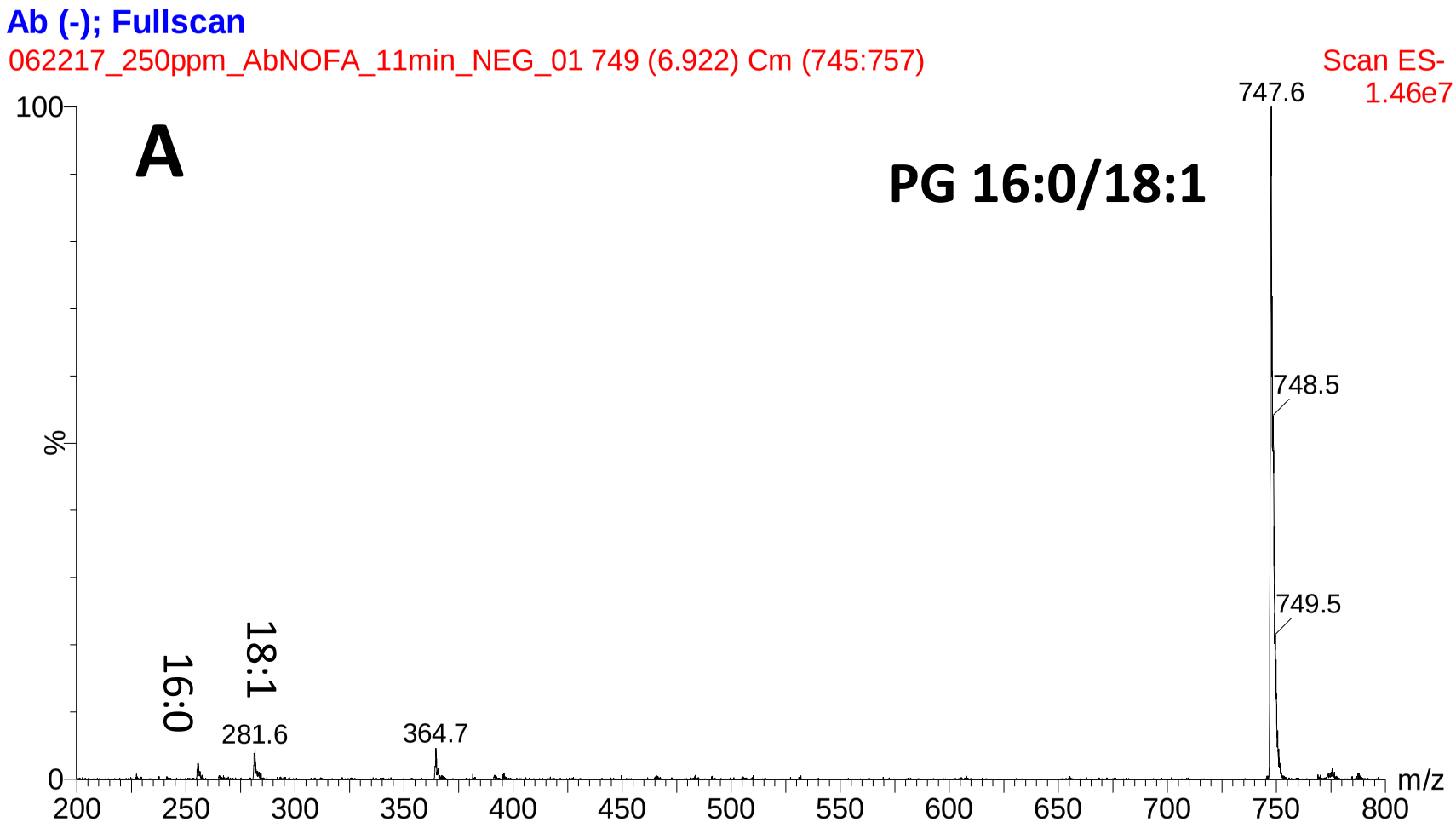

Figure 3.3: The average mass spectrum of chromatogram peak A in the control *A. baumannii* chromatogram

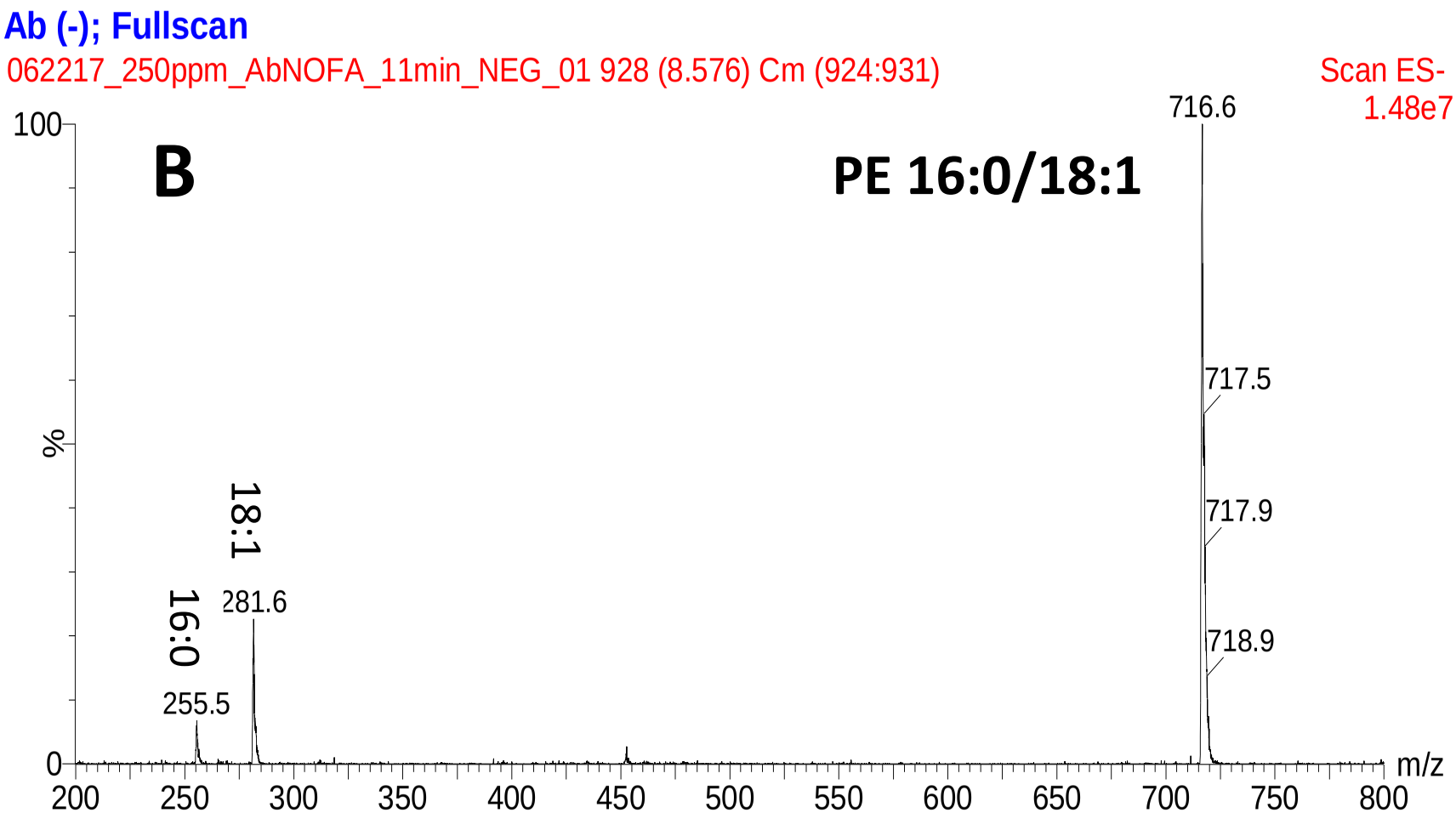

Figure 3.4: The average mass spectrum of chromatogram peak B in the control *A. baumannii* chromatogram

The average mass spectra of the two chromatogram peaks labeled as A and B at 6.92 minutes and 8.58 minutes respectively were examined to identify the phospholipids corresponding to those peaks. The 747.5 m/z value in the average mass spectrum of chromatogram peak A corresponds to the $[M-H]^-$ ion of PG 16:0/18:1. In addition to referencing LIPID MAPS, this was confirmed by the presence of the 16:0 and 18:1 cone fragments that correspond to the 255.5 m/z and 281.5 m/z values, respectively. The 716.5 m/z value in the average mass spectrum of chromatogram peak B corresponds to the $[M-H]^-$ ion of PE 16:0/18:1, as was confirmed by referencing LIPID MAPS and noting the presence of the 16:0 and 18:1 cone fragments. The other chromatogram peaks in Figure 3.2 were labeled following a similar procedure as for peaks A and B. Therefore, the average mass spectra of these peaks are not presented for the sake of cogency.

The phospholipid region of the 18:2 *A. baumannii* sample chromatogram is presented in Figure 3.5 and the average mass spectra of the 6.23 minute, 7.82 minute, and 8.10 minute chromatogram peaks labeled as A, B, and C are presented in Figures 3.6, 3.7, and 3.8, respectively.

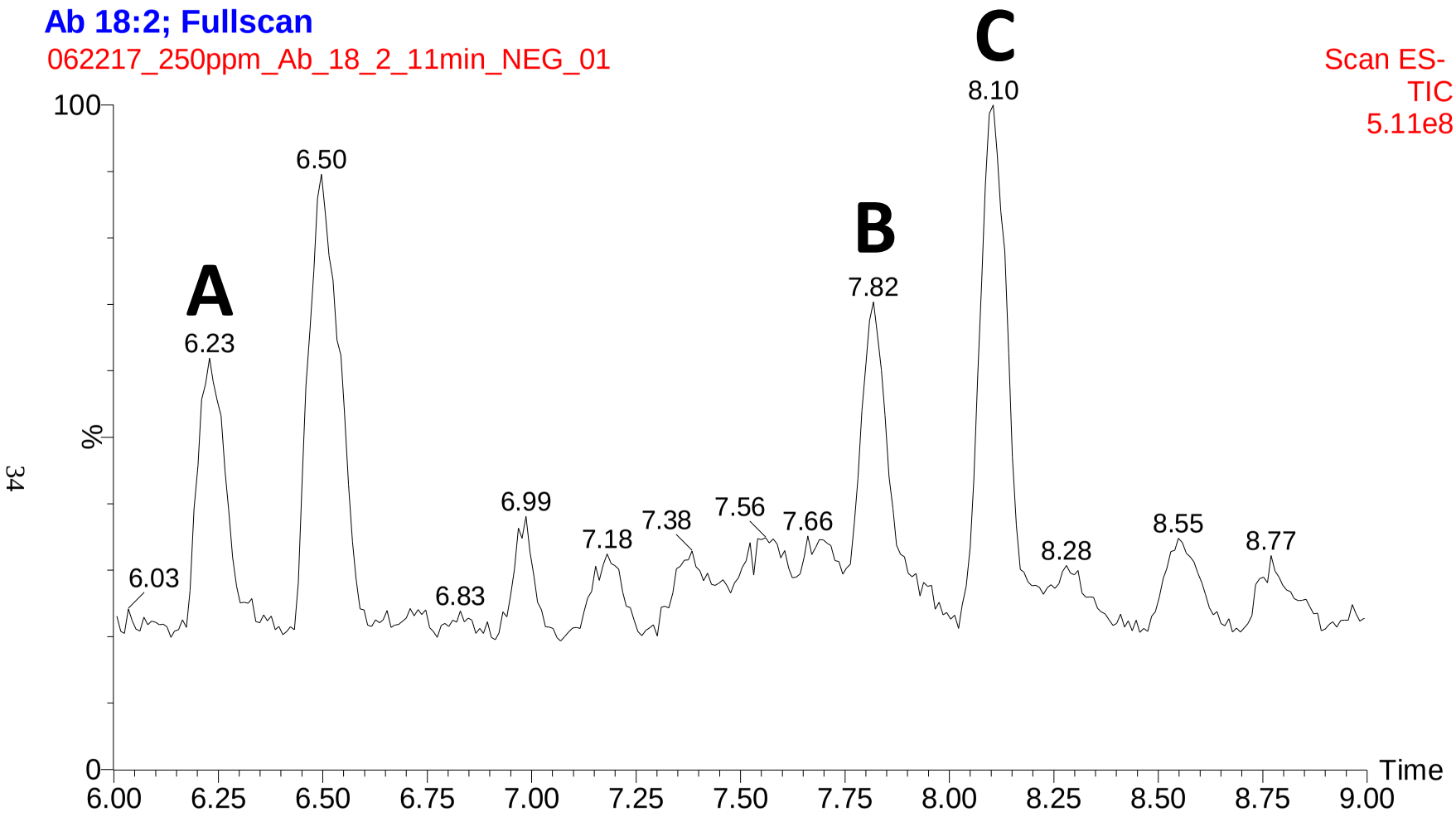

Figure 3.5: The phospholipid region of the 18:2 *A. baumannii* sample chromatogram

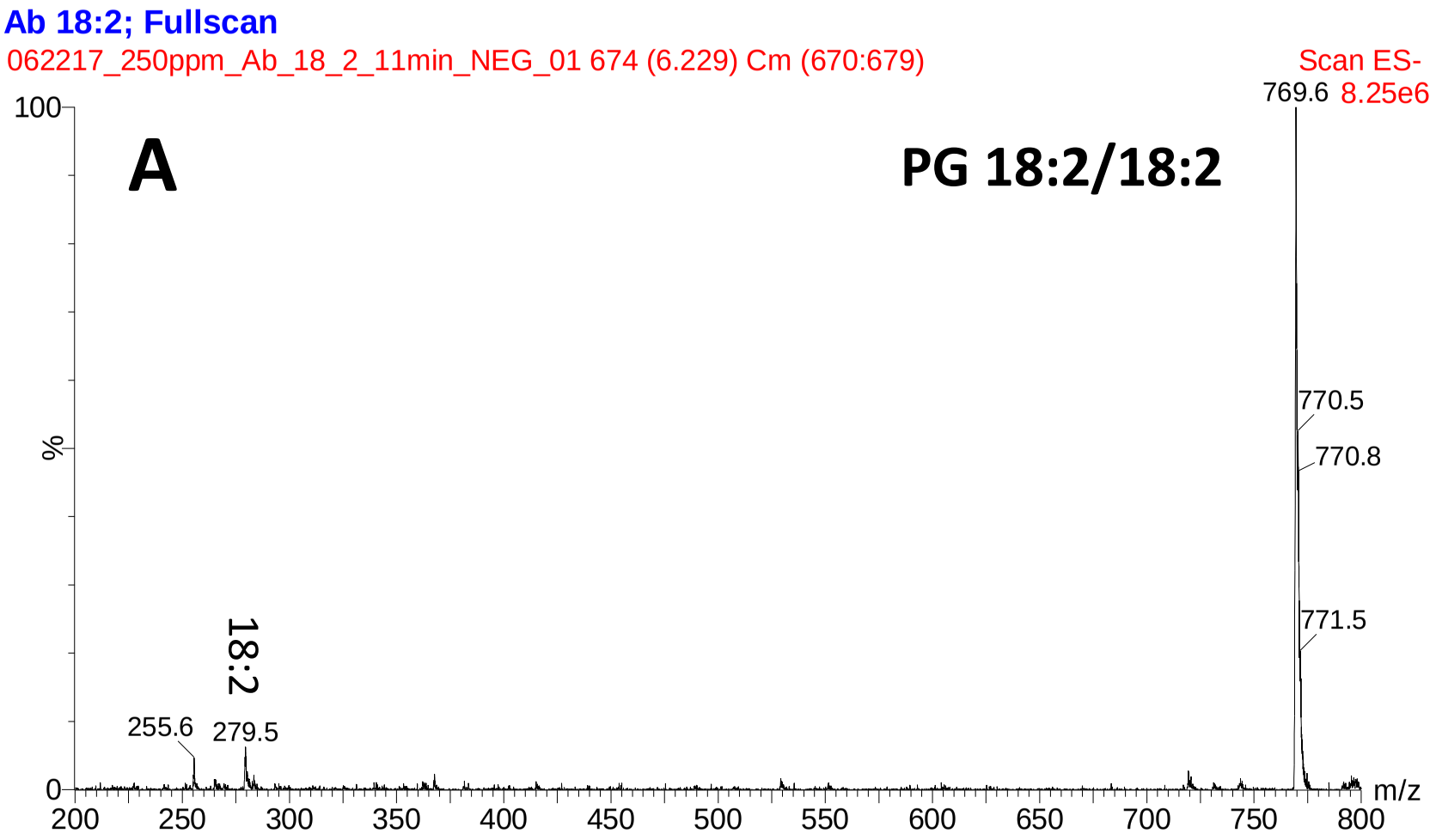

Figure 3.6: The average mass spectrum of peak A in the 18:2 *A. baumannii* sample chromatogram

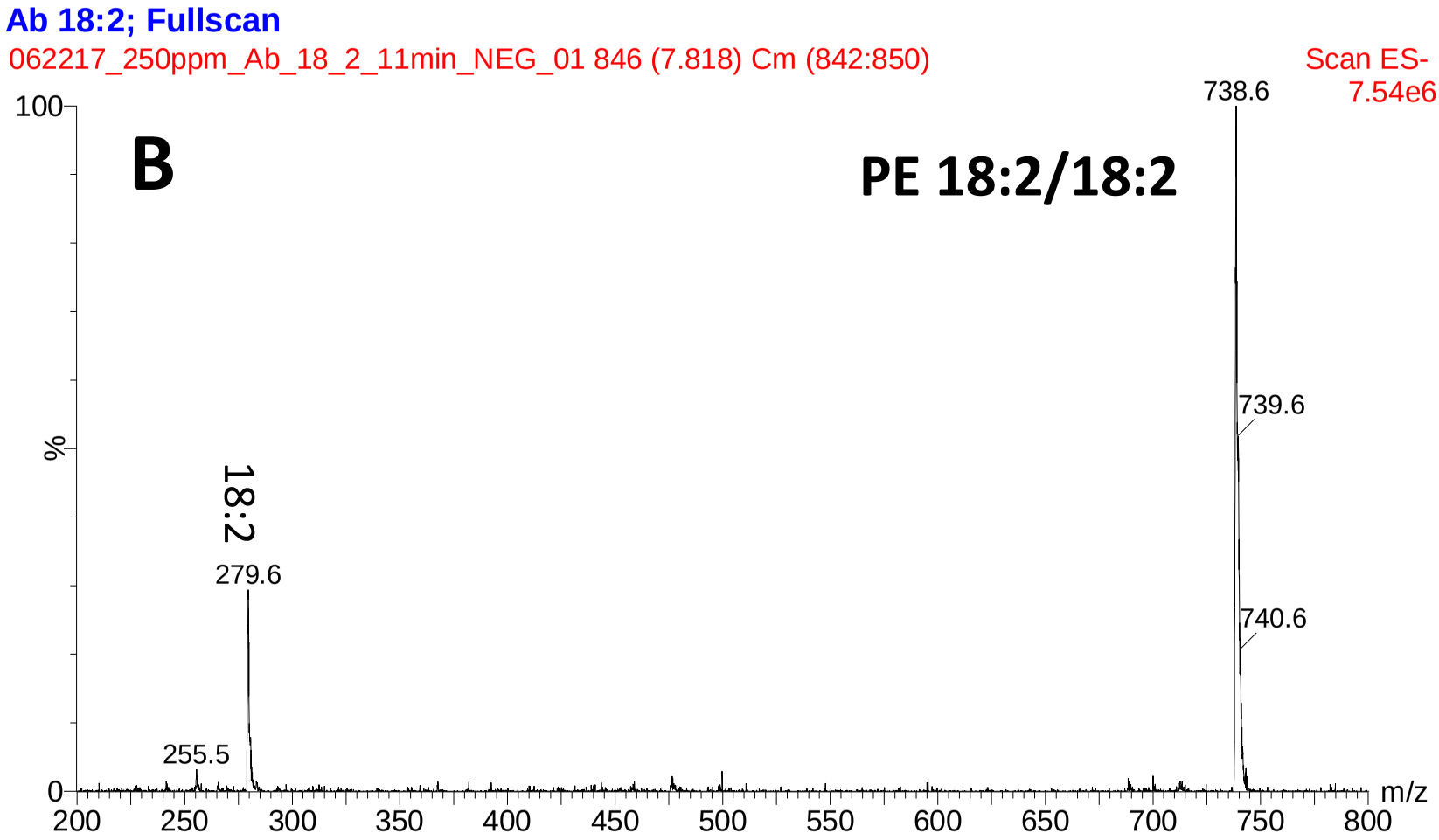

Figure 3.7: The average mass spectrum of peak B in the 18:2 *A. baumannii* sample chromatogram

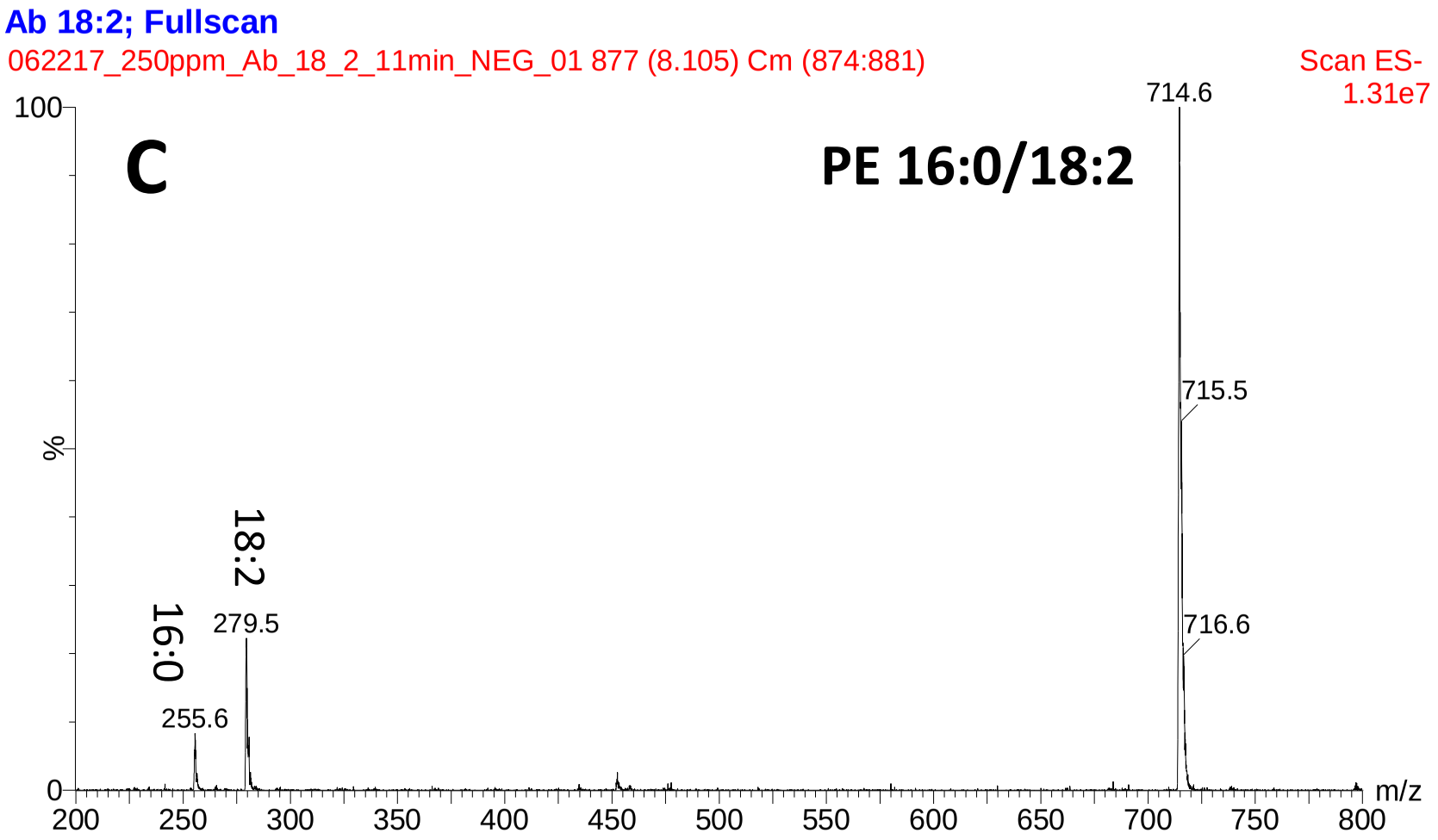

Figure 3.8: The average mass spectrum of peak C in the 18:2 *A. baumannii* sample chromatogram

The average mass spectra of chromatogram peaks A and B display a PG and PE, respectively, that have been doubly substituted with exogenously supplied 18:2 fatty acid chains. The 769.5 m/z peak in the average mass spectrum of chromatogram peak A corresponds to the $[M-H]^-$ ion of PG 18:2/18:2, and the 738.5 m/z peak in the average mass spectrum of chromatogram peak B corresponds to PE 18:2/18:2. The identification of these phospholipids was achieved by referencing LIPID MAPS and observing the relatively high intensity 18:2 cone fragments, which correspond to the 279.5 m/z peaks. It should be noted that 255.5 m/z peaks can be observed in the average mass spectra of chromatogram peaks A and B, but these peaks do not originate as 16:0 cone fragments from the parent ions. The identities of these 255.5 m/z peaks have not yet been elucidated and may result from a contaminant or from a higher mass lipid such as a cardiolipin. The 714.5 m/z peak in the average mass spectrum of chromatogram peak C corresponds to the $[M-H]^-$ ion of PE 16:0/18:2. This identification was confirmed using LIPID MAPS and by the presence of the 16:0 and 18:2 cone fragments.

The phospholipid region of the 18:3-α *A. baumannii* sample chromatogram is presented in Figure 3.9 and the average mass spectrum of the 7.66 minute chromatogram peak labeled as A is presented in Figure 3.10.

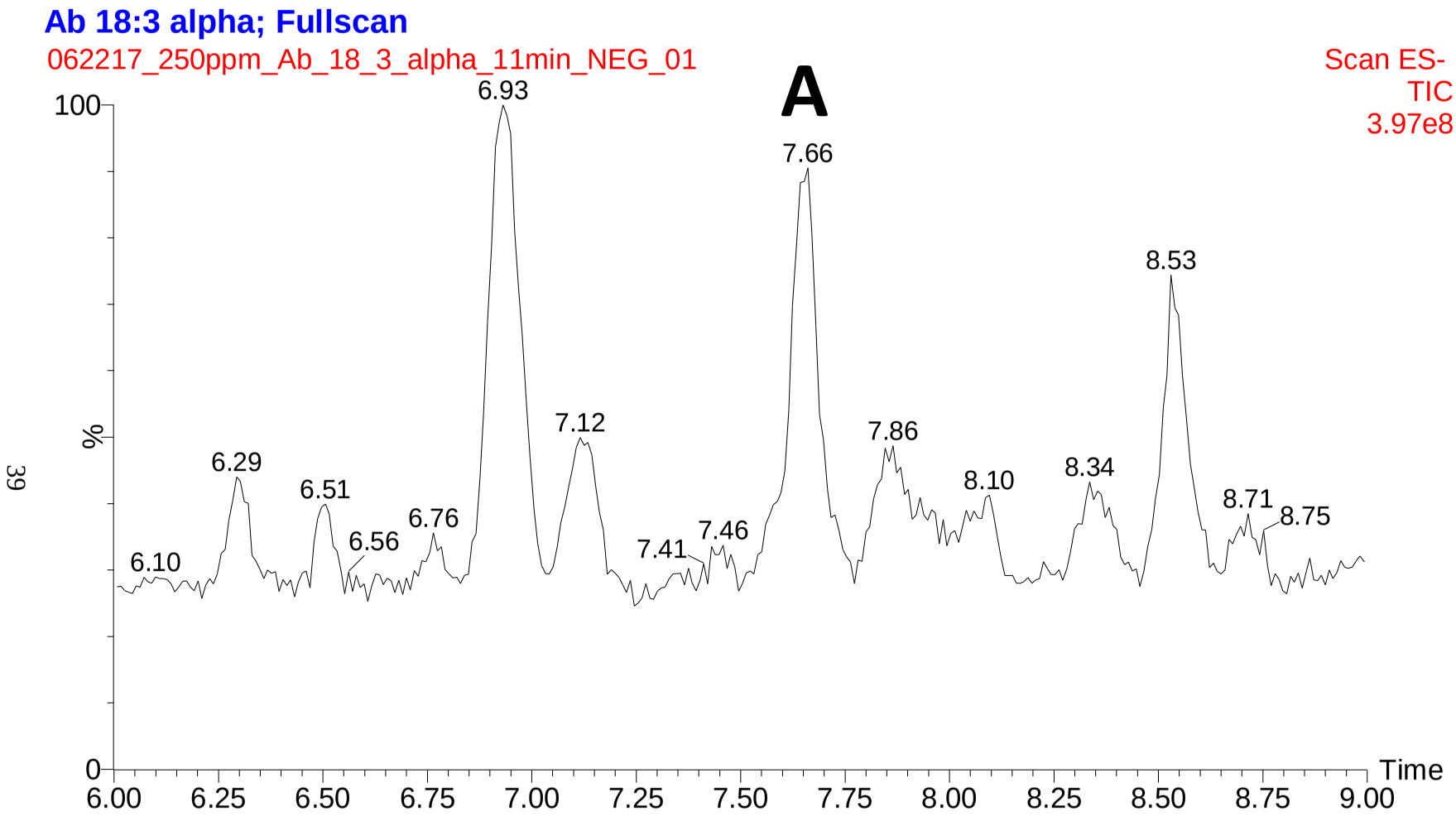

Figure 3.9: The phospholipid region of the 18:3-α *A. baumannii* sample chromatogram

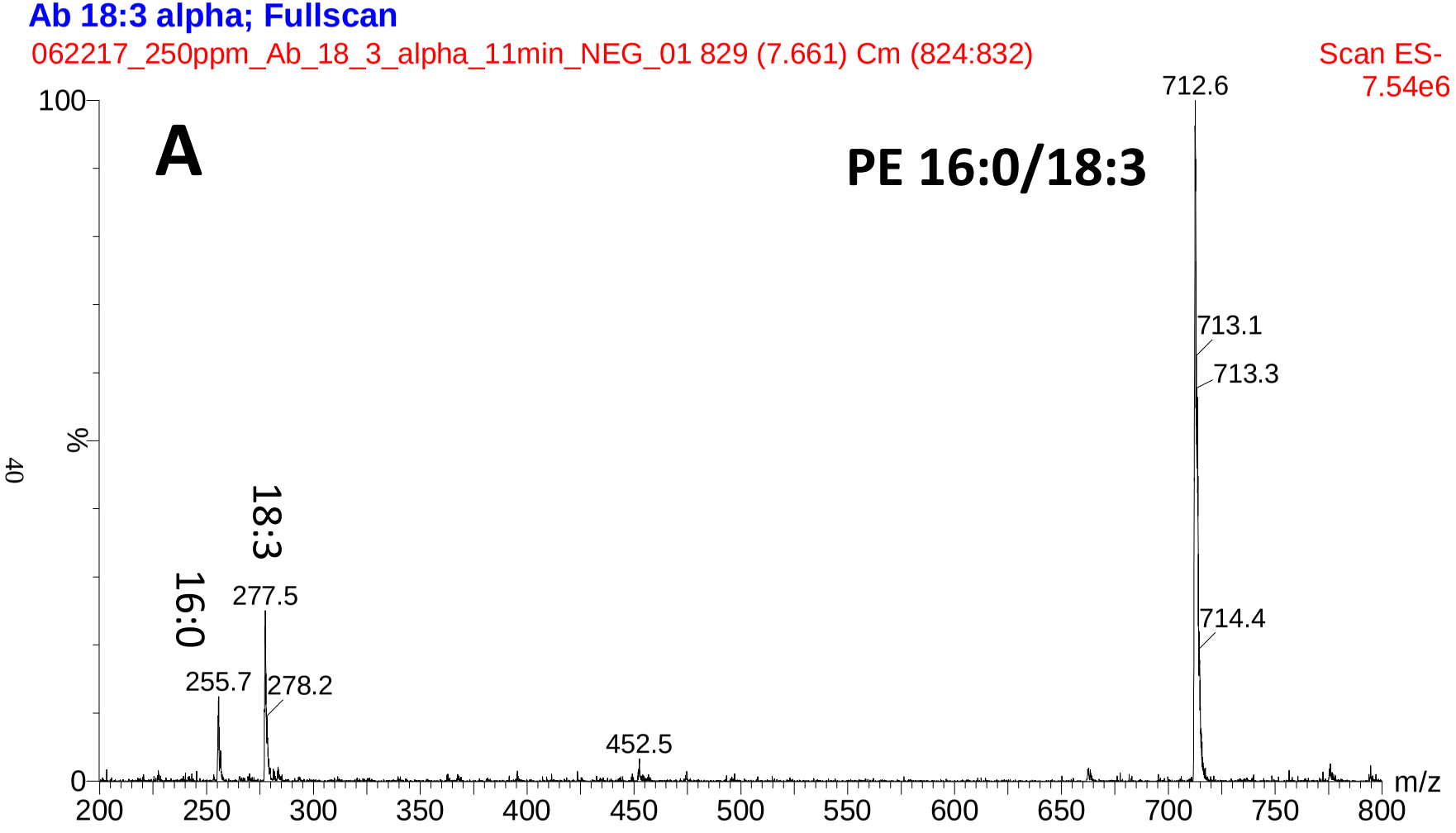

Figure 3.10: The average mass spectrum of peak A in the 18:3-α *A. baumannii* sample chromatogram

The 712.5 m/z peak in the average mass spectrum of chromatogram peak A corresponds to the $[M-H]^-$ ion of PE 16:0/18:3, as confirmed by LIPID MAPS and the 16:0 and 18:3 cone fragments corresponding to the 255.5 m/z and 277.5 m/z peaks, respectively.

The phospholipid region of the 18:3-γ *A. baumannii* sample chromatogram is presented in Figure 3.11 and the average mass spectra of the 6.17 minute and 7.76 minute chromatogram peaks labeled as A and B respectively are presented in Figures 3.12 and 3.13 respectively.

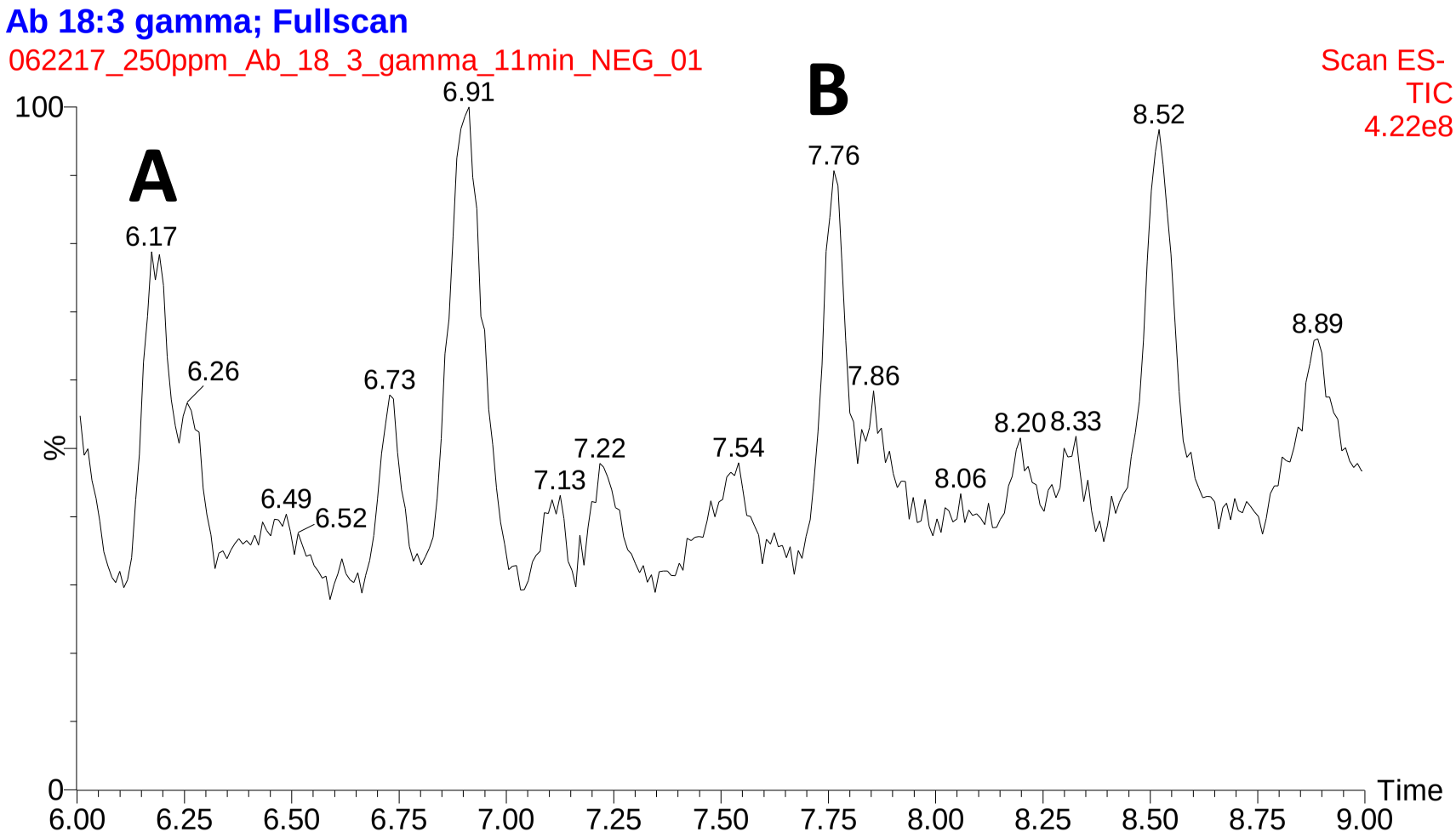

Figure 3.11: The phospholipid region of the 18:3-γ *A. baumannii* sample chromatogram

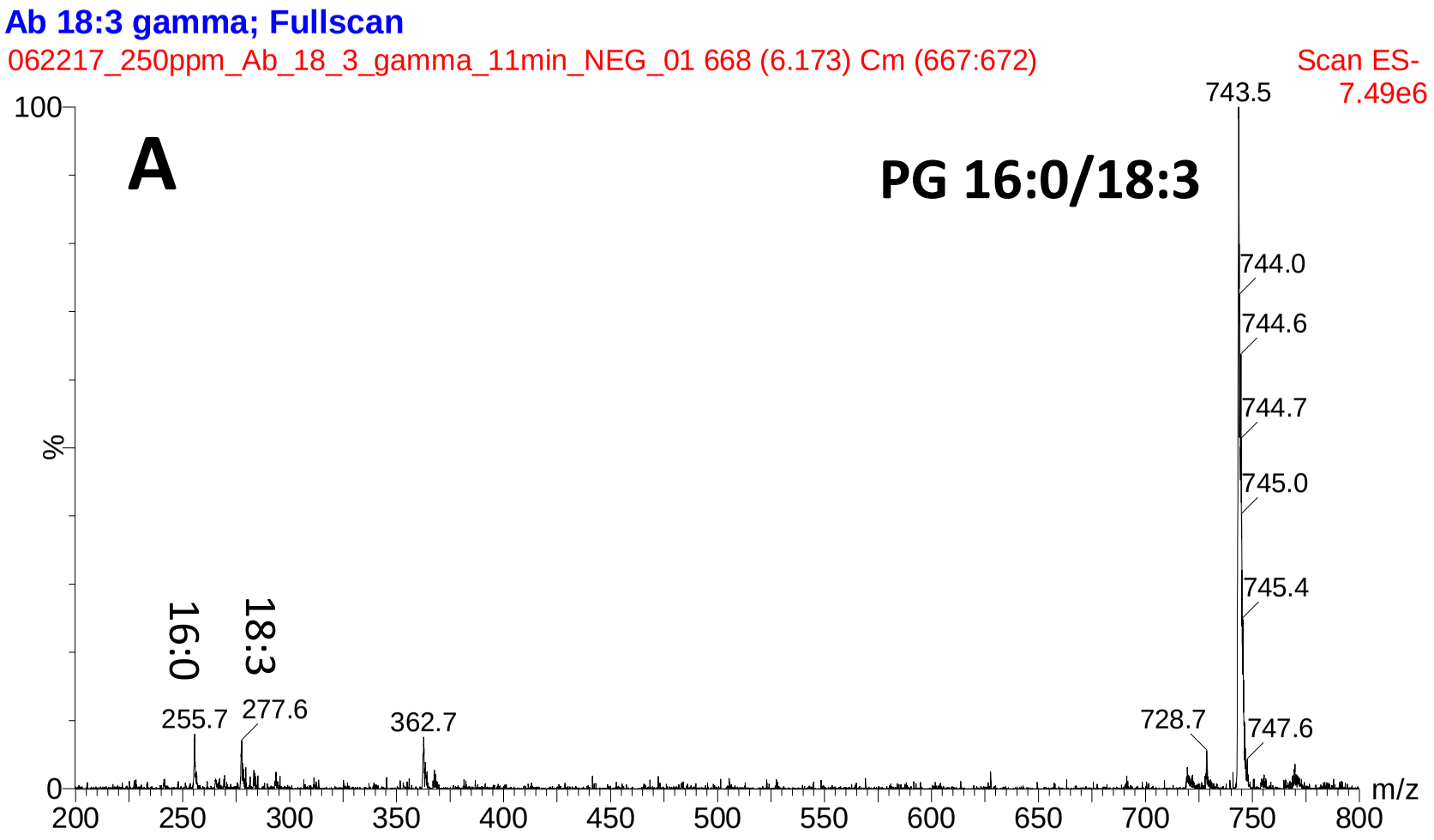

Figure 3.12: The average mass spectrum of peak A in the 18:3-γ *A. baumannii* sample chromatogram

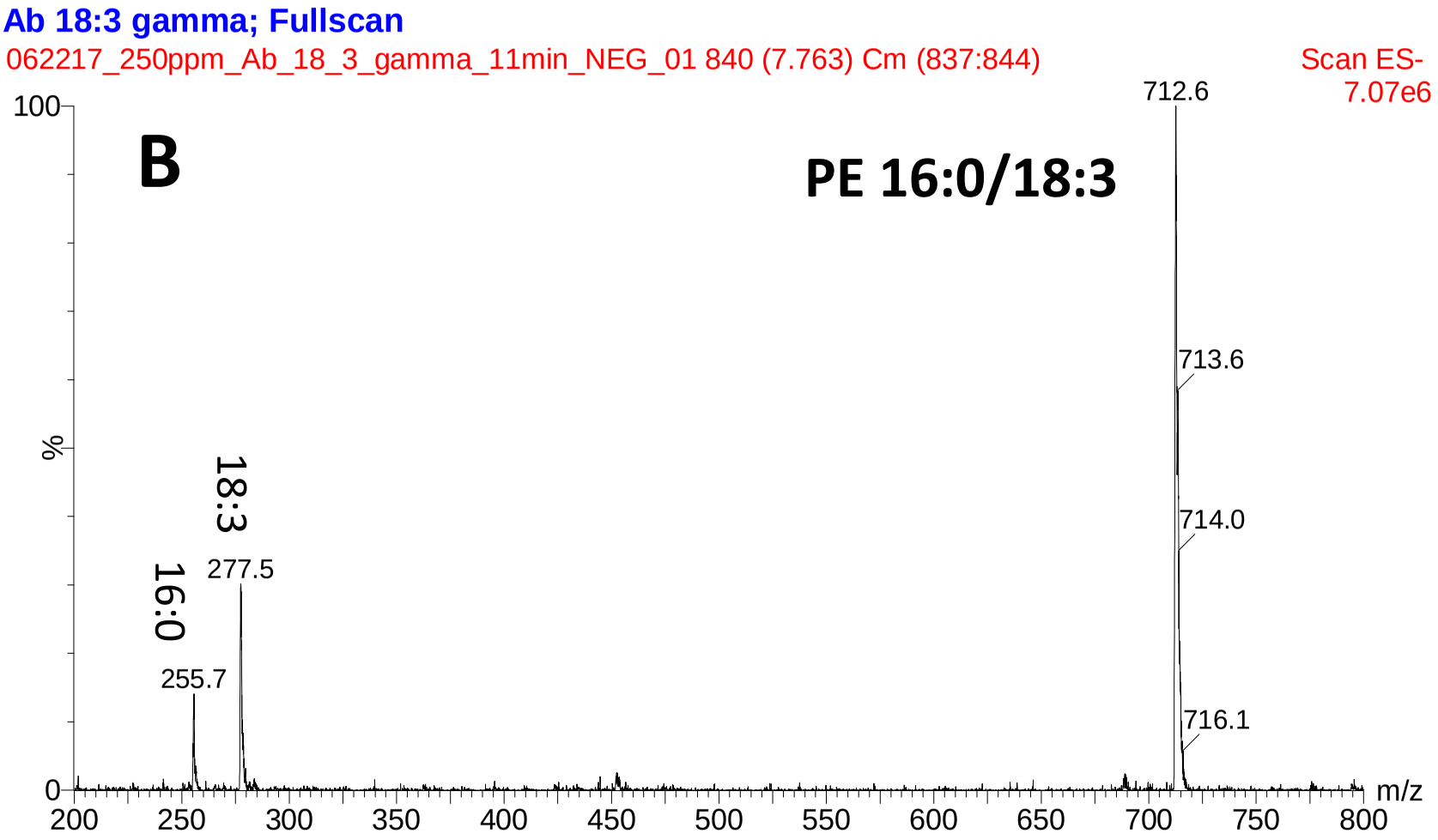

Figure 3.13: The average mass spectrum of peak B in the 18:3-γ *A. baumannii* sample chromatogram

The 743.5 m/z peak in the average mass spectrum of chromatogram peak A corresponds to the $[M-H]^-$ ion of PG 16:0/18:3, and the 712.5 m/z peak in the average mass spectrum of chromatogram peak B corresponds to the $[M-H]^-$ ion of PE 16:0/18:3. These identities were confirmed by the LIPID MAPS database and by observing the 16:0 and 18:3 cone fragments that correspond to the 255.5 m/z and 277.5 m/z peaks, respectively.

The phospholipid region of the 20:3 *A. baumannii* sample chromatogram is presented in Figure 3.14 and the average mass spectra of the 6.71 minute and 8.31 minute chromatogram peaks labeled as A and B respectively are presented in Figures 3.15 and 3.16 respectively.

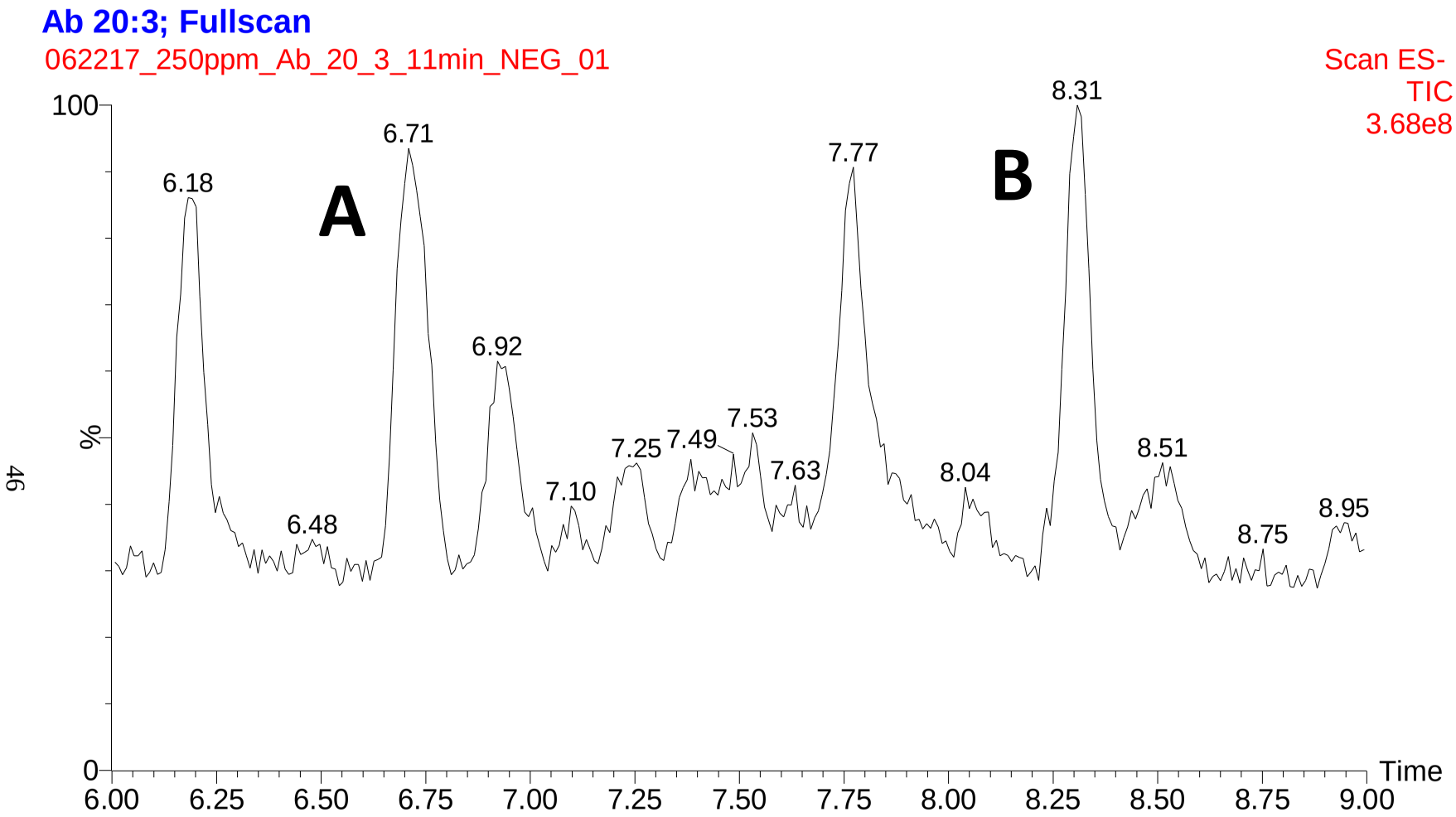

Figure 3.14: The phospholipid region of the 20:3 *A. baumannii* sample chromatogram

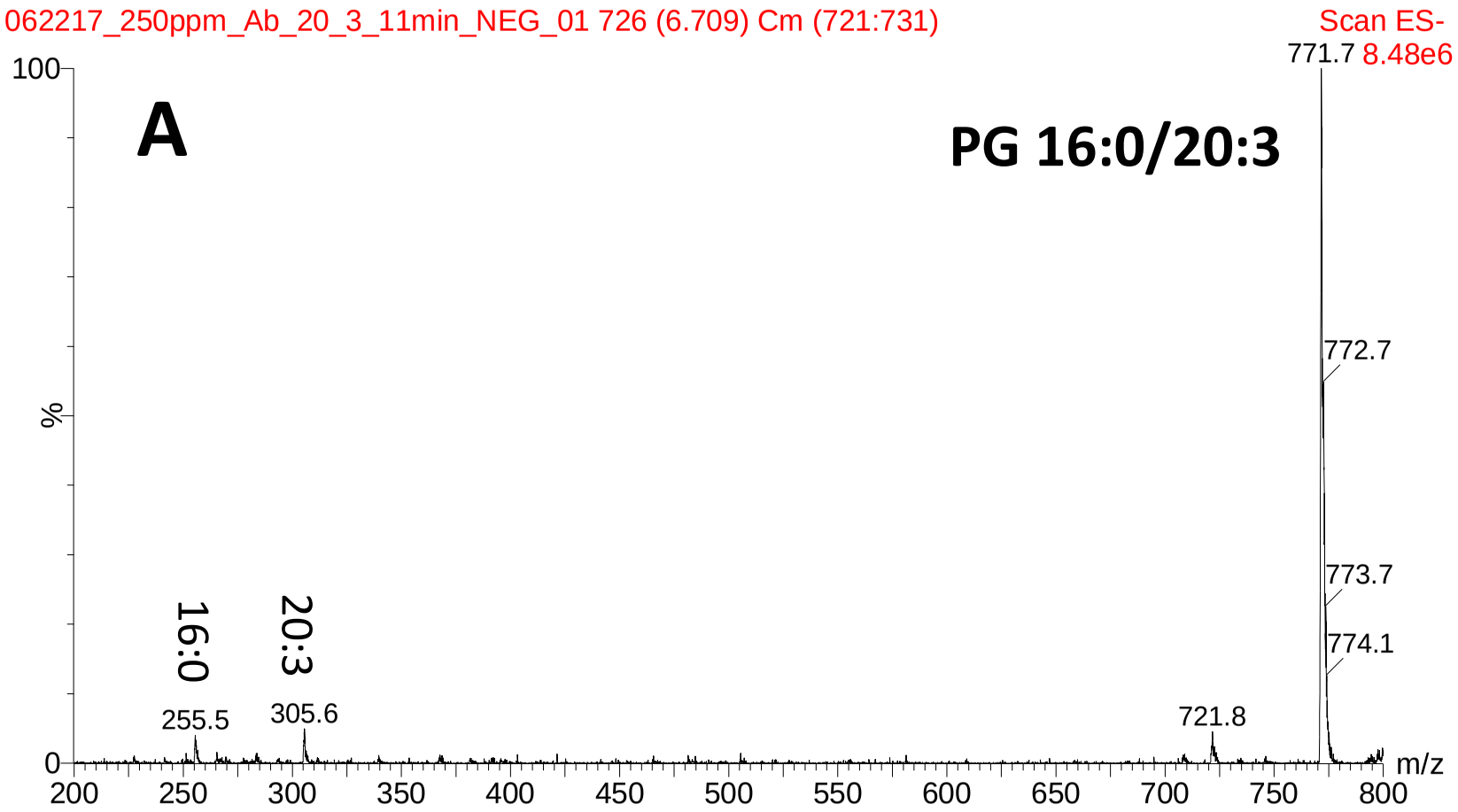

Figure 3.15: The average mass spectrum of peak A in the 20:3 *A. baumannii* sample chromatogram

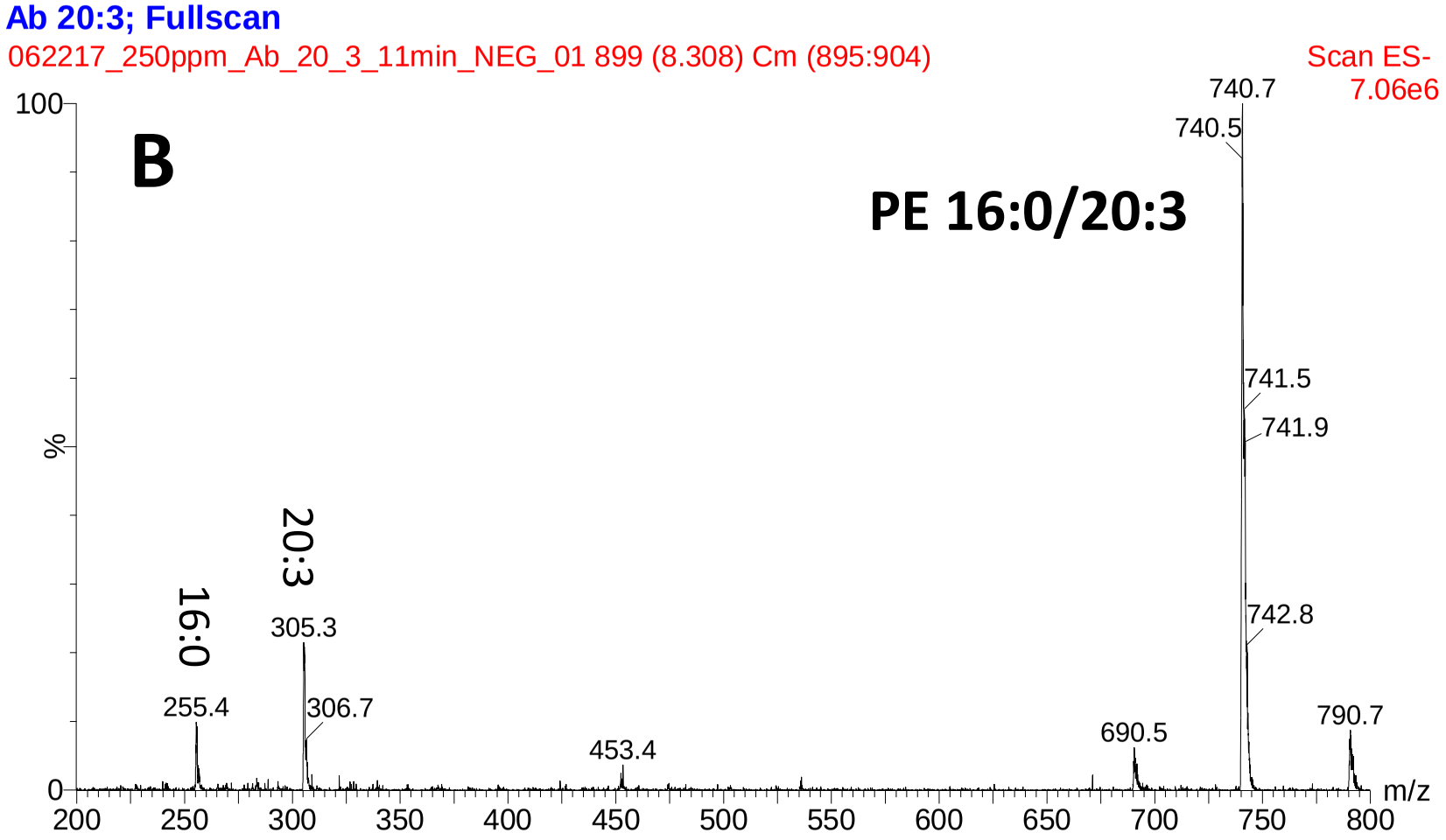

Figure 3.16: The average mass spectrum of peak B in the 20:3 *A. baumannii* sample chromatogram

The 771.5 m/z peak in the average mass spectrum of chromatogram peak A corresponds to the $[M-H]^-$ ion of PG 16:0/20:3, and the 740.5 m/z peak in the average mass spectrum of chromatogram peak B corresponds to the $[M-H]^-$ ion of PE 16:0/20:3. These identities were confirmed by referencing LIPID MAPS and noting the 16:0 and 20:3 cone fragments that correspond to the 255.5 m/z and 305.5 m/z peaks, respectively.

The phospholipid region of the 20:4 *A. baumannii* sample chromatogram is presented in Figure 3.17 and the average mass spectra of the 6.49 minute and 8.08 minute chromatogram peaks labeled as A and B respectively are presented in Figures 3.18 and 3.19 respectively.

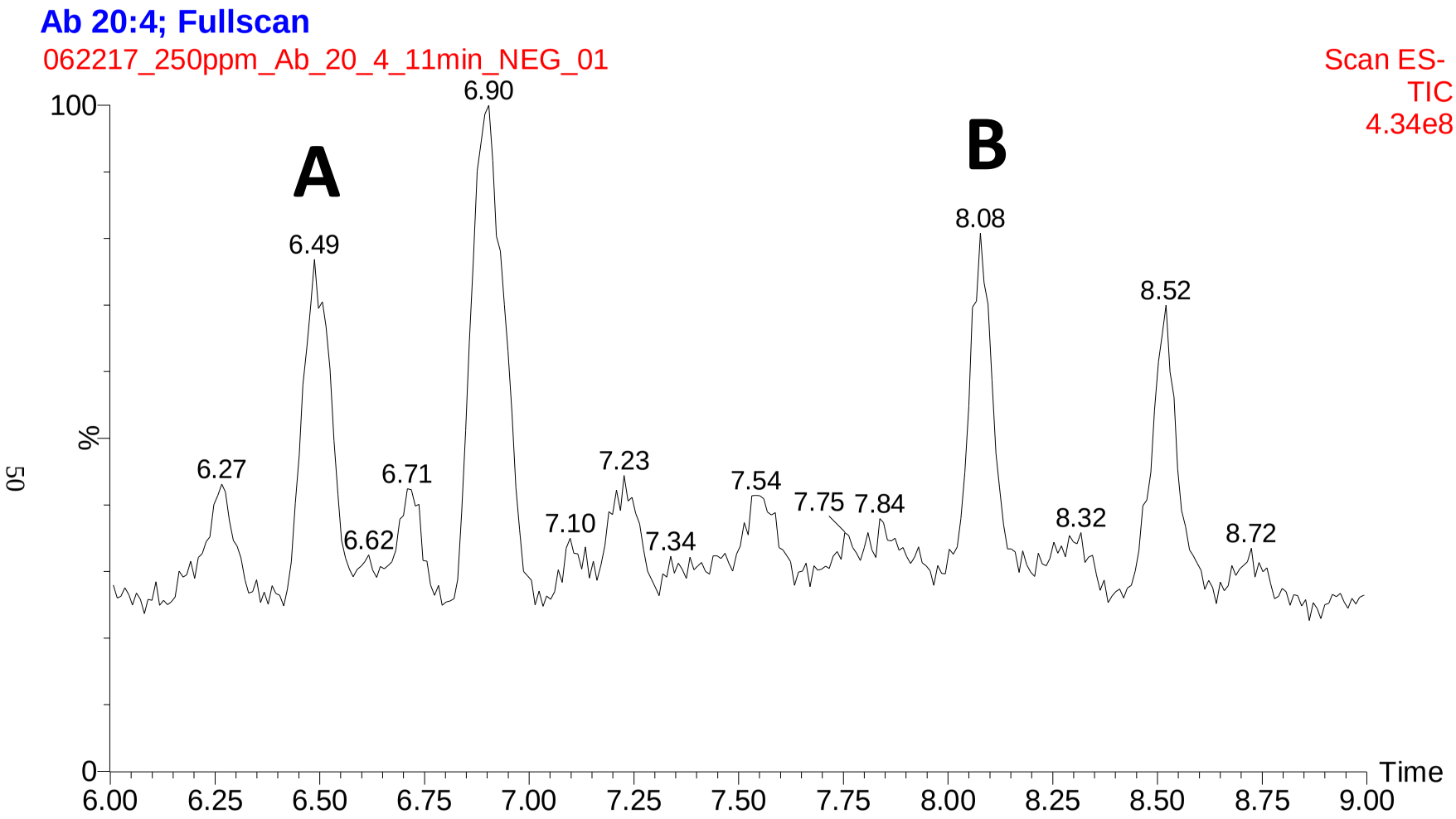

Figure 3.17: The phospholipid region of the 20:4 *A. baumannii* sample chromatogram

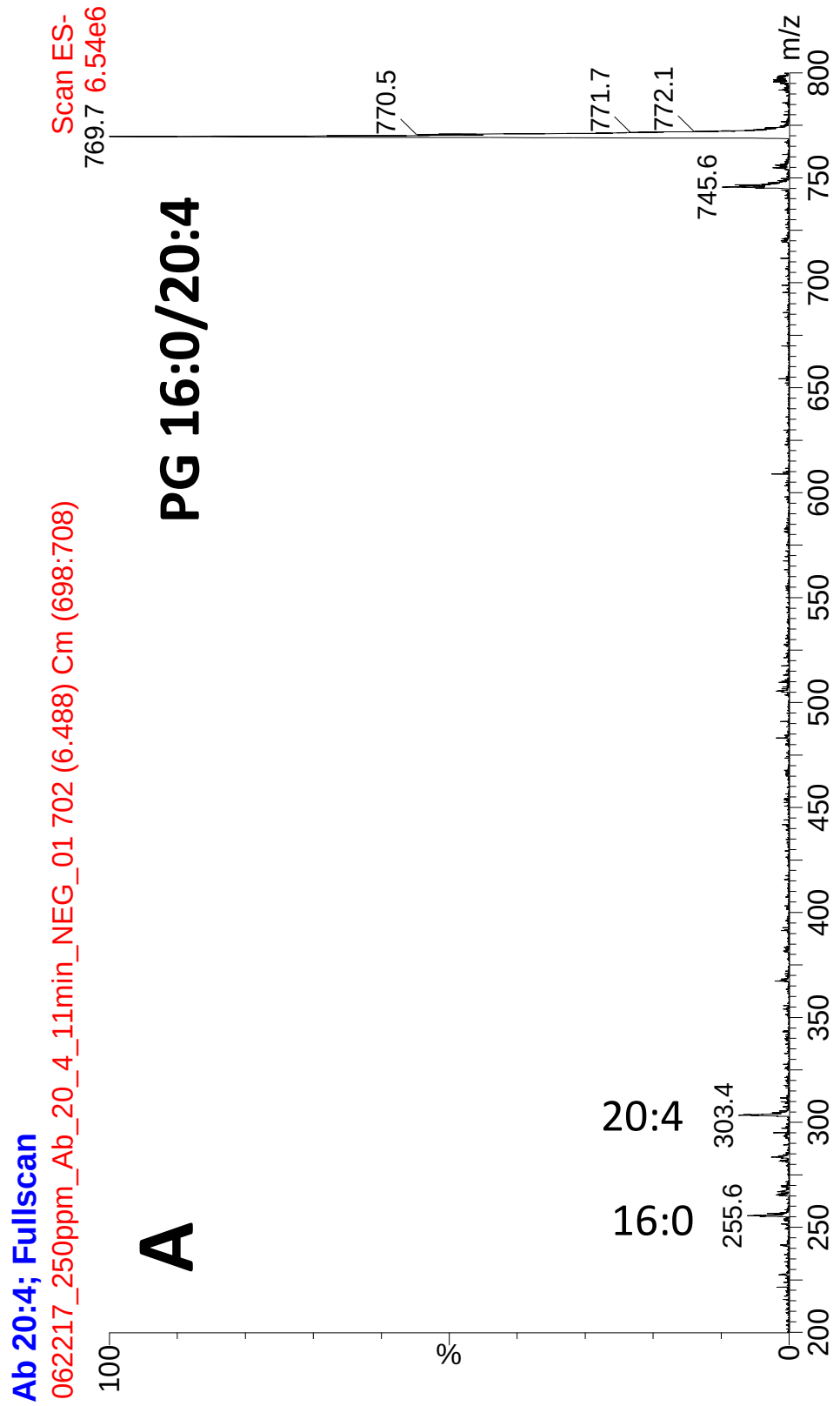

Figure 3.18: The average mass spectrum of peak A in the 20:4 *A. baumannii* sample chromatogram

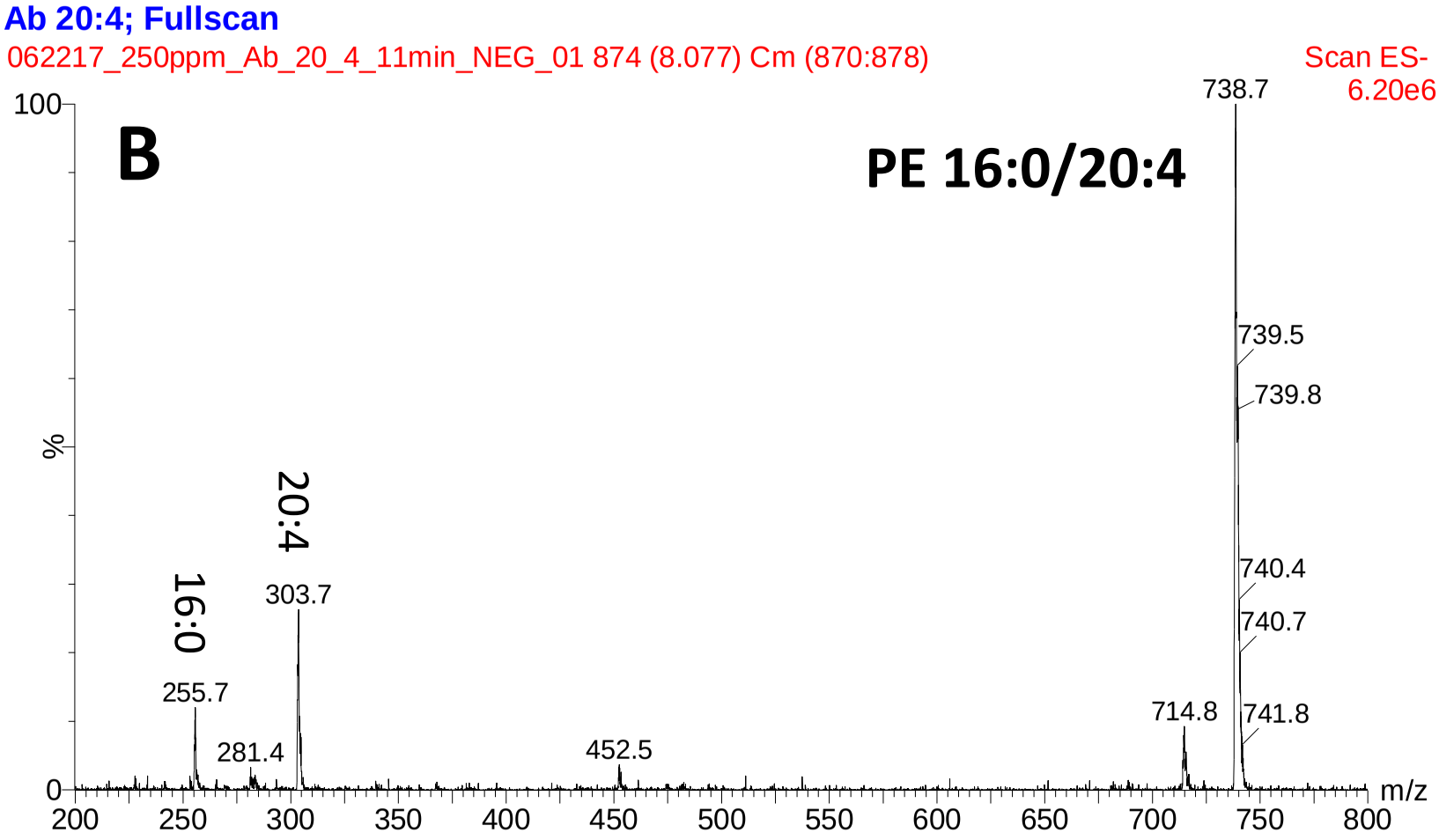

Figure 3.19: The average mass spectrum of peak B in the 20:4 *A. baumannii* sample chromatogram

The 769.5 m/z peak in the average mass spectrum of peak A corresponds to the $[M-H]^-$ ion of PG 16:0/20:4, and the 738.5 m/z peak in the average mass spectrum of peak B corresponds to the $[M-H]^-$ ion of PE 16:0/20:4; these identifications were confirmed by referencing LIPID MAPS and by the presence of the 16:0 and 20:4 cone fragments, which correspond to the 255.5 m/z and 303.5 m/z peaks, respectively.

The phospholipid region of the 20:5 *A. baumannii* sample chromatogram is presented in Figure 3.20 and the average mass spectrum of the 7.67 minute chromatogram peak labeled as A is presented in Figure 3.21.

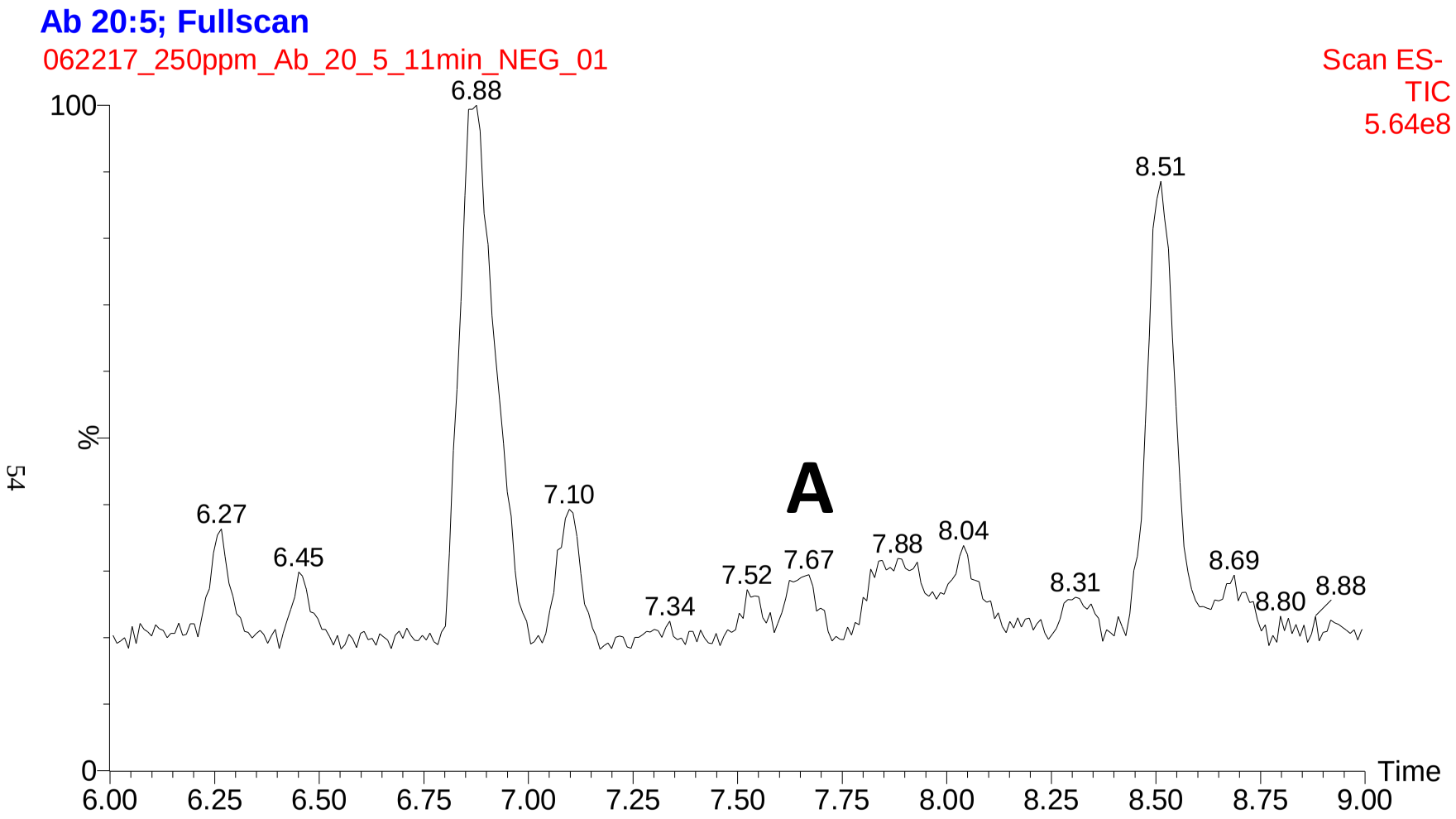

Figure 3.20: The phospholipid region of the 20:5 *A. baumannii* sample chromatogram

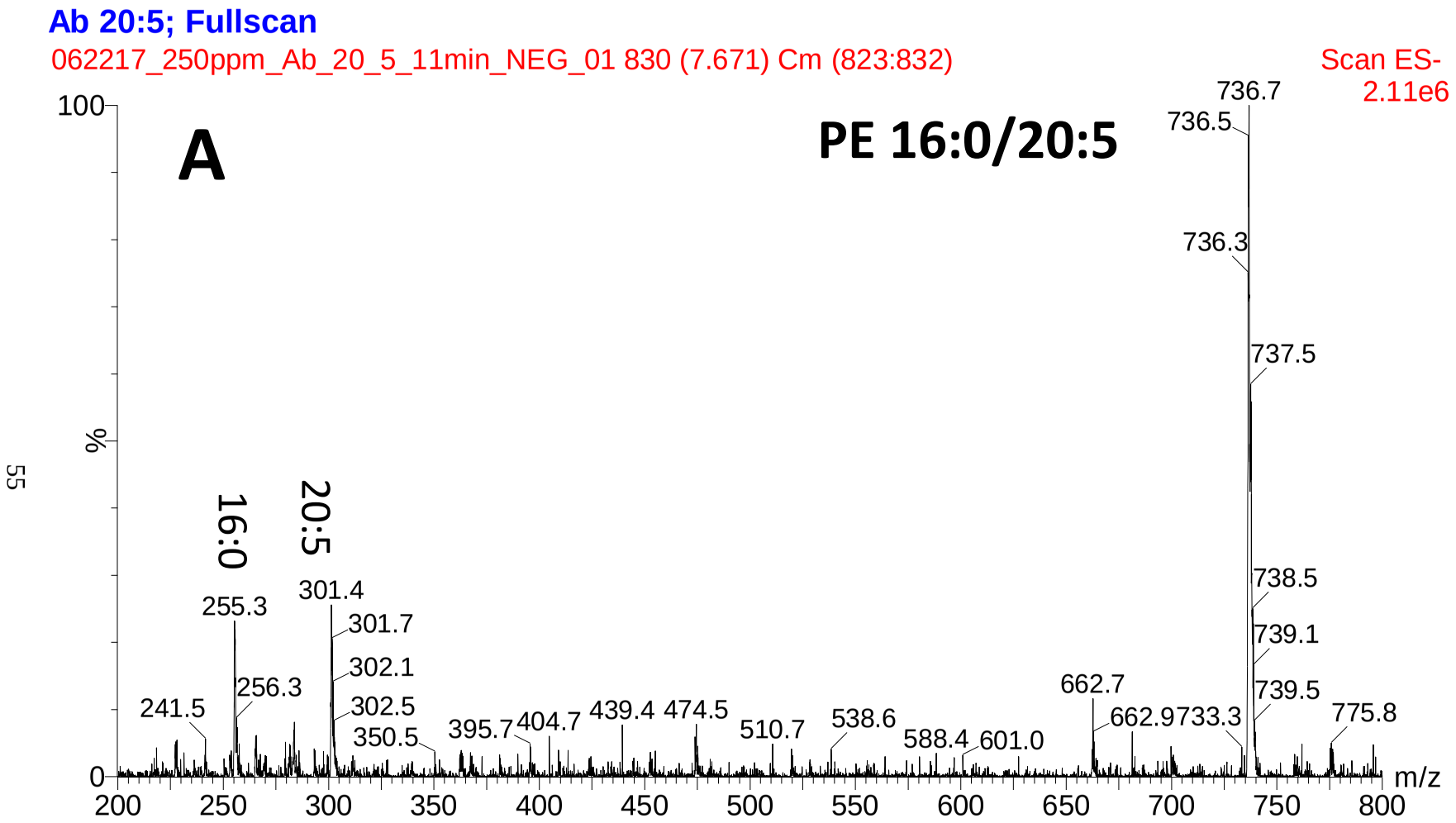

Figure 3.21: The average mass spectrum of peak A in the 20:5 *A. baumannii* sample chromatogram

The 736.5 m/z peak in the average mass spectrum of peak A corresponds to the $[M-H]^-$ ion of PE 16:0/20:5, which was confirmed through the LIPID MAPS database and by observing the 16:0 and 20:5 cone fragments that correspond to the 255.5 m/z and 301.5 m/z peaks, respectively.

The phospholipid region of the 22:6 *A. baumannii* sample chromatogram is presented in Figure 3.22 and the average mass spectrum of the 6.27 minute chromatogram peak labeled as A is presented in Figure 3.23.

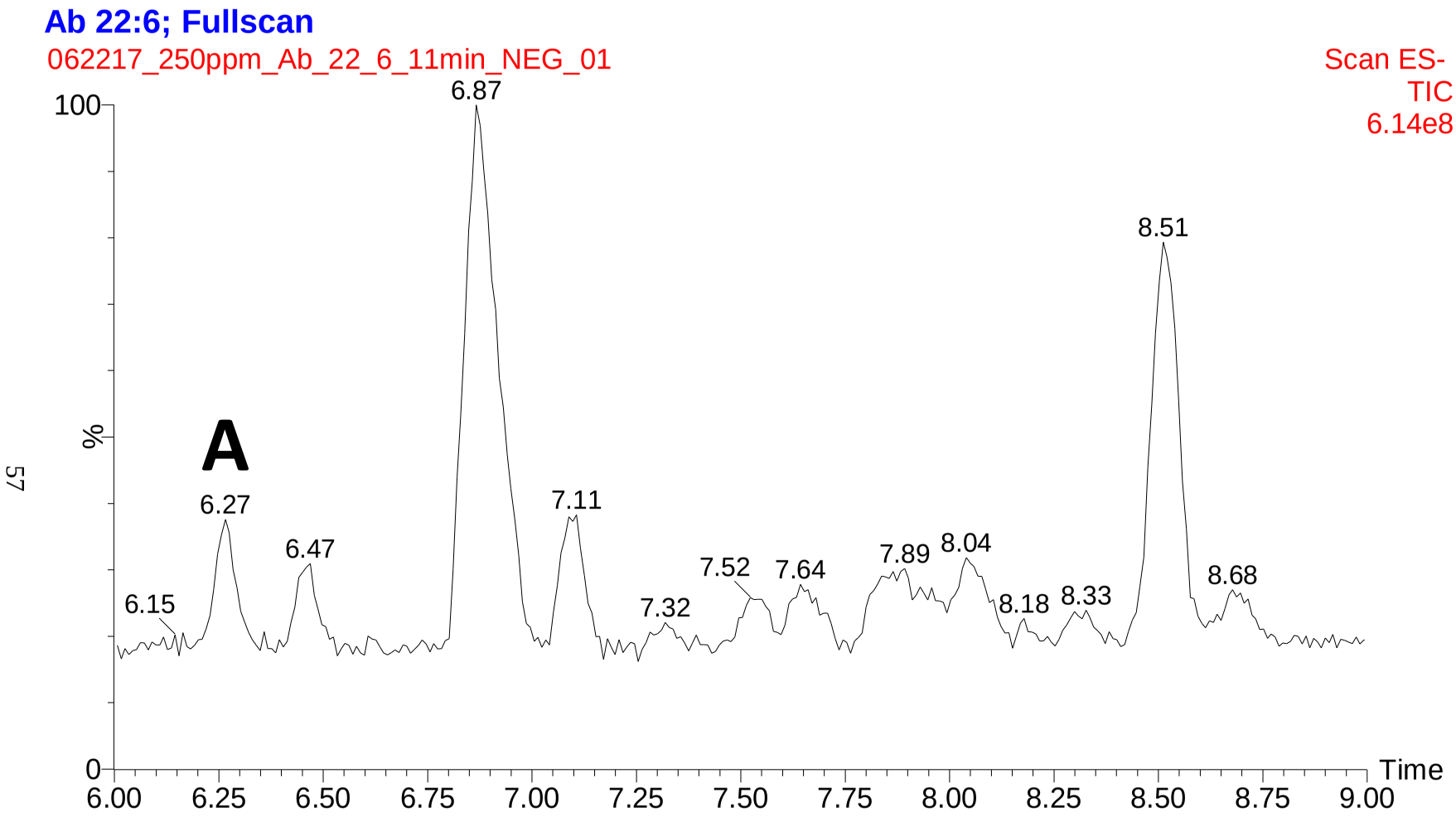

Figure 3.22: The phospholipid region of the 22:6 *A. baumannii* sample chromatogram

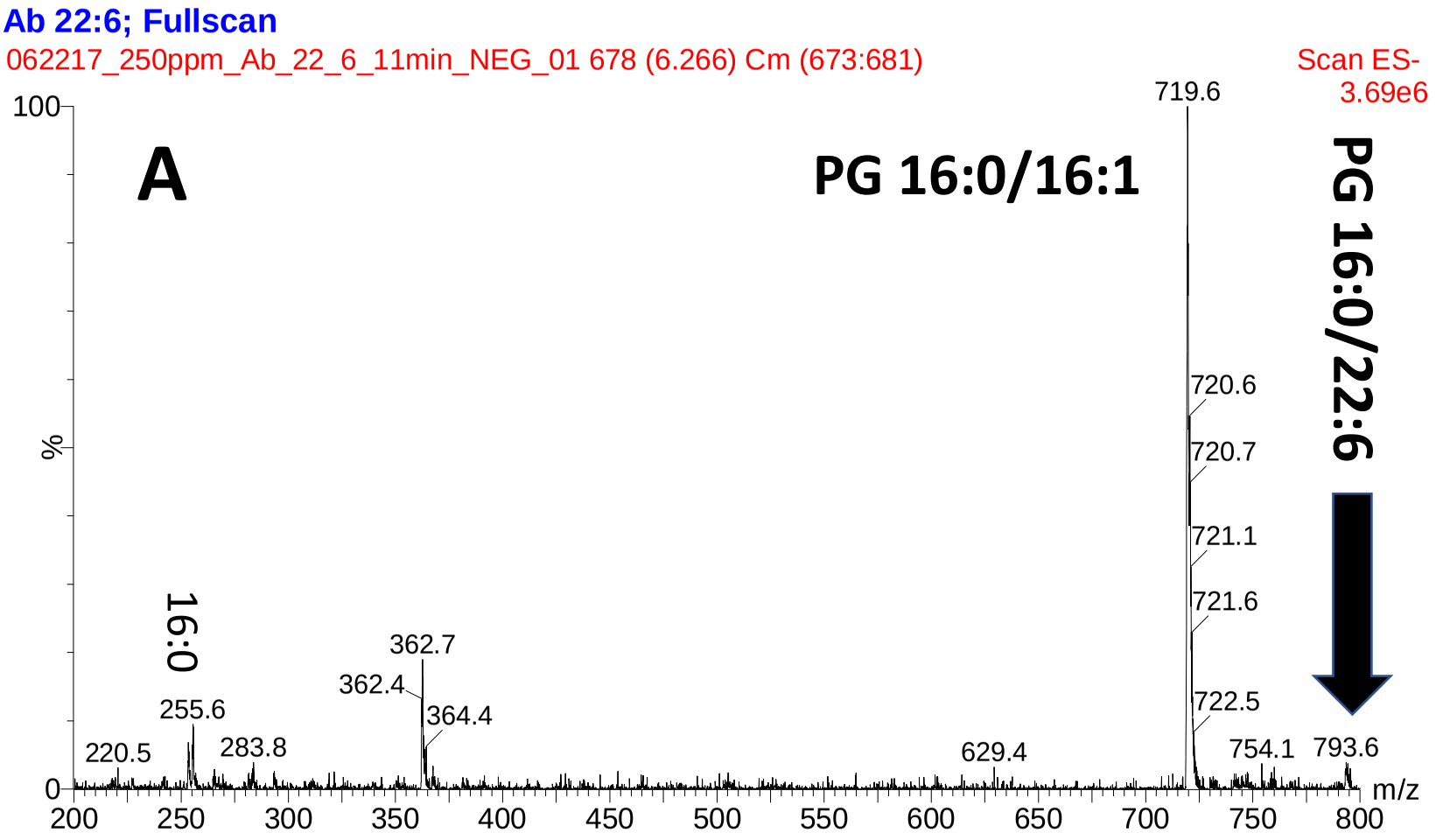

Figure 3.23: The average mass spectrum of peak A in the 22:6 *A. baumannii* sample chromatogram

The 793.5 m/z peak in the average mass spectrum of peak A corresponds to the $[M-H]^-$ ion of PG 16:0/22:6. This was confirmed by referencing LIPID MAPS. While the 22:6 cone fragment signal has a very low intensity, it was found to be present as well. PG 16:0/22:6 coeluted with PG 16:0/16:1, which is a much more abundant phospholipid within *A. baumannii* that is made natively. The low intensity of the PG 16:0/22:6 signal suggests that *A. baumannii* does not incorporate 22:6 into its cell membrane as well as the other PUFAs used in this experiment.

Mass filtering is a useful technique for finding chromatogram peaks in the total ion chromatogram (TIC) of a given sample. It is achieved using the MassLynx software to display an extracted ion chromatogram (XIC) featuring only the chromatogram peaks corresponding to a chosen m/z value. Mass filtering was employed in this experiment to show that PE and PG species possessing one of the seven exogenous PUFAs as a constituent are not natively produced by *A. baumannii*. To avoid excessive repetition, only one example of mass filtering in the *A. baumannii* chromatograms is shown here. The XICs generated by mass filtering for the m/z value of PE 16:0/20:4 in the control and 20:4 *A. baumannii* samples are presented in Figure 3.24.

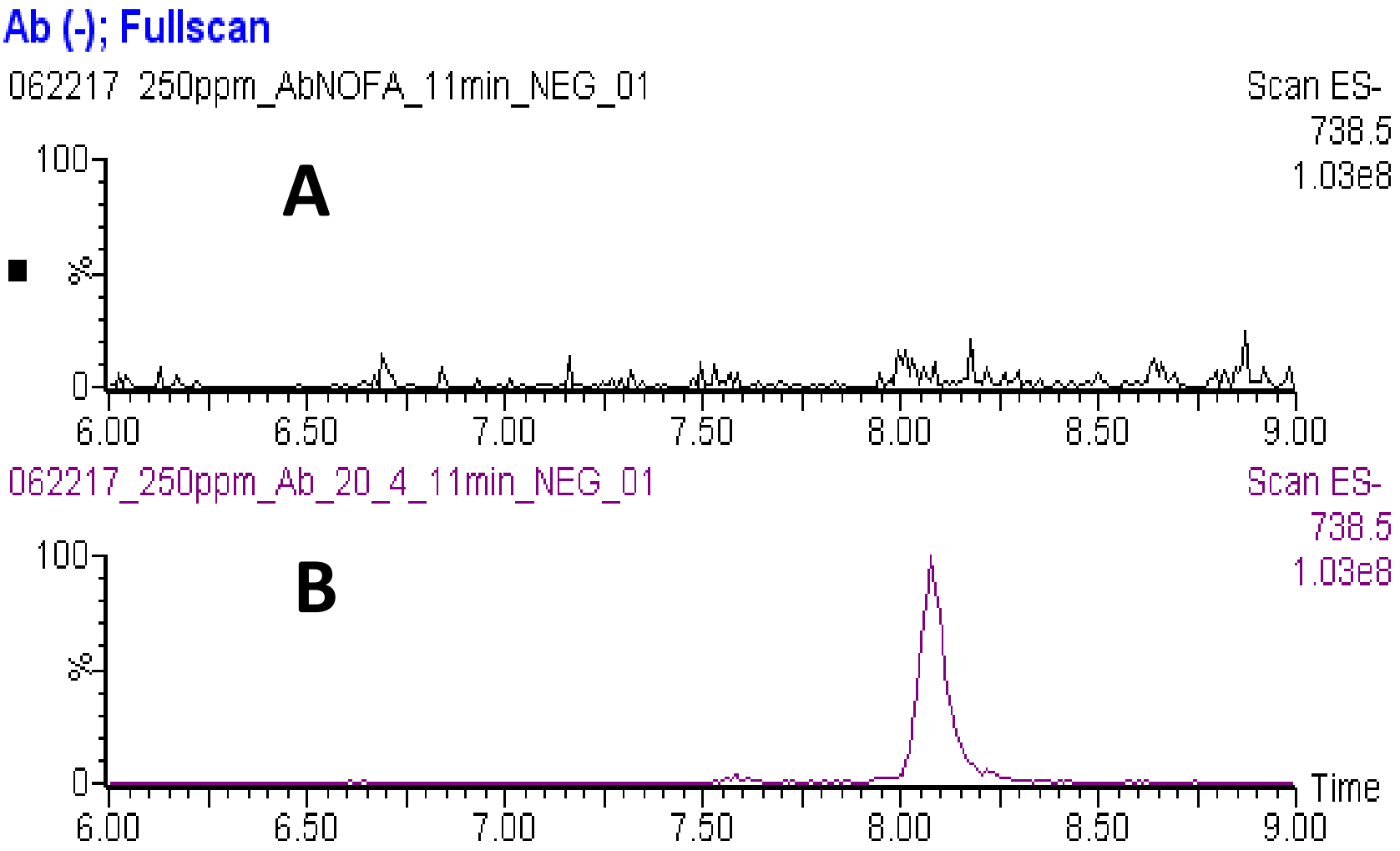

Figure 3.24: The XICs of the control and 20:4 *A. baumannii* samples after mass filtering for 738.5 m/z

"A" represents the XIC of the control *A. baumannii* sample generated after filtering for the 738.5 m/z value, and "B" represents the XIC of the 20:4 *A. baumannii* sample generated after filtering for the 738.5 m/z. Clearly, only noise peaks are present in the control XIC, but a chromatogram peak corresponding to the $[M-H]^-$ ion of PE 16:0/20:4 (738.5 m/z) is present in the 20:4 XIC. This demonstrates that *A. baumannii* does not natively produce phospholipid species possessing 20:4 acyl chains, and that *A. baumannii* successfully incorporated 20:4 into its cell membrane following exposure to it.

3.3 *Klebsiella Pneumoniae* Results

3.3.1 *Klebsiella Pneumoniae* Mass Spectra and Chromatograms

The complete chromatogram of the *K. pneumoniae* control sample is presented in Figure 3.25 and the phospholipid region of the chromatogram is presented in Figure 3.26. The average mass spectra of the 6.90 minute and 7.65 minute chromatogram peaks labeled as A and B respectively are presented in Figures 3.27 and Figure 3.28 respectively.

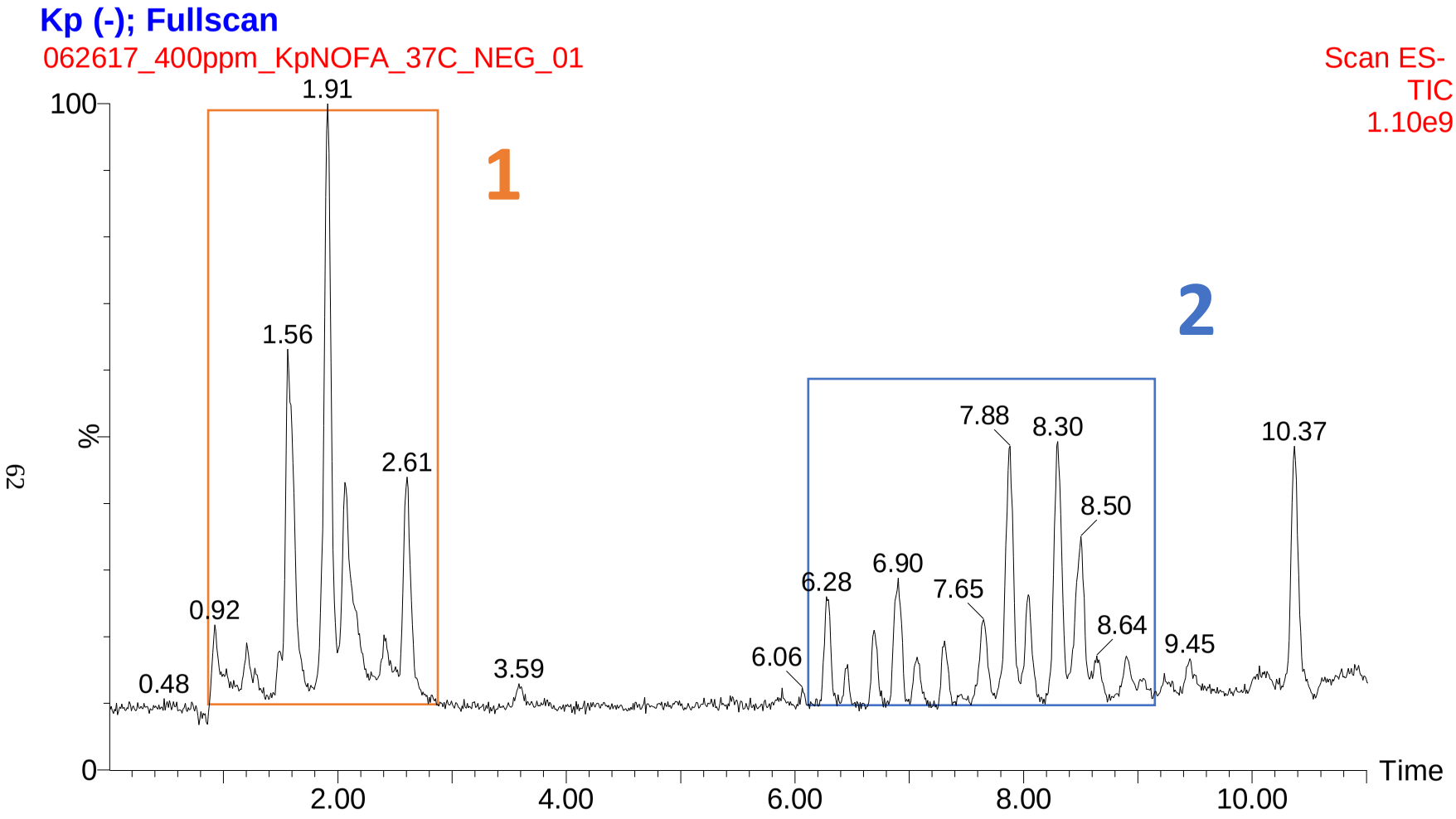

Figure 3.25: The complete chromatogram of the control *K. pneumoniae* sample

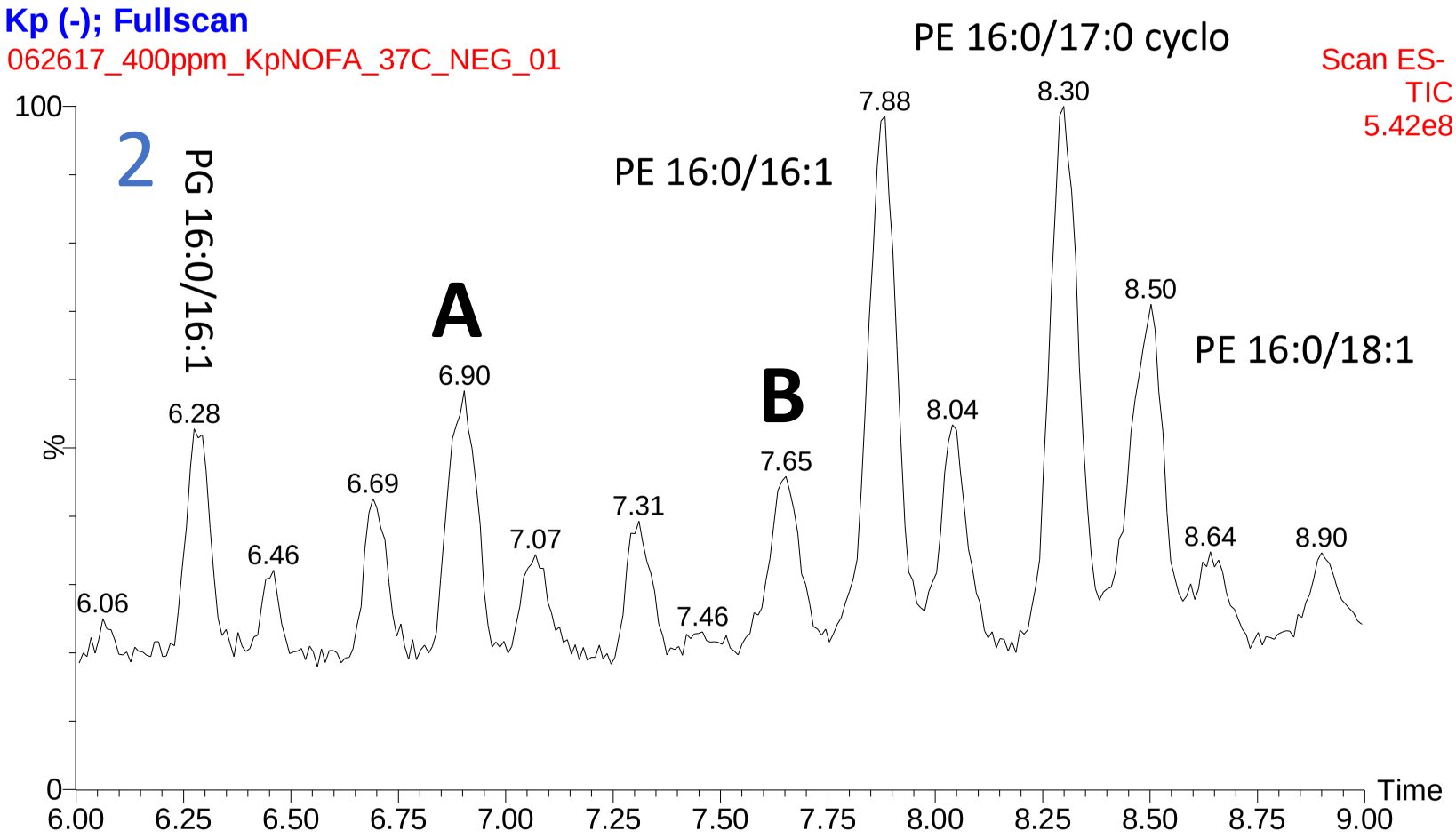

Figure 3.26: The phospholipid region of the control *K. pneumoniae* sample chromatogram

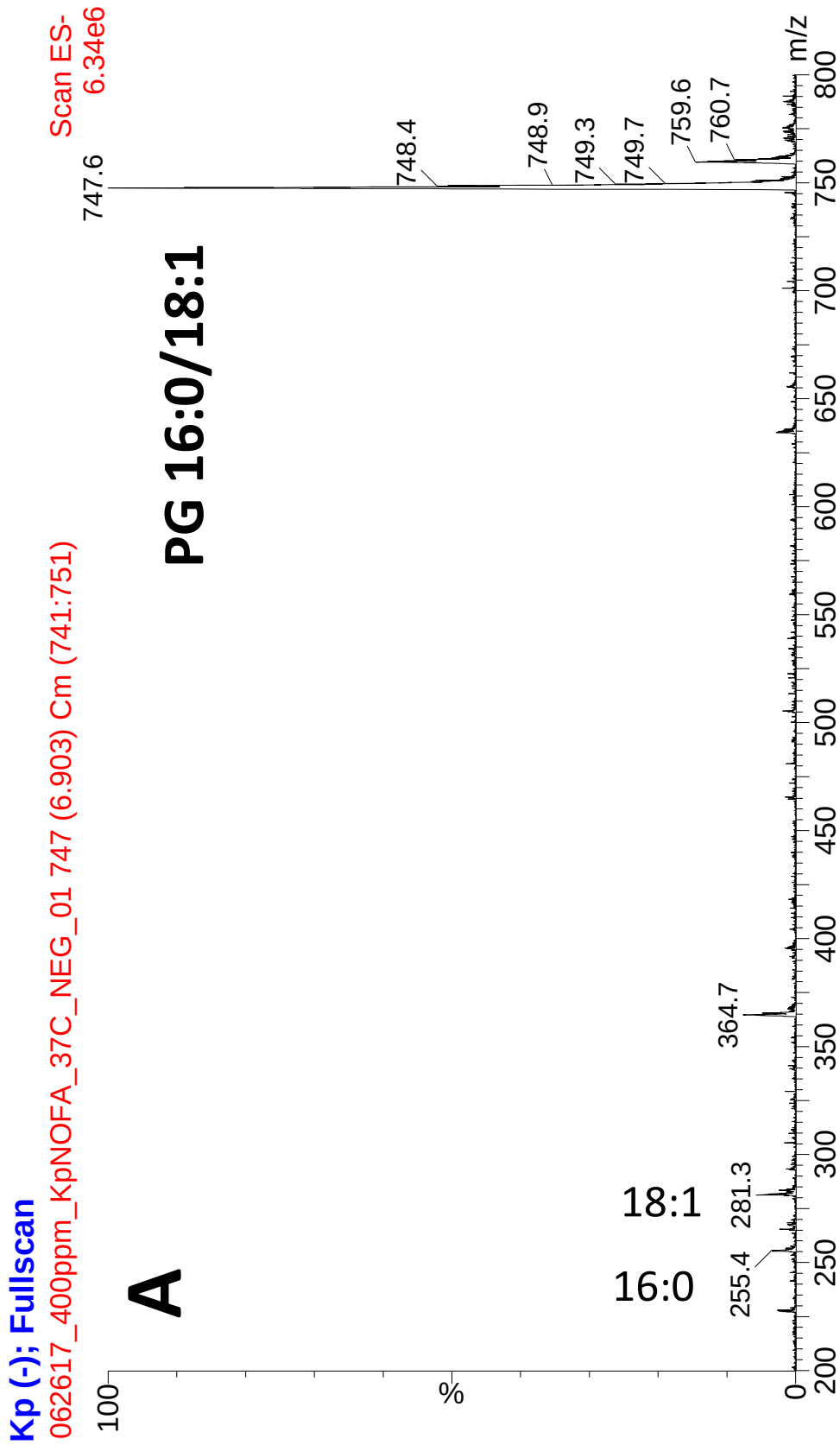

Figure 3.27: The average mass spectrum of peak A in the control *K. pneumoniae* sample chromatogram

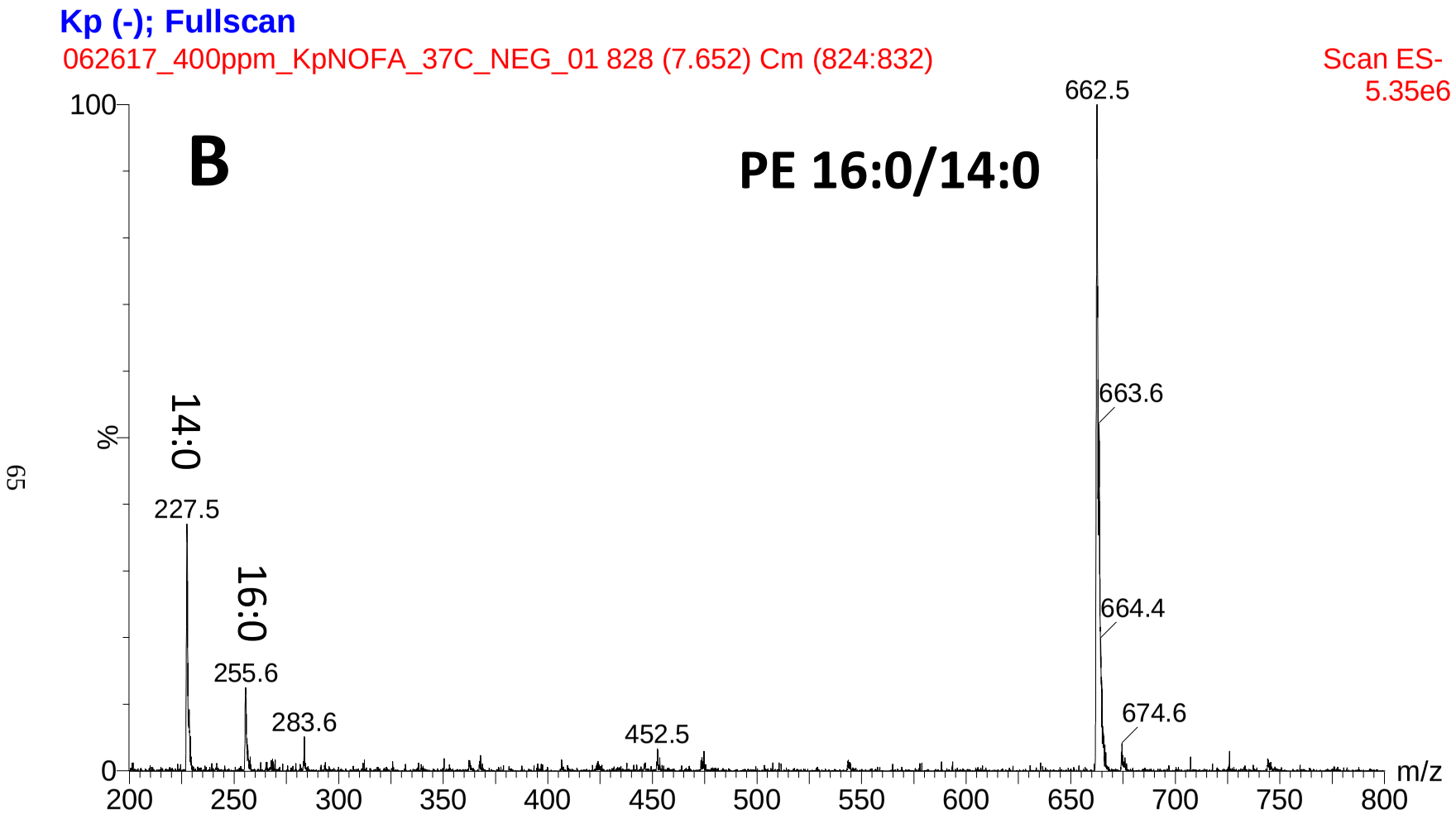

Figure 3.28: The average mass spectrum of peak B in the control *K. pneumoniae* sample chromatogram

The regions labeled as 1 and 2 in the complete chromatogram of the *K. pneumoniae* control sample represent the fatty acid region and the phospholipid region respectively. These distinct regions arise due to the LC gradient used in this experiment and the polarity differences between fatty acids and phospholipids; fatty acids are more polar than phospholipids, and as a result they elute from the C8 reversed-phase column sooner than the phospholipids. The 747.5 m/z peak in the average mass spectrum of chromatogram peak A corresponds to the $[M-H]^-$ ion of PG 16:0/18:1, and the 662.5 m/z peak in the average mass spectrum of chromatogram peak B corresponds to the $[M-H]^-$ ion of PE 16:0/14:0. These identifications were confirmed using the LIPID MAPS database and by the presence of 16:0 and 18:1 cone fragments in the average mass spectrum of chromatogram peak A that correspond to the 255.5 m/z and 281.5 m/z peaks respectively, and the 16:0 cone fragment and 14:0 cone fragment that corresponds to the 227.5 m/z peak in the average mass spectrum of chromatogram peak B. It is important to note that although there is a 283.5 m/z peak in the mass spectrum of chromatogram peak B, it does not correlate to an 18:0 cone fragment originating from the parent PE 16:0/14:0 ion. It is possible that this may reflect a contaminant in the system or, more likely, it may be an 18:0 cone fragment that originated from another lipid that coeluted with the parent ion.

The phospholipid region of the 18:2 *K. pneumoniae* sample chromatogram is presented in Figure 3.29 and the average mass spectra of the 6.51 minute and 8.07 minute chromatogram peaks labeled as A and B respectively are presented in Figures 3.30 and 3.31 respectively.

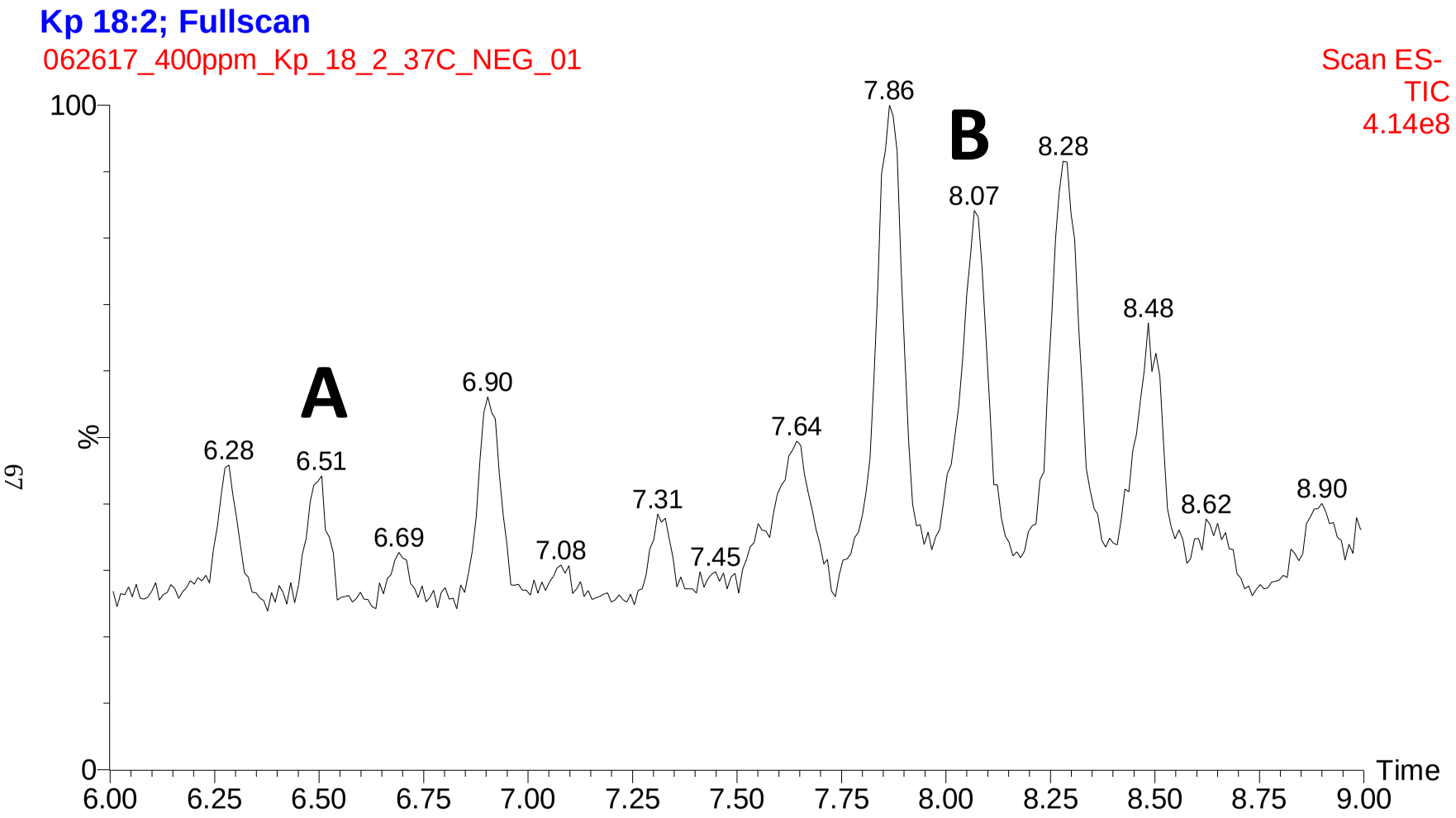

Figure 3.29: The phospholipid region of the 18:2 *K. pneumoniae* sample chromatogram

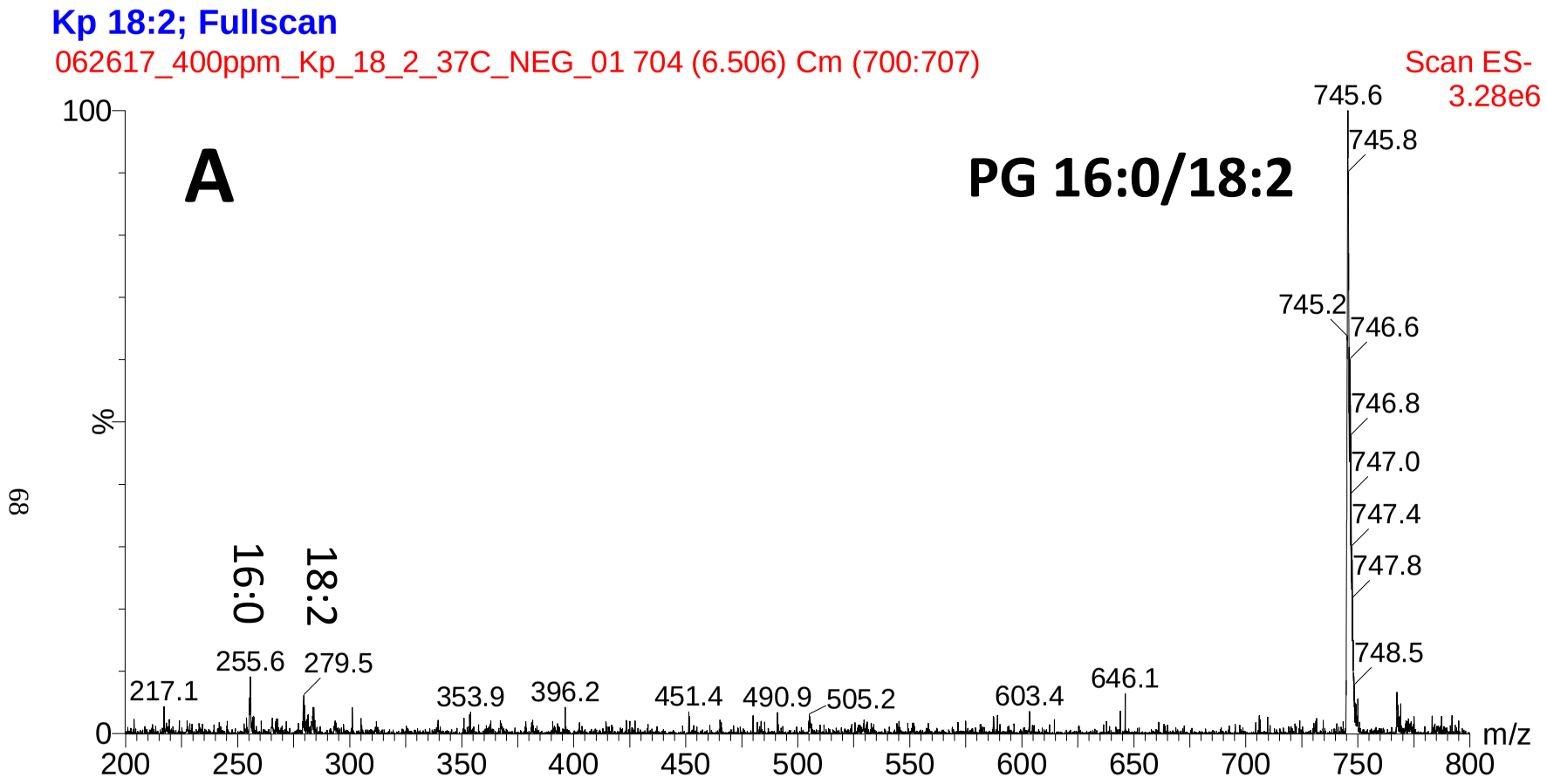

Figure 3.30: The average mass spectrum of peak A in the 18:2 *K. pneumoniae* sample chromatogram

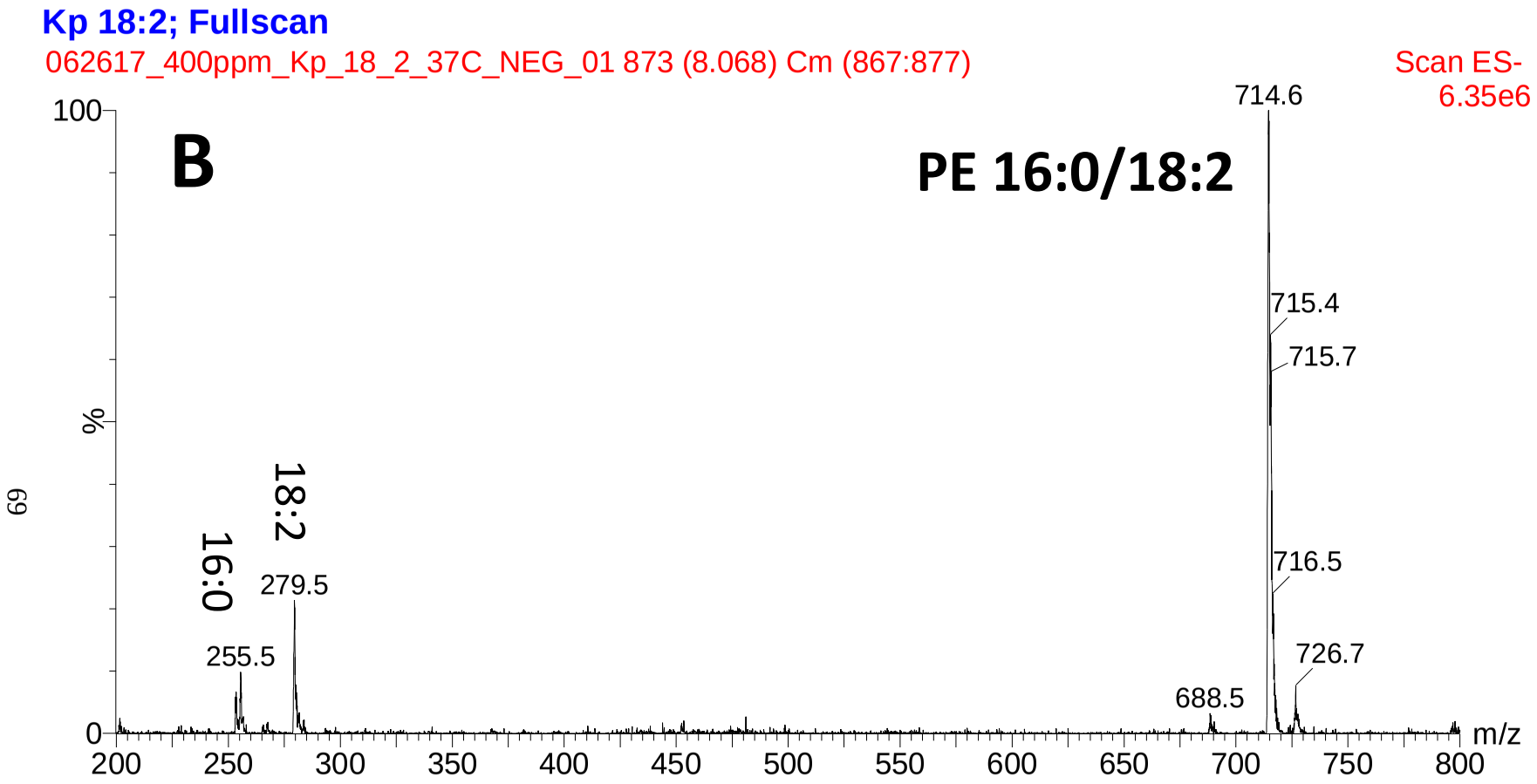

Figure 3.31: The average mass spectrum of peak B in the 18:2 *K. pneumoniae* sample chromatogram

The 745.5 m/z peak in the average mass spectrum of chromatogram peak A corresponds to the $[M-H]^-$ ion of PG 16:0/18:2, and the 714.5 m/z peak in the average mass spectrum of chromatogram peak B corresponds to the $[M-H]^-$ ion of PE 16:0/18:2. These identities were confirmed by referencing the LIPID MAPS database and by noting the presence of the 16:0 and 18:2 cone fragments that correspond to the 255.5 m/z and 279.5 m/z peaks respectively.

The phospholipid region of the 18:3-γ *K. pneumoniae* sample chromatogram is presented in Figure 3.32 and the average mass spectrum of the 7.74 minute chromatogram peak labeled as A is presented in Figure 3.33.

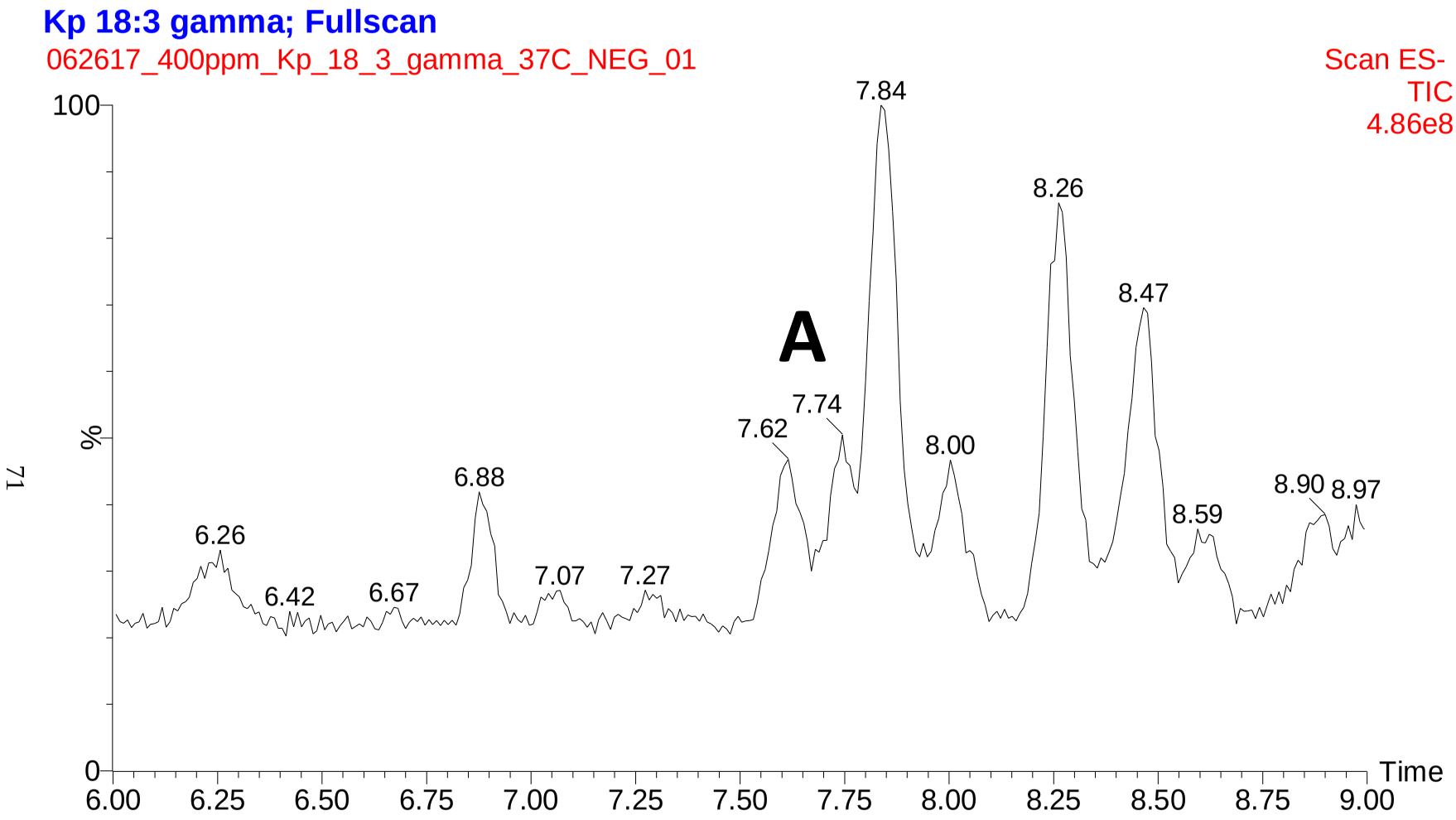

Figure 3.32: The phospholipid region of the 18:3-γ *K. pneumoniae* sample chromatogram

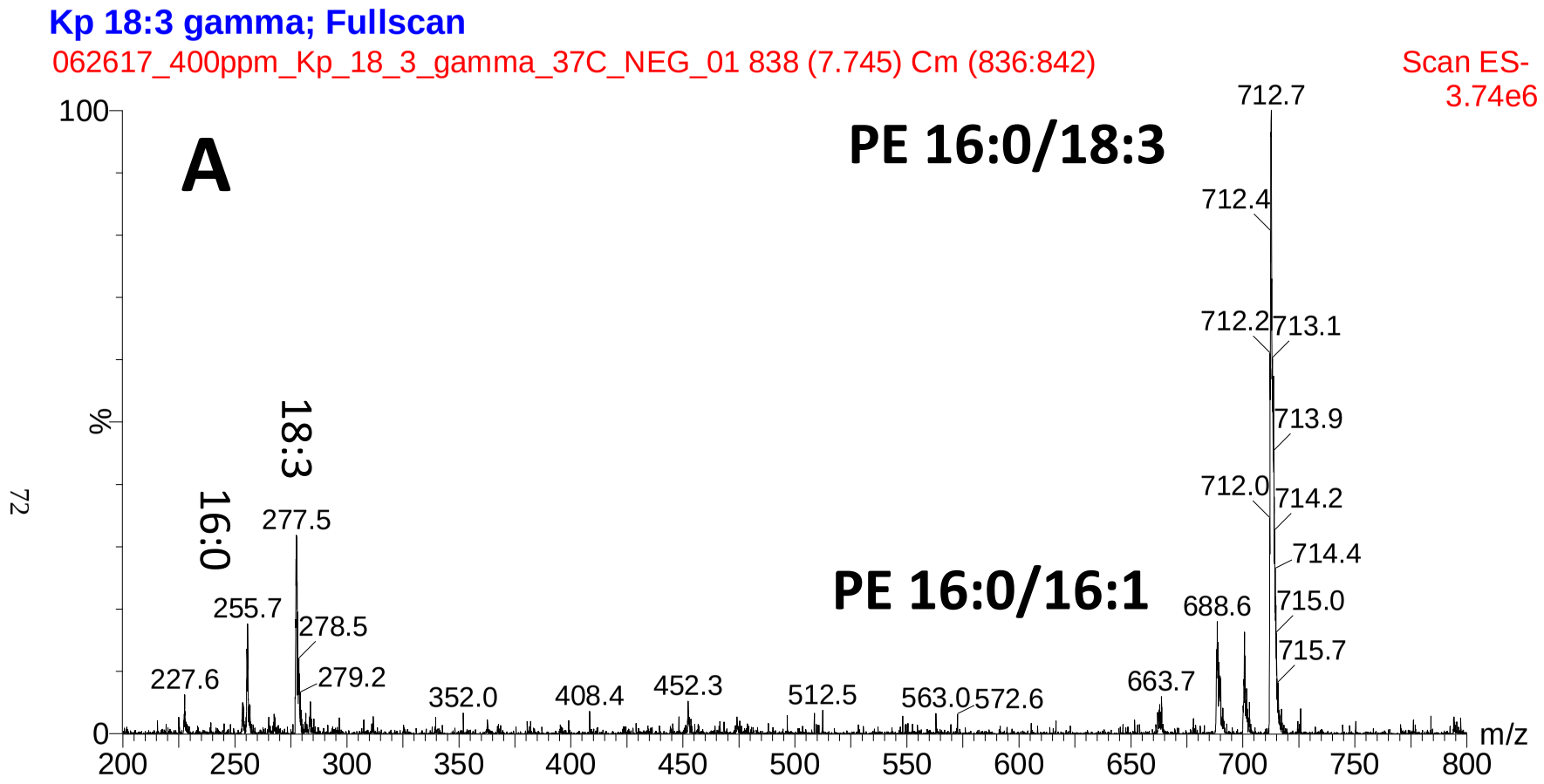

Figure 3.33: The average mass spectrum of peak A in the 18:3-γ *K. pneumoniae* sample chromatogram

The 712.5 m/z peak in the average mass spectrum of peak A corresponds to the $[M-H]^-$ ion of PE 16:0/18:3. This was confirmed by referencing the LIPID MAPS database and by the presence of the 16:0 and 18:3 cone fragments that correspond to the 255.5 m/z and 277.5 m/z peaks respectively. The $[M-H]^-$ ion of PE 16:0/16:1 coeluted with the PE 16:0/18:3 ion, as evidenced by the 688.5 m/z peak. Although a 227.5 m/z peak is present, it does not originate from a 14:0 cone fragment from either of the phospholipid ions represented in this mass spectrum.

The chromatograms and mass spectra of the 18:3-α, 20:3, 20:4, 20:5, and 22:6 *K. pneumoniae* samples are not presented here to avoid excessive repetition. *K. pnuemoniae* was shown to incorporate these PUFAs into its cell membrane via UPLC/MS analysis as well, and phospholipid identifications were confirmed using the same methods described above: referencing the LIPID MAPS database and observing the characteristic cone fragments in the mass spectra for each phospholipid of interest.

Mass filtering was an efficient technique employed in this experiment to show that PUFA-substituted PE and PG species are not natively produced by *K. pneumoniae*. One example of mass filtering in *K. pneumoniae* is shown here. The XICs generated after mass filtering for the m/z value of PE 16:0/20:5 in the control and 20:5 *K. pneumoniae* samples are presented in Figure 3.34.

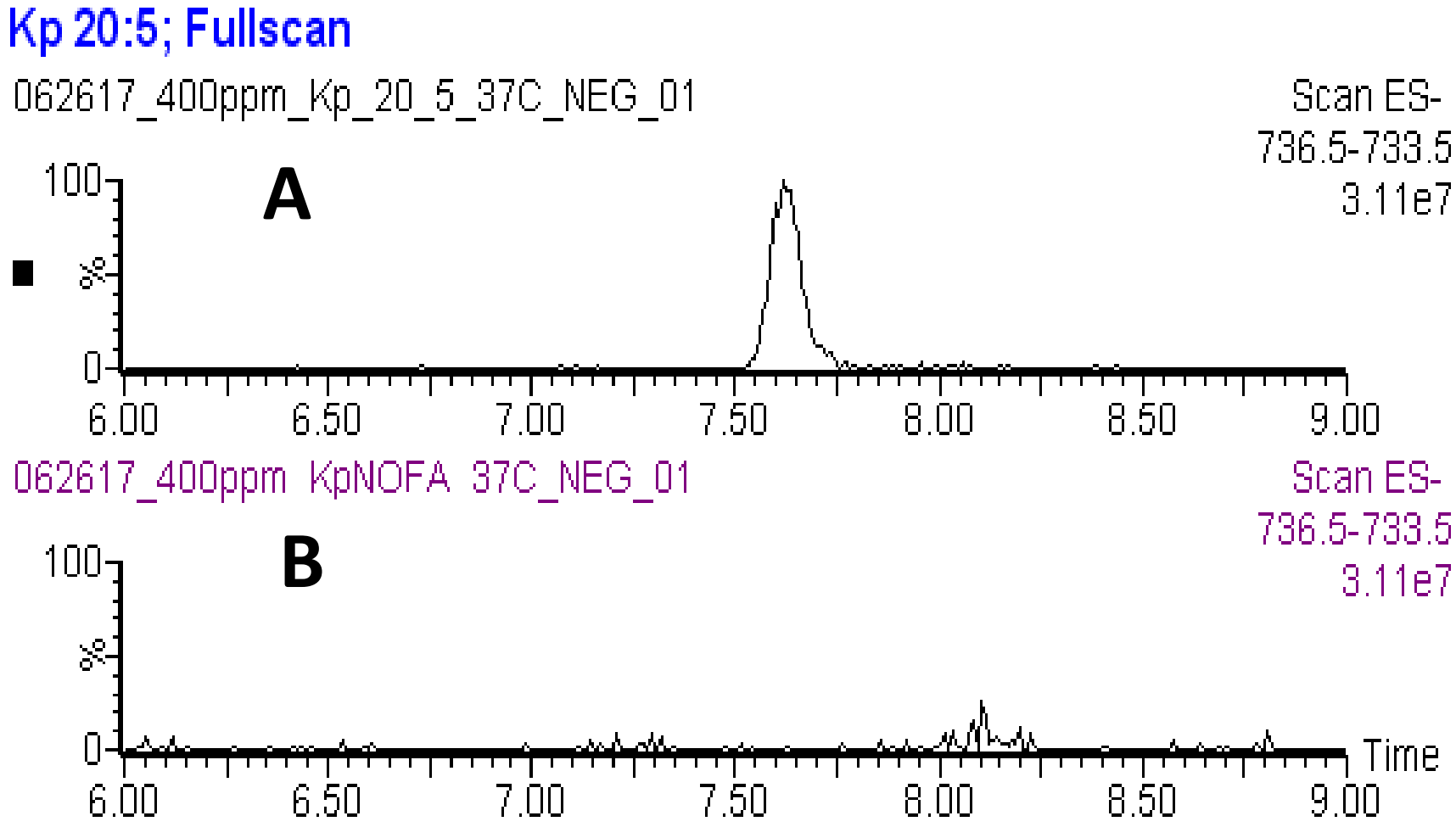

Figure 3.34: The XICs generated after mass filtering for 736.5 m/z in the control and 20:5 *K. pnuemoniae* chromatograms

"A" represents the XIC of the 20:4 *K. pneumoniae* sample after mass filtering for the 736.5 m/z value, and "B" represents the XIC of the control *K. pneumoniae* sample after mass filtering for the 736.5 m/z value. The peak in the XIC of the 20:4 sample corresponds to the $[M-H]^-$ ion of PE 16:0/20:5, showing that *K. pneumoniae* remodeled its cell membrane with 20:5. Only noise peaks are present in the control sample following mass filtering, suggesting that *K. pneumoniae* does not natively make phospholipids possessing 20:5 acyl chains.

3.4 *Escherichia coli* Results

3.4.1 *Escherichia coli* Mass Spectra and Chromatograms

The complete chromatogram of the *E. coli* control sample is presented in Figure 3.35 and the phospholipid region of the chromatogram is presented in Figure 3.36. The average mass spectra of the 6.81 minute and 8.57 minute chromatogram peaks labeled as A and B respectively are presented in Figures 3.37 and 3.38 respectively.

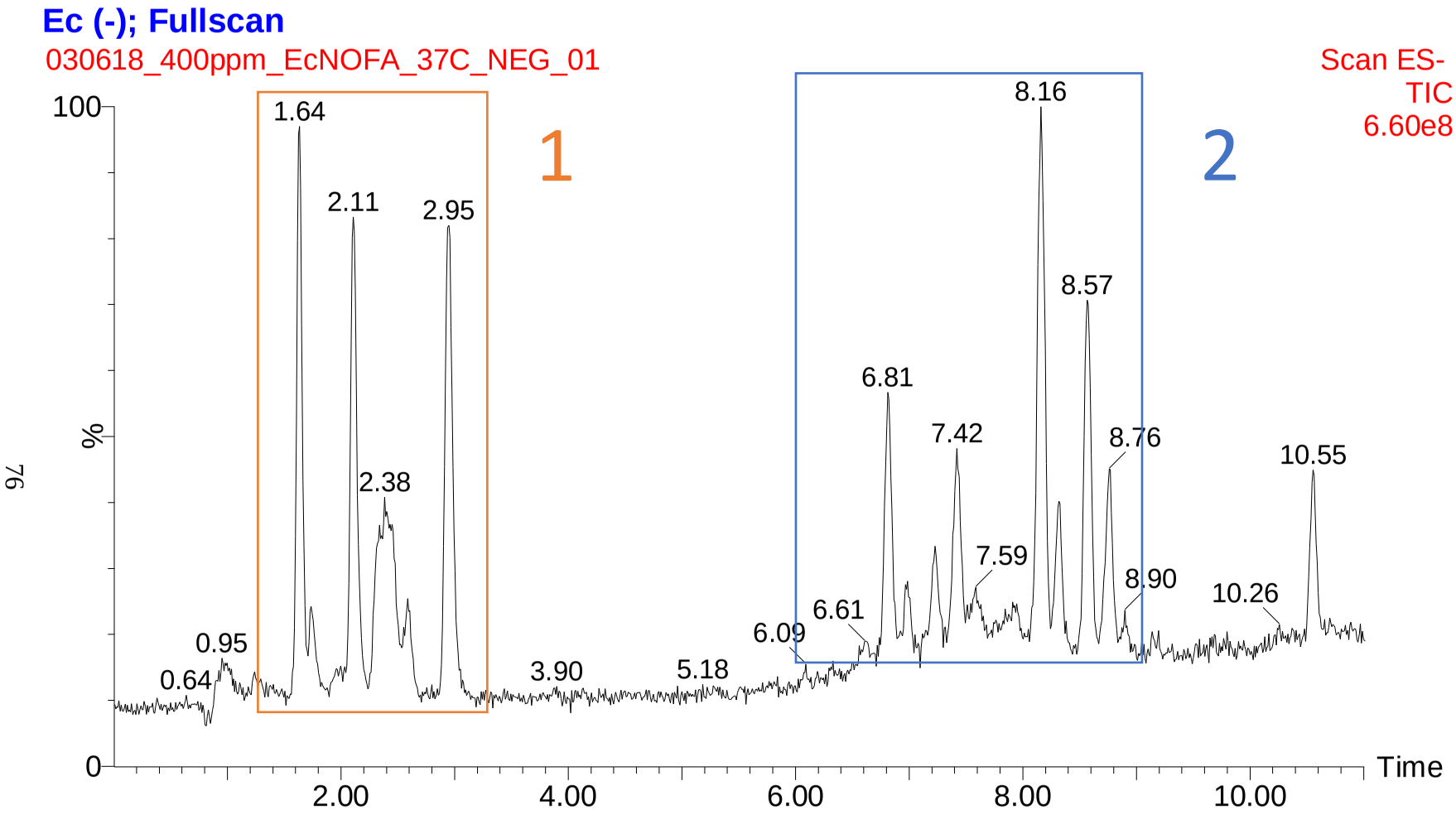

Figure 3.35: The complete chromatogram of the control *E. coli* sample

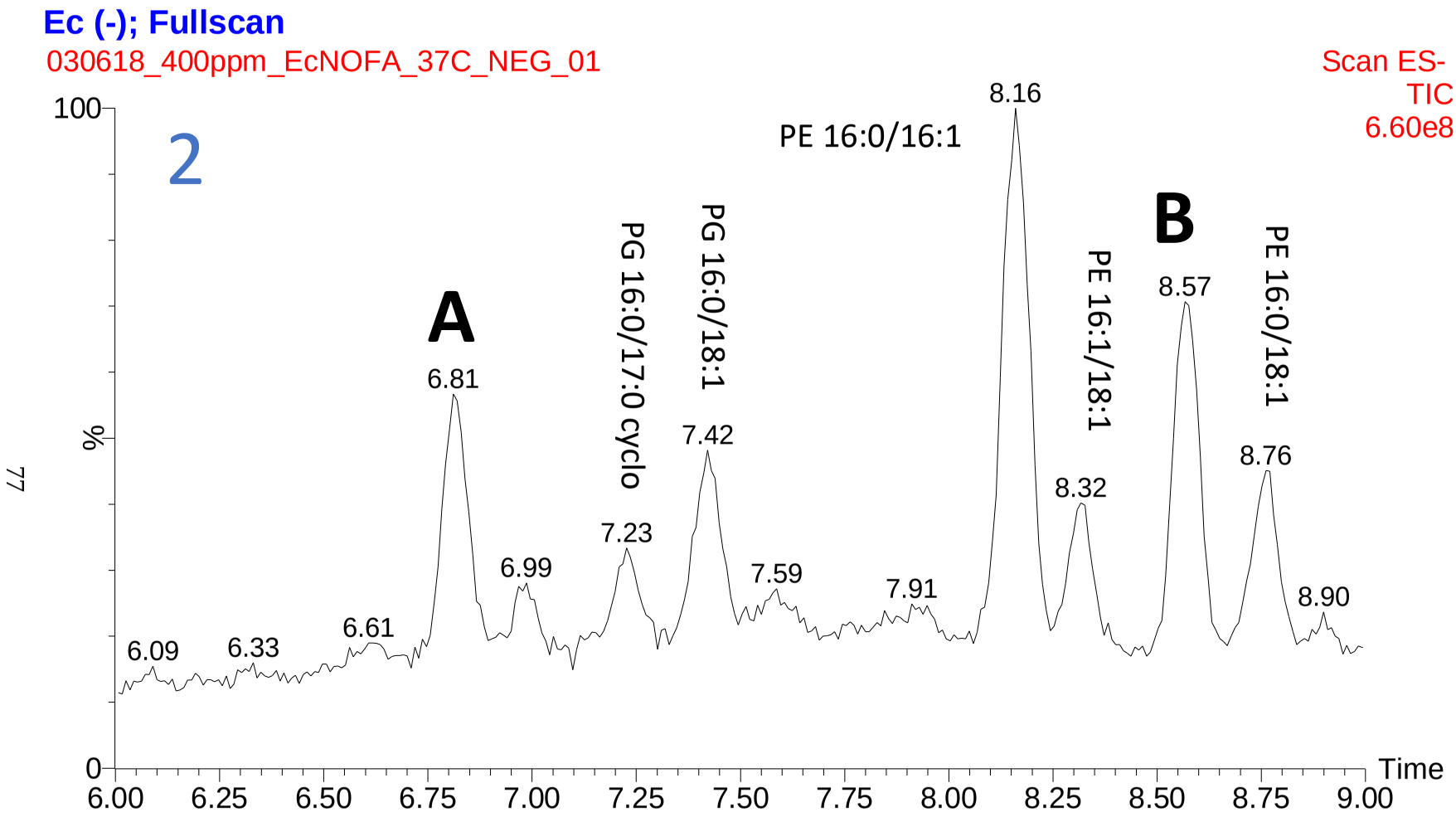

Figure 3.36: The phospholipid region of the control *E. coli* sample chromatogram

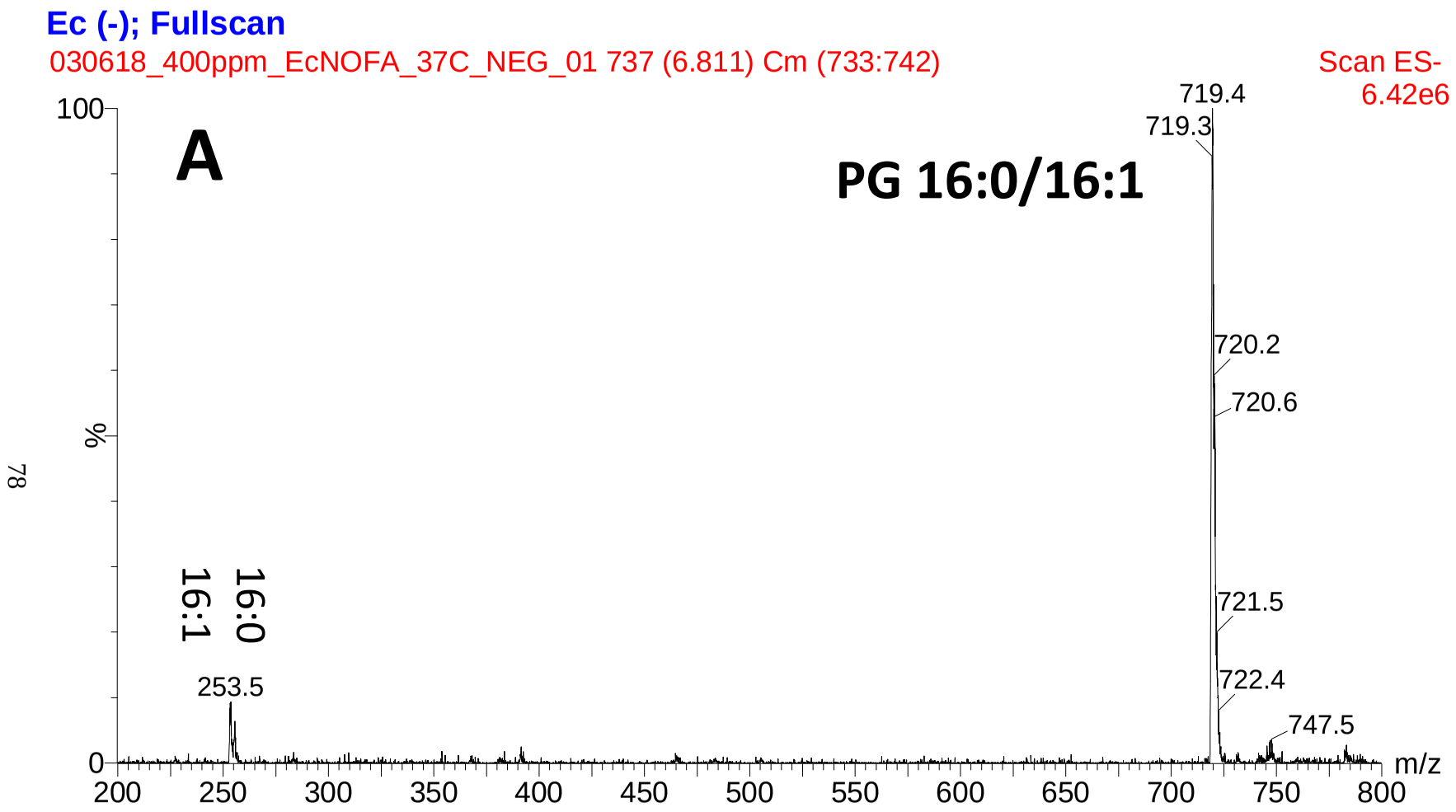

Figure 3.37: The average mass spectrum of peak A in the control *E. coli* sample chromatogram

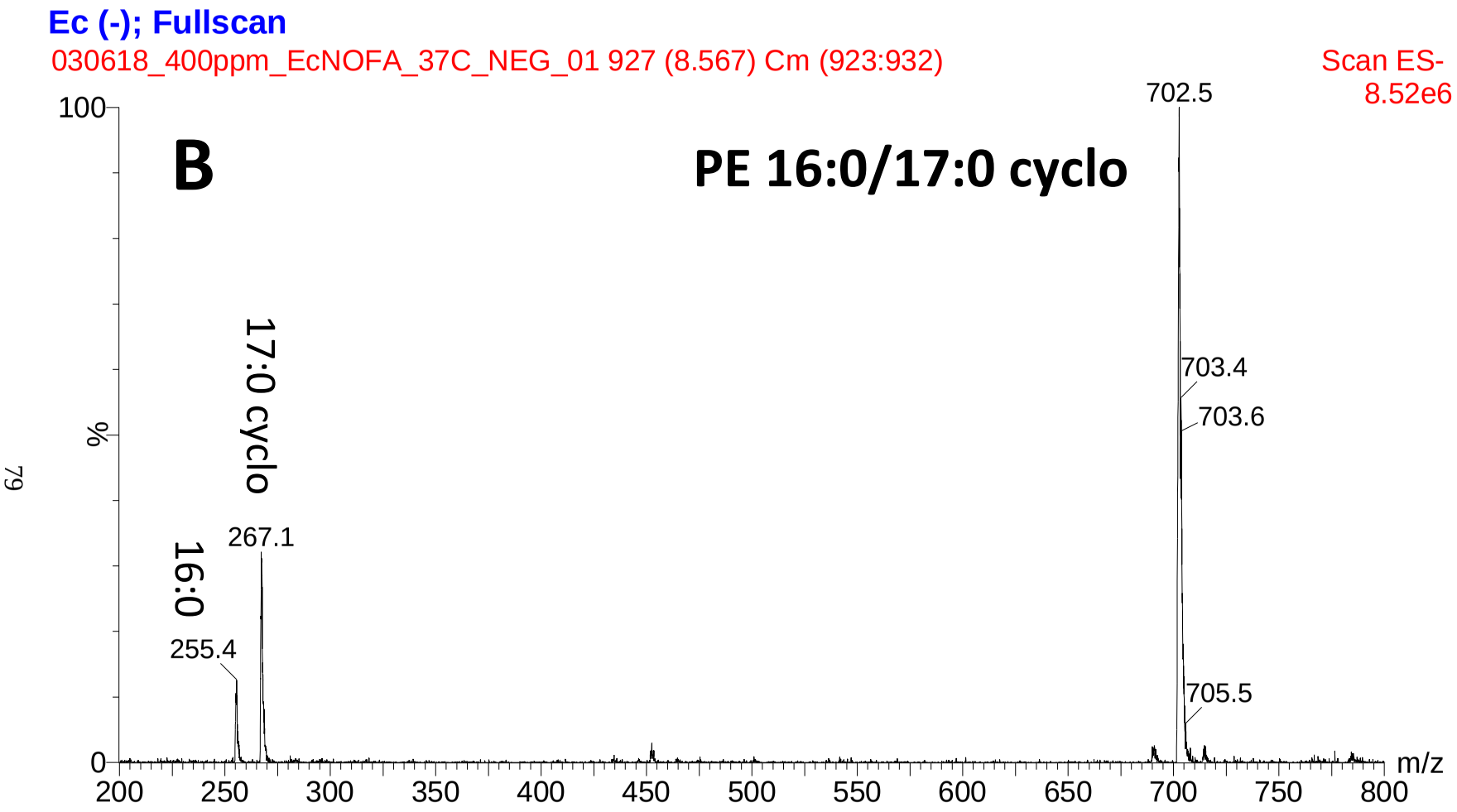

Figure 3.38: The average mass spectrum of peak B in the control *E. coli* sample chromatogram

Region 1 and Region 2 represent the fatty acid region and the phospholipid region of the complete chromatogram, respectively. The 719.5 m/z peak in the average mass spectrum of chromatogram peak A corresponds to the $[M-H]^-$ ion of PG 16:0/16:1. This identification was confirmed using the LIPID MAPS database and by observing the 16:0 and 16:1 cone fragments that correspond to the 255.5 m/z and 253.5 m/z peaks, respectively. These peaks nearly overlap, so only the label for the 16:1 cone fragment peak is displayed since it is more intense than the 16:0 cone fragment peak. The 702.5 m/z peak in the average mass spectrum of chromatogram peak B corresponds to the $[M-H]^-$ ion of PE 16:0/17:0 cyclo. The 16:0 and 17:0 cyclo cone fragments can be observed in the average mass spectrum; the 267.5 m/z peak corresponds to the 17:0 cyclo cone fragment. Further confirmation of this identification was achieved using the LIPID MAPS database.

The phospholipid region of the 18:2 *E. coli* chromatogram is presented in Figure 3.39, and the average mass spectra of the 7.01 minute and 8.34 minute chromatogram peaks labeled as A and B respectively are presented in Figures 3.40 and 3.41 respectively.

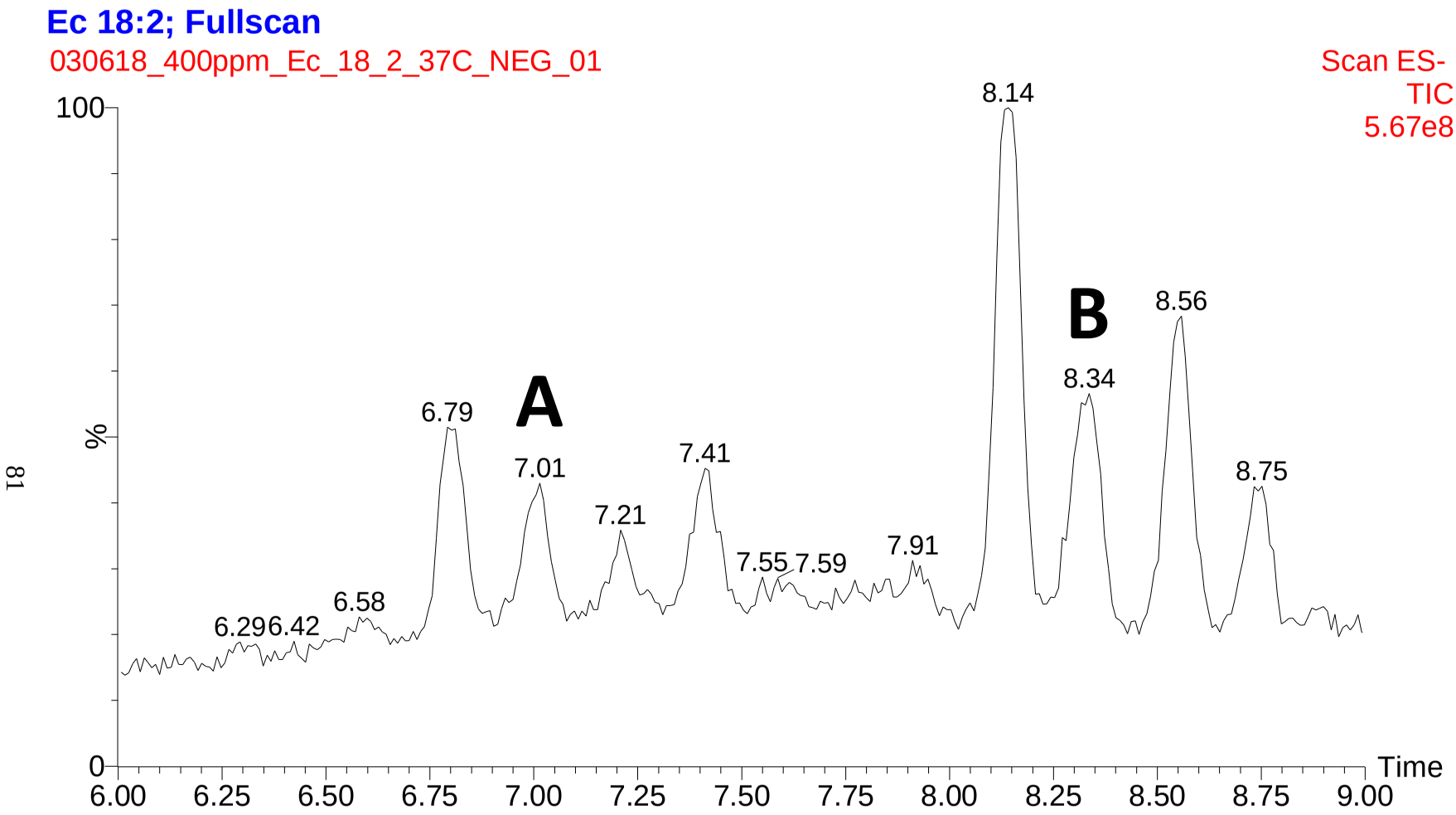

Figure 3.39: The phospholipid region of the 18:2 *E. coli* sample chromatogram

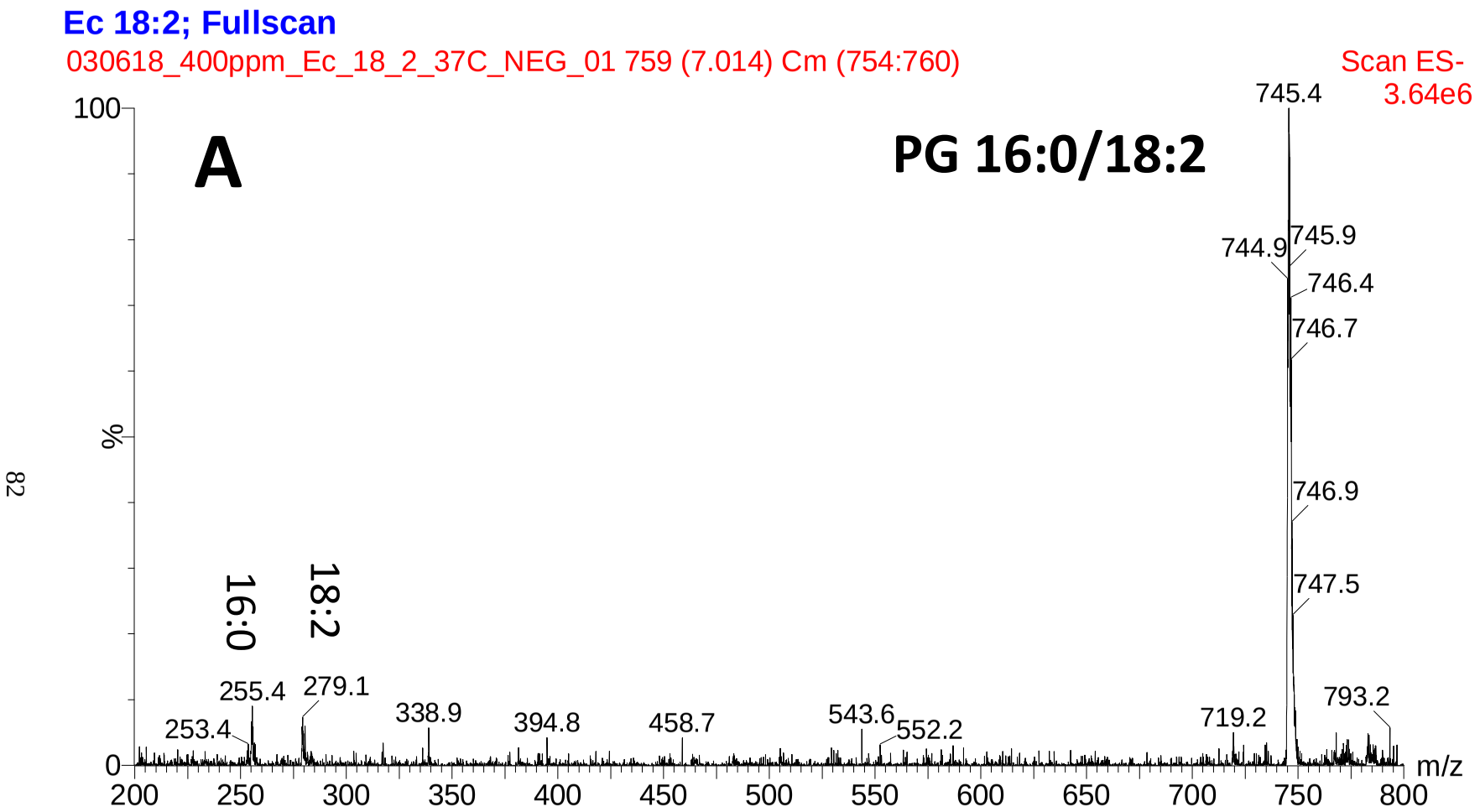

Figure 3.40: The average mass spectrum of peak A in the 18:2 *E. coli* sample chromatogram

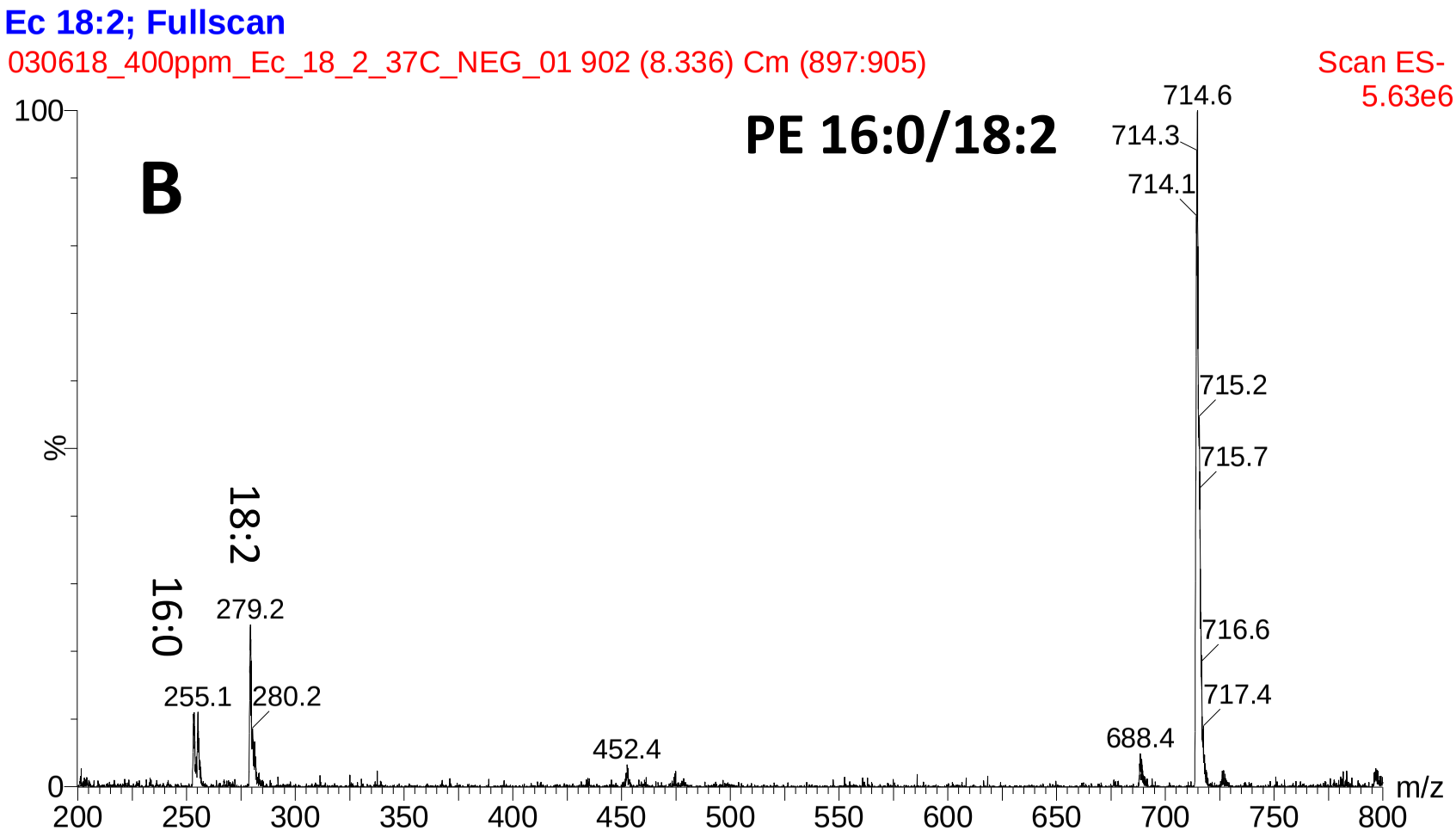

Figure 3.41: The average mass spectrum of peak B in the 18:2 *E. coli* sample chromatogram

The 745.5 m/z peak in the average mass spectrum of chromatogram peak A corresponds to the $[M-H]^-$ ion of PG 16:0/18:2, which was confirmed by the LIPID MAPS database and by the presence of the 16:0 and 18:2 cone fragments that correspond to the 255.5 m/z and 279.5 m/z peaks respectively. The 714.5 m/z peak in the average mass spectrum of chromatogram peak B corresponds to the $[M-H]^-$ ion of PE 16:0/18:2. This identity was confirmed using the same technique described above for PG 16:0/18:2.

The phospholipid region of the 20:4 *E. coli* sample chromatogram is presented in Figure 3.42 and the average mass spectrum of the 8.23 minute chromatogram peak labeled as A is presented in Figure 3.43.

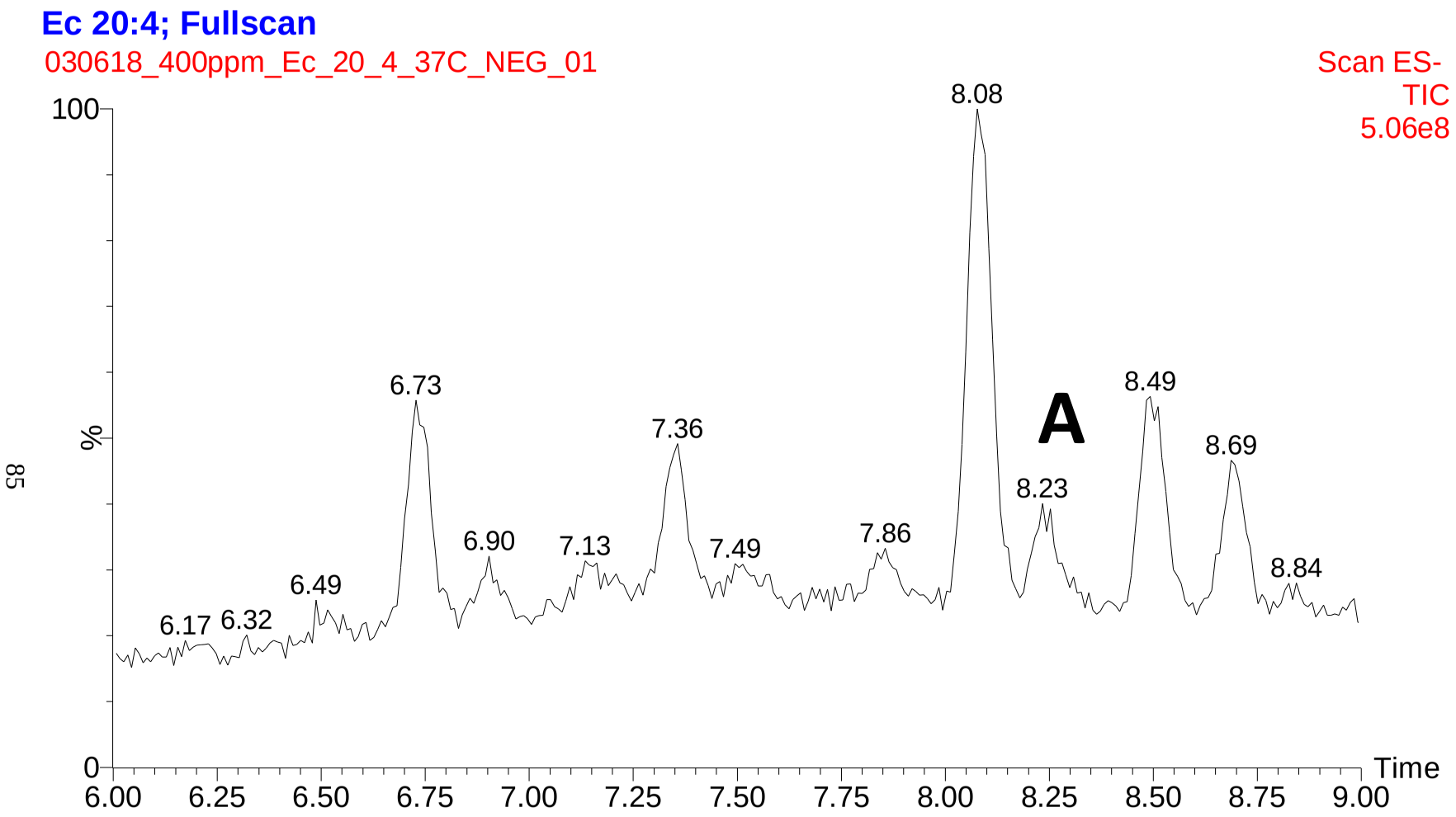

Figure 3.42: The phospholipid region of the 20:4 *E. coli* sample chromatogram

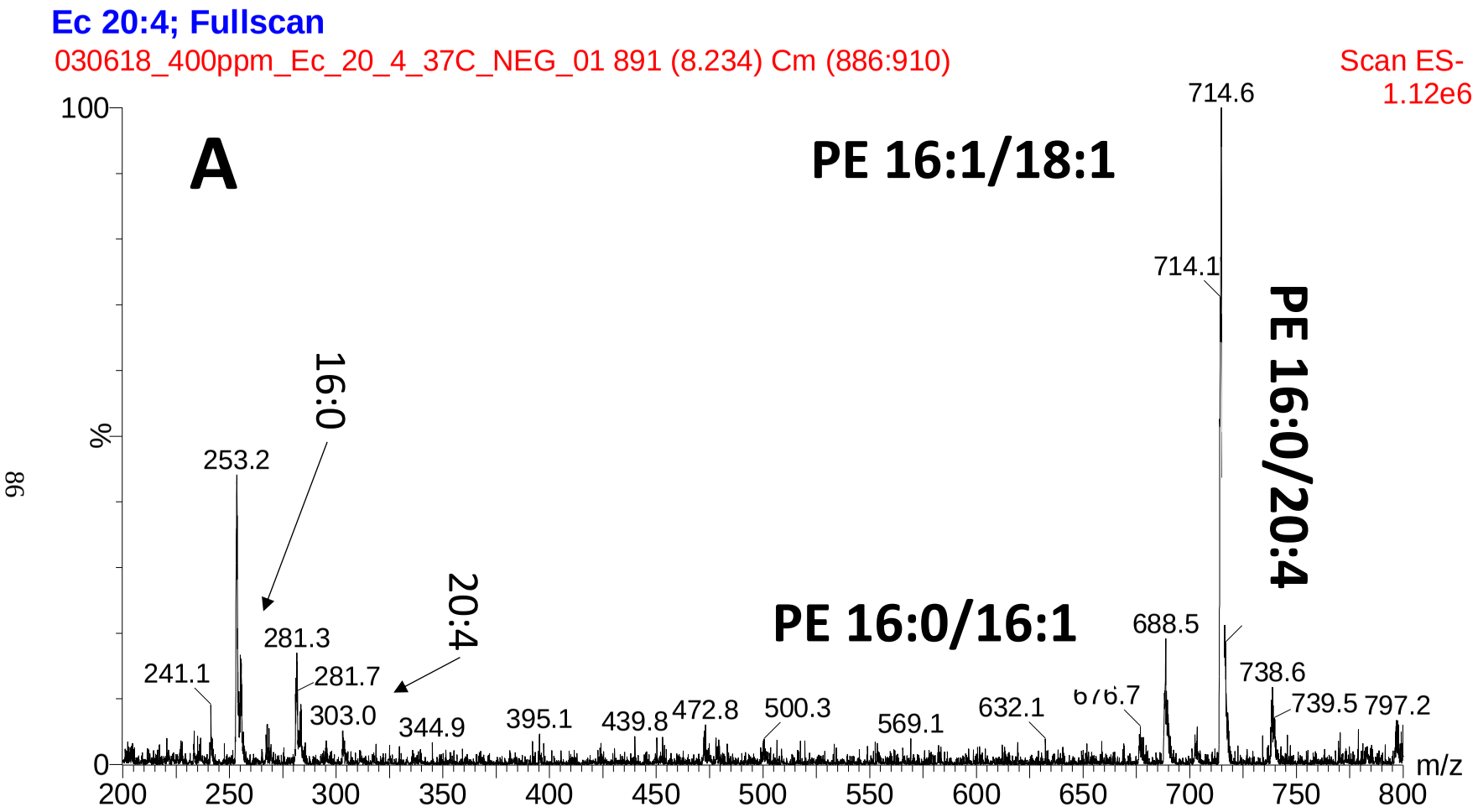

Figure 3.43: The average mass spectrum of peak A in the 20:4 *E. coli* sample chromatogram

The 738.5 m/z peak in the average mass spectrum of chromatogram peak A represents the signal of the $[M-H]^-$ ion of PE 16:0/20:4. This identification was confirmed by the LIPID MAPS database and by the presence of the 16:0 and 20:4 cone fragments that correspond to the 255.5 m/z and 303.5 m/z peaks respectively. The 738.5 m/z peak is not the dominant peak in this mass spectrum, possibly reflecting the limited capability of *E. coli* to undergo membrane remodeling with exogenous PUFAs. The $[M-H]^-$ ions of PE 16:1/18:1 and PE 16:0/16:1 coeluted with the $[M-H]^-$ ion of PE 16:0/20:4. This is shown in the mass spectrum by the 714.5 m/z and 688.5 m/z peaks and the abundant 16:1 and 18:1 cone fragments that correspond to the 253.5 m/z and 281.5 m/z peaks respectively.

Although *E. coli* was shown to remodel its cell membrane with the exogenous PUFAs 18:3-α, 18:3-γ, 20:3, and 20:5 via UPLC/MS analysis, the chromatograms and mass spectra for the *E. coli* cultures grown in the presence of these PUFAs are not presented to avoid excessive repetition. Interestingly, *E. coli* was shown to be incapable of remodeling its cell membrane with 22:6 following UPLC/MS analysis. This will be discussed further in Chapter 4.

The technique of mass filtering was employed to show that phospholipids possessing any of the PUFAs used in this experiment are not natively found in the cell membranes of *E. coli* cells. One example of mass filtering in the *E. coli* samples is shown here. The XICs generated after mass filtering for the m/z value of PE 16:0/18:3 in the control and 18:3-α *E. coli* samples are presented in Figure 3.44.

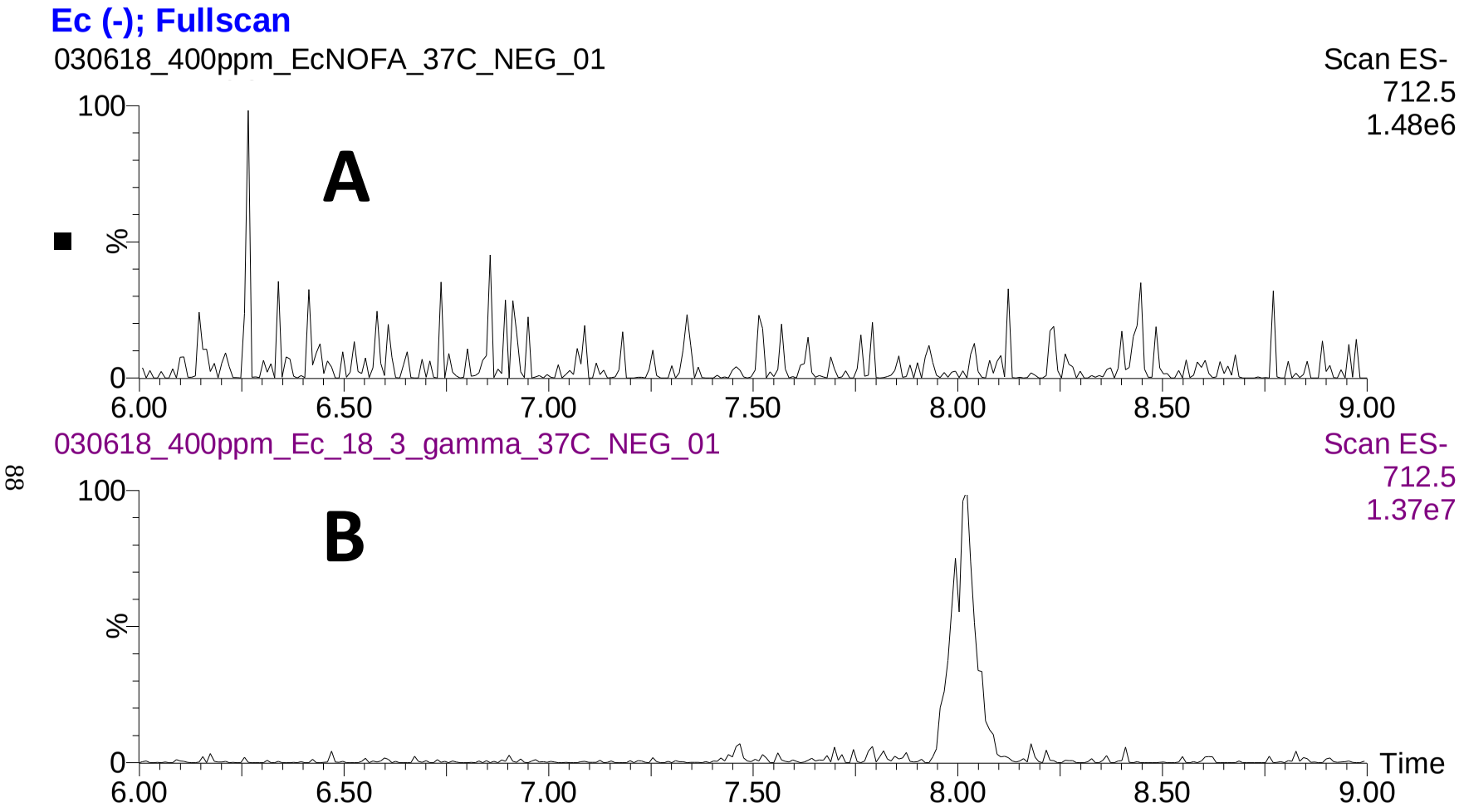

Figure 3.44: The XICs generated after mass filtering for 712.5 m/z in the control and 18:3-α *E. coli* chromatograms

"A" represents the XIC generated after mass filtering for 712.5 m/z in the *E. coli* sample grown in the absence of PUFAs, and "B" represents the XIC generated after mass filtering for 712.5 m/z in the *E. coli* sample grown in the presence of 18:3-α. Only noise peaks are present in the XIC of the control sample. The large peak in the XIC of the 18:3-α sample corresponds to the $[M-H]^-$ ion of PE 16:0/18:3. This shows that *E. coli* does not natively produce phospholipids with 18:3-α acyl chains, but it is capable of remodeling its cell membrane with 18:3-α following exposure to it. Mass filtering was performed on the other PUFA-exposed *E. coli* samples and showed similar results (except for the culture exposed to 22:6).

3.4.2 *Escherichia coli* Motility Results

E. coli cultures were grown in M9 minimal medium to roughly OD_{600} 0.9, pelleted, washed with PBS, resuspended in PBS, and diluted to roughly OD_{600} 1.0. A volume of 2 µL of the diluted culture was injected into the center of each quadrant of each motility plate that had been prepared. Eight motility plates were prepared, one containing no PUFA and the other seven containing one of the seven PUFAs used in this experiment. The plates were incubated for 12 hours at 37 °C. Following this incubation period, the diameter of the motility halo in each quadrant of each plate was measured. The measurements from each plate were averaged together and the standard deviations were calculated. The average swimming motility of the *E. coli* culture on each plate is presented in Figure 3.45 and the standard deviations are represented by the error bars.

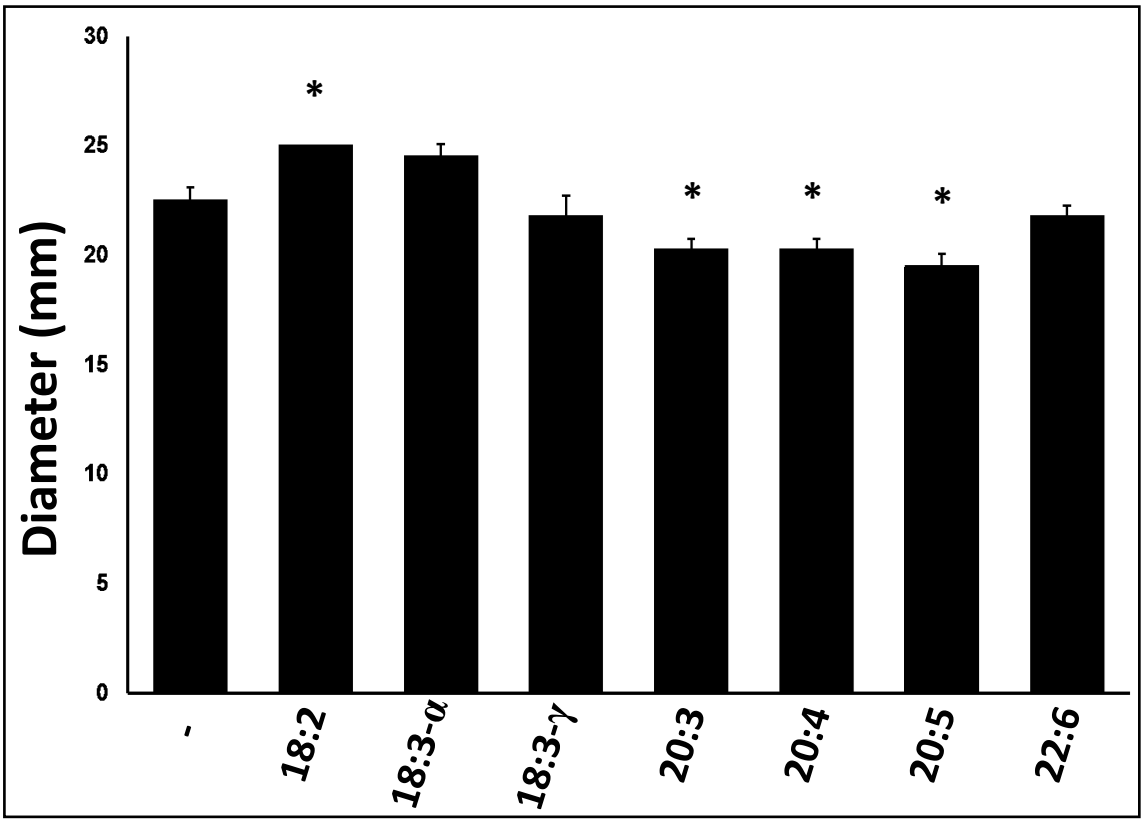

Figure 3.45: The motility of *E. coli* cells following PUFA exposure. Asterisks indicate significant deviations in motility from the control sample ($\alpha = 0.01$, $p < 0.01$).

The *E. coli* cells grown in the presence of 18:2 exhibited significantly ($p < 0.01$) higher swimming motility than the control cells. The 20:3, 20:4, and 20:5 samples exhibited significantly lower levels of swimming motility than the control sample.

3.4.3 *Escherichia coli* Permeability Results

E. coli cultures were grown in M9 minimal medium at 37 °C in either the presence or absence of exogenous PUFAs to roughly OD_{600} 0.8. The cultures were pelleted, washed with PBS, and resuspended in PBS. The hydrophobic compound crystal violet (CV) was added to each of the cultures to yield a final concentration of 5 µg/mL. The cultures were agitated at 50 rpm, and a 1 mL aliquot was removed from each of the cultures in 5 minute increments to be centrifuged. Following centrifugation, the supernatant of each culture was spectrophotometrically measured at a wavelength of 590 nm to determine the percentage of CV in the supernatant of each culture; these percentages were used to determine the percentage of CV taken up by each culture. A control sample containing CV but no *E. coli* culture was included in this experiment to allow for normalization of the data. The percentage of CV taken up by each culture over a 20 minute time period is presented in Figure 3.46.

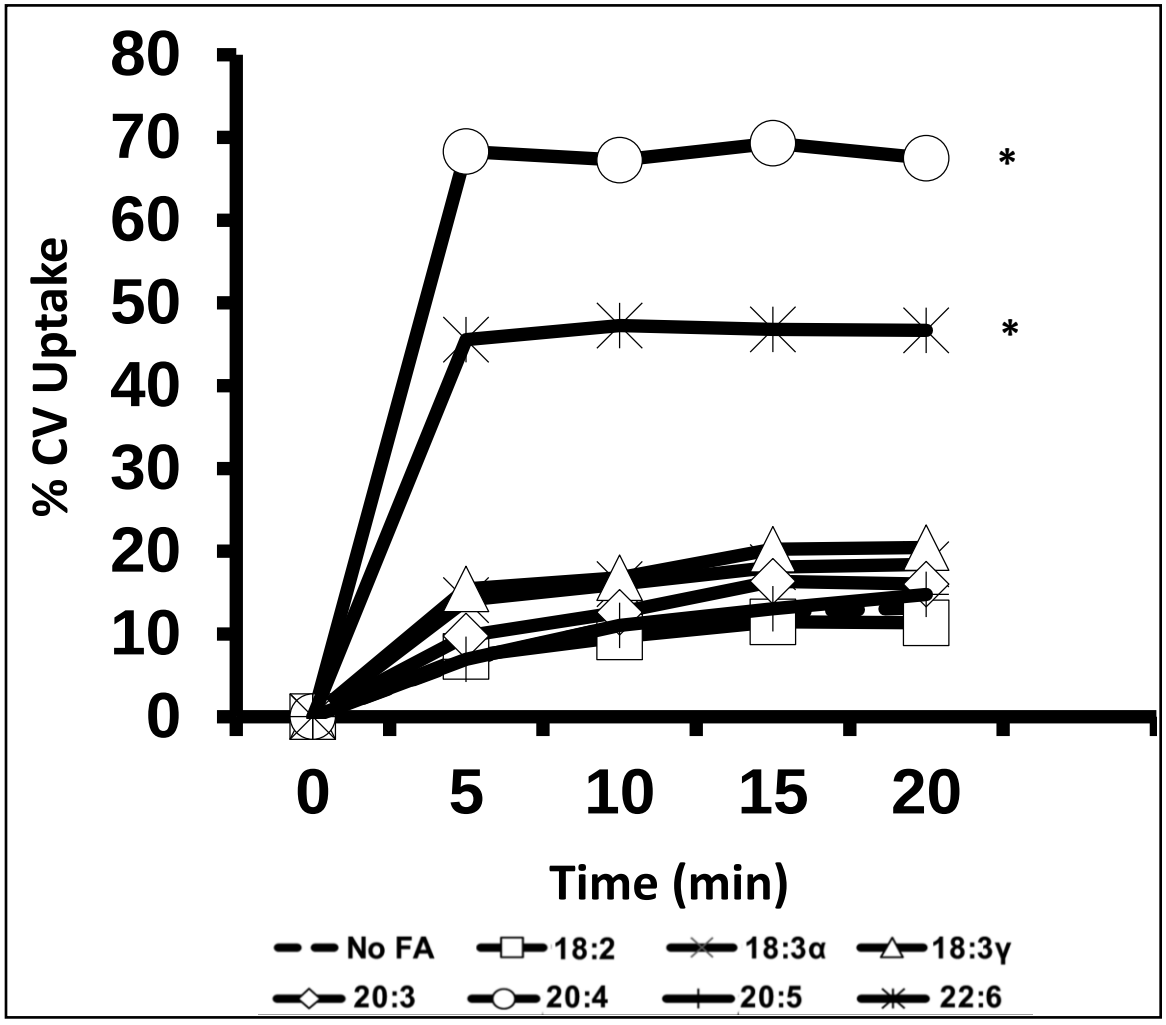

Figure 3.46: The % CV uptake of *E. coli* cells following PUFA exposure. Asterisks indicate significant deviations in membrane permeability from the control sample ($\alpha = 0.002$, $p < 0.002$).

The *E. coli* cells grown in the presence of 20:4 and 22:6 exhibited significantly ($p < 0.002$) greater permeability to CV than the culture grown in the absence of PUFAs, which is indicated by the asterisks. The culture grown in the presence of 20:4 demonstrated the greatest permeability to CV out of all of the cultures used in this assay.

Similar growth conditions were used for the ethidium bromide (EtBr) uptake assay. EtBr was added to each of the samples to yield a final concentration of 5 μg/mL. The cultures were agitated at 50 rpm, and a 1 mL aliquot was removed from each culture in 5 minute

increments to be pelleted via centrifugation. The supernatants were measured fluorimetrically using an excitation wavelength of 530 nm, an emission wavelength of 585 nm, and a slit width of 20 nm. A control containing EtBr but no *E. coli* cells was included to allow for normalization of the data and was measured using an excitation wavelength of 420 nm. The average fluorescence intensities of three biological replicates for each of the *E. coli* cultures are presented in Figure 3.47.

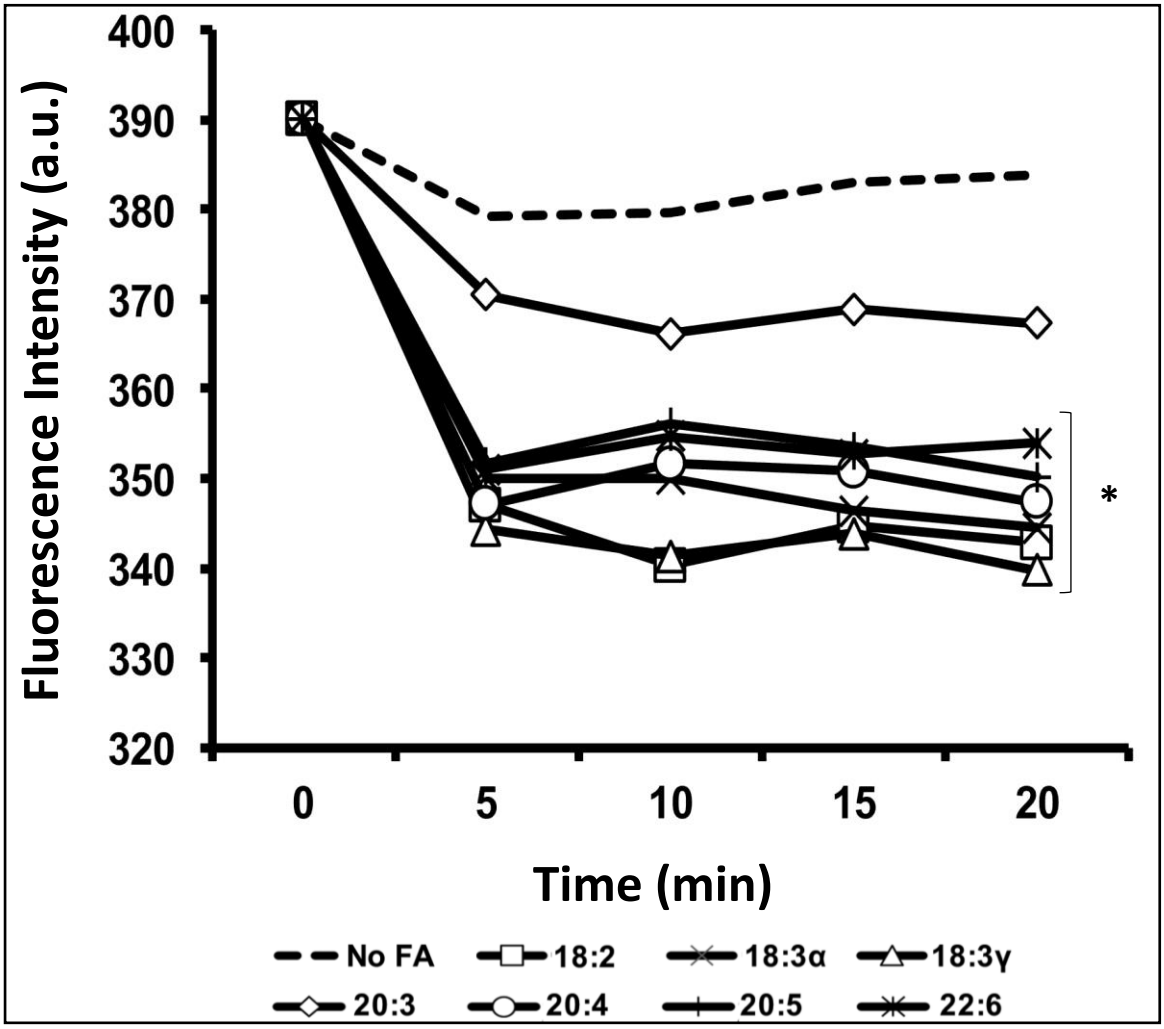

Figure 3.47: The fluorescence intensities of *E. coli* cells following PUFA exposure. Asterisks indicate significant deviations in membrane permeability from the control sample ($\alpha = 0.002$, $p < 0.002$).

The average fluorescence intensities measured over the 20 minute period of each *E. coli* culture grown in the presence of a particular PUFA were lower than the control. This indicates that each of the seven PUFAs used in this assay increased the permeability of the cell membrane to EtBr, with 18:3-γ increasing permeability the most. The average fluorescence intensities of the *E. coli* cultures grown in the presence of 18:2, 18:3-α, 18:3-γ, 20:4, 20:5, and 22:6 were all significantly ($p < 0.002$) different from the average fluorescence intensities of the *E. coli* culture grown in the absence of PUFAs.

3.4.4 *Escherichia coli* Biofilm Formation Results

E. coli cultures were prepared in 96-well microtiter plates containing M9 minimal medium supplemented with casamino acids (CM9) and either one of the seven exogenous PUFAs used in this experiment or no exogenous PUFAs. The cultures were inoculated onto the plates in octuplet and incubated for 24 hours at 37 °C to allow for biofilm formation within the wells. A volume of 125 µL of a 3 % crystal violet solution was added to each of the wells, and following a short incubation period, 125 µL of a 30 % acetic acid solution was added to each well to solubilize the crystal violet. The solubilized crystal violet was transferred to a fresh 96-well microtiter plate and absorbance measurements were made at 550 nm with a Biotek Synergy microplate reader. The results of the biofilm assay are presented in Figure 3.48.

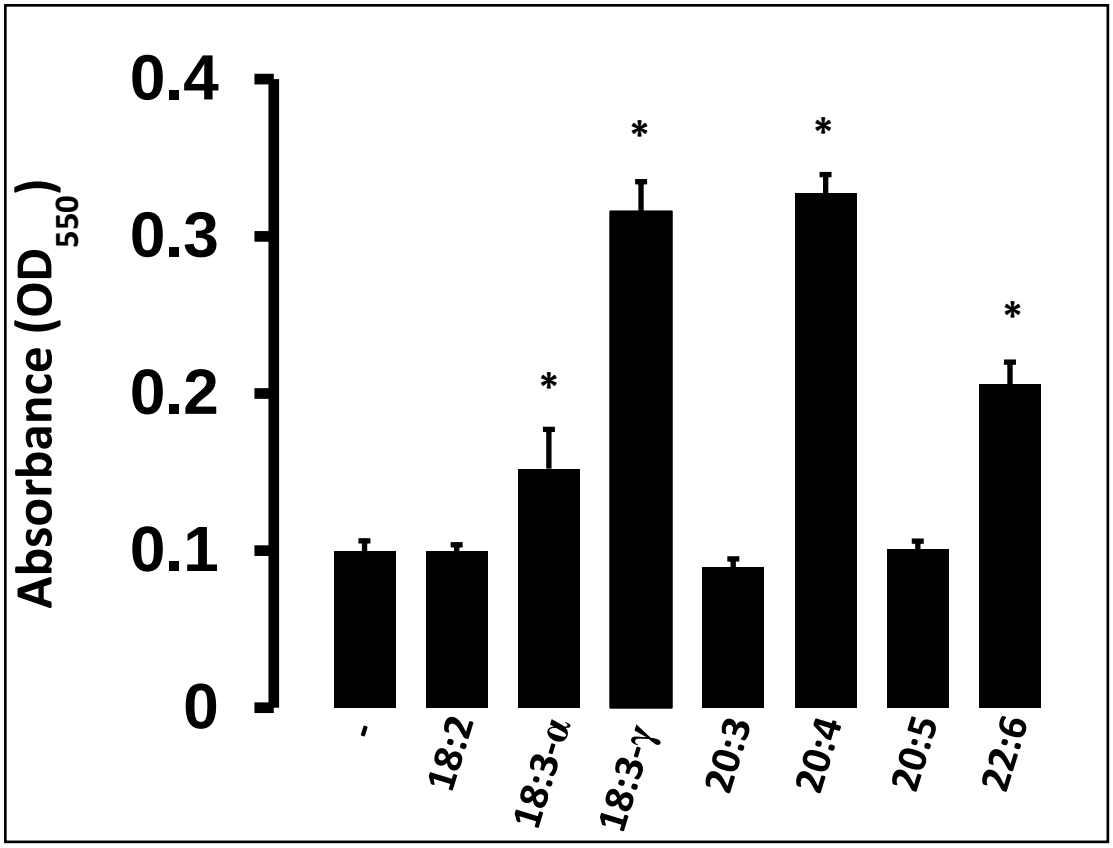

Figure 3.48: *E. coli* biofilm formation following PUFA exposure. Asterisks indicate significant deviations in biofilm formation from the control sample ($\alpha = 0.002$, $p < 0.002$).

The absorbance values for each of the samples are reported as the average absorbance of three biological replicates and the standard deviations are represented by the error bars. The asterisks indicate the 18:3-α, 18:3-γ, 20:4, and 22:6 samples displayed significantly different ($p < 0.002$) biofilm formation from the control sample. This was determined after performing a student's t-test. Therefore, 18:3-α, 18:3-γ, 20:4, and 22:6 appear to increase biofilm formation in *E. coli*, and the greatest increases were observed in the 20:4 and 22:6 samples. The other PUFAs used in this assay did not significantly alter biofilm formation in *E. coli*.

3.4.5 *Escherichia coli* Antimicrobial Peptide Susceptibility Results

E. coli cultures were grown to approximately OD_{600} 0.9 in M9 minimal medium supplemented with casamino acids and either 300 µM of one of the seven PUFAs or no PUFAs. The cultures were pelleted, washed with CM9, resuspended in CM9, and diluted to OD_{600} 0.1. Using two 96-well microtiter plates, each of the *E. coli* samples were exposed to increasing concentrations of the antimicrobial peptide colistin in triplicate and incubated at 37 °C for 20 hours in an enclosed shaker. Following this incubation period, the plates were spectrophotometrically assessed at 600 nm using a Biotek Synergy microplate reader. The average absorbance values of the three biological replicates for each *E. coli* culture grown in the presence of different colistin concentrations are presented in Figure 3.49.

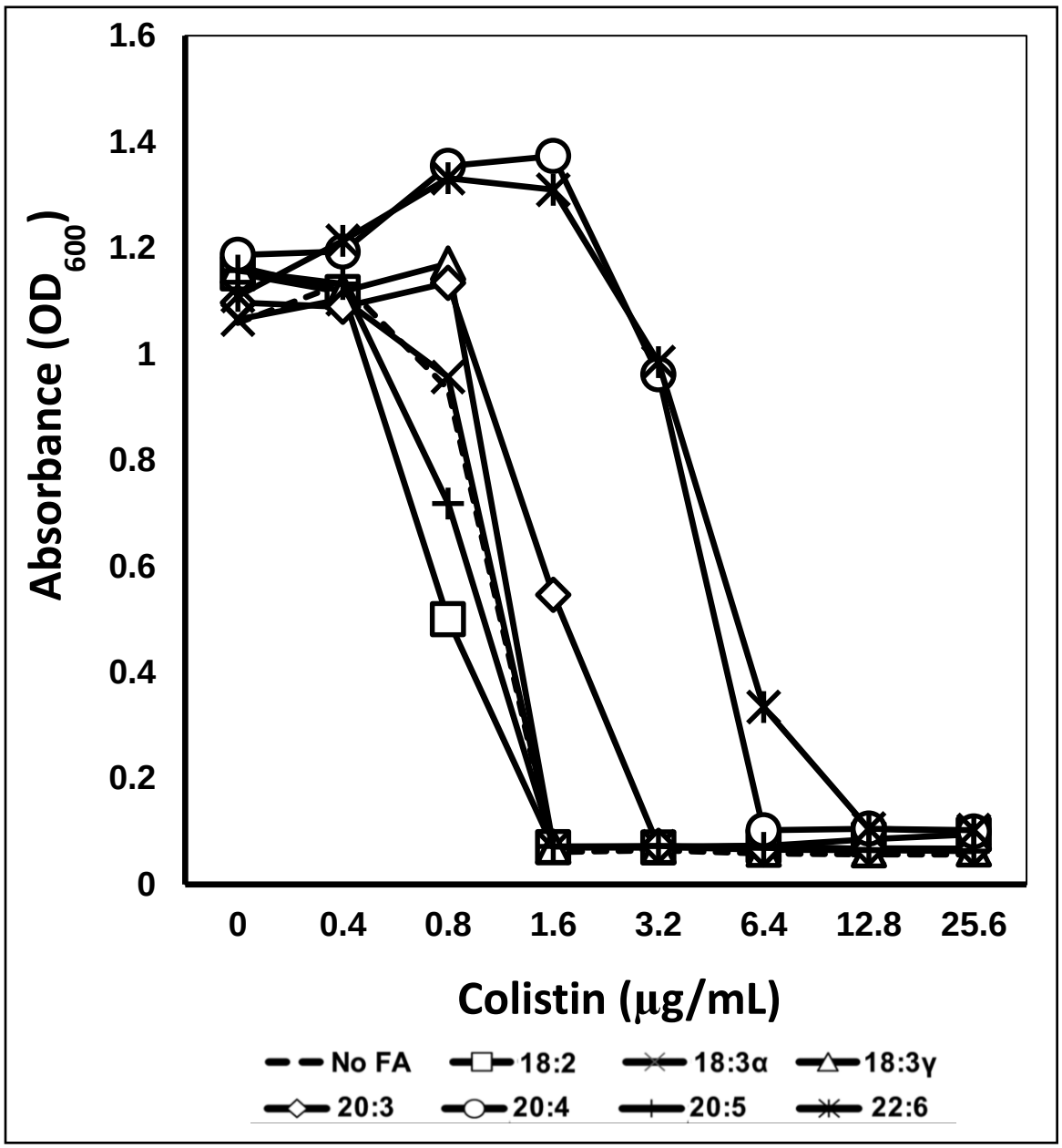

Figure 3.49: The colistin susceptibility of *E. coli* cells following PUFA exposure

The *E. coli* samples grown in the presence of 20:4 and 22:6 increased the resistance of *E. coli* to colistin at each concentration compared to the culture that was grown in the absence PUFAs. The *E. coli* cultures grown in the presence of 18:2 and 20:5 were more susceptible to colistin than the culture grown in the absence of PUFAs at concentrations

greater than 0.4 µg/mL. The *E. coli* cultures grown in the presence of 20:4 and 22:6 displayed significantly (two-fold MIC) different susceptibility to colistin than the control sample at all concentrations greater than 0.4 µg/mL. The *E. coli* cultures grown in the presence of 20:5 and 18:2 displayed significantly different susceptibility to colistin than the control sample at a concentration of 0.8 µg/mL, and the culture grown in the presence of 20:3 displayed significantly different susceptibility to colistin than the control at a concentration of 1.6 µg/mL.

A similar assay was performed using the cAMP polymyxin B. The average absorbance values of the three biological replicates for each *E. coli* culture grown in the presence of different polymyxin B concentrations are presented in Figure 3.50.

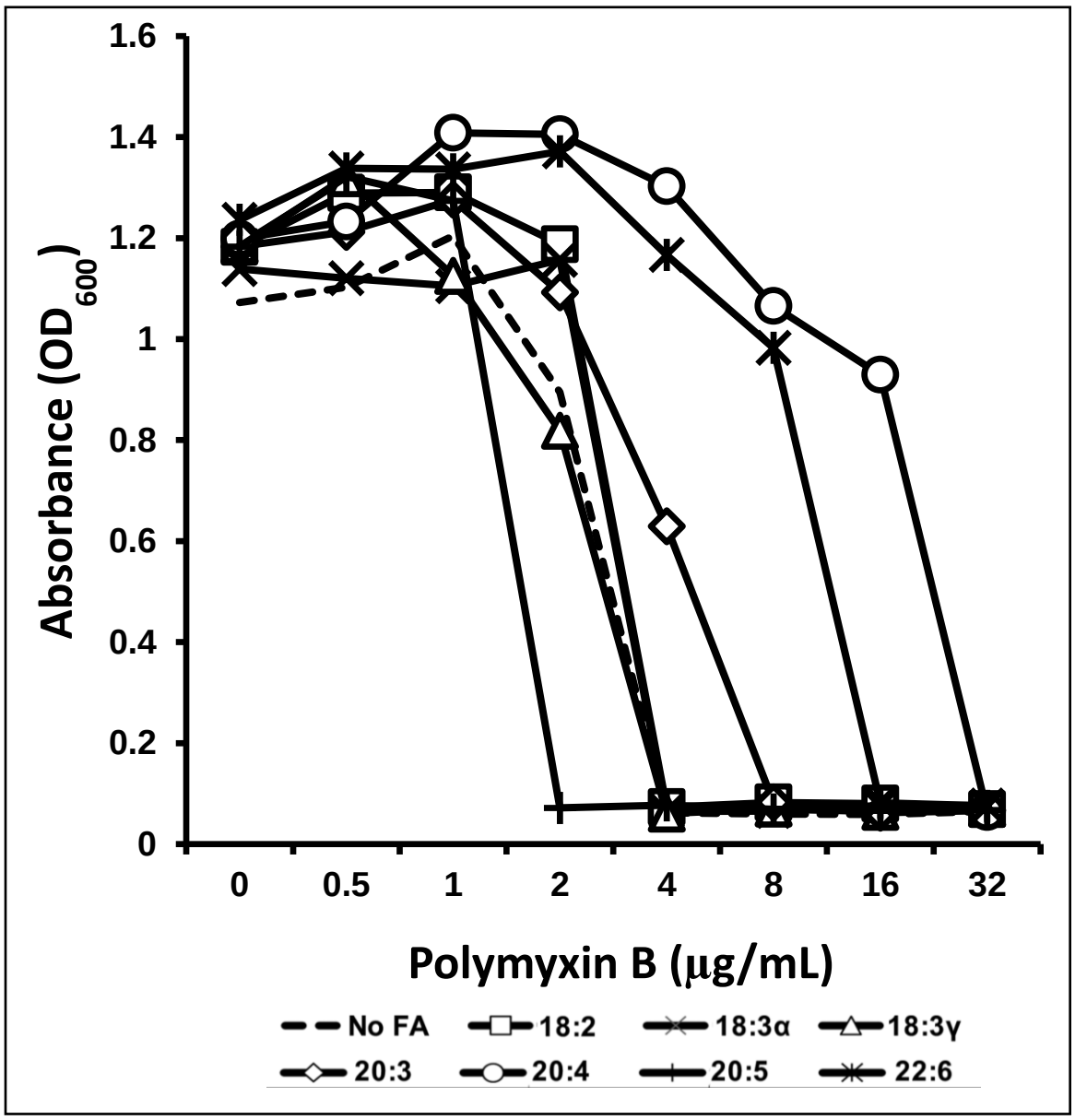

Figure 3.50: The polymyxin B susceptibility of *E. coli* cells following PUFA exposure

The *E. coli* samples grown in the presence of 18:2, 20:3, 20:4, and 22:6 increased the resistance of *E. coli* to polymyxin B at all concentrations tested. The cultures grown in 20:4 and 22:6 increased the resistance to *E. coli* the most at concentrations greater than 0.5 µg/mL; the 20:4 culture showed growth at a concentration of 16 µg/mL when all

other samples demonstrated no growth at that concentration. The 20:4 and 22:6 samples displayed significantly (two-fold MIC) higher resistance to polymyxin B compared to the control sample at concentrations of 2 µg/mL, 4 µg/mL, and 8 µg/mL; 22:6 also displayed significantly different growth at the concentration of 16 µg/mL. The 20:5 sample displayed significantly lower resistance to polymyxin B from the control sample at a concentration of 2 µg/mL, and the 20:3 sample displayed significantly higher resistance to polymyxin B compared to the control at a concentration of 4 µg/mL.

CHAPTER FOUR

4. Discussion

4.1 Discussion and Future Direction

Multi-drug resistant bacteria have become a major concern for public well-being, particularly in health care facilities housing numerous immunocompromised individuals. Nosocomial infection rates have increased over the past few decades along with the advent of MDR bacteria, resulting in the need for novel techniques or outright treatments to deal with these bacteria. Rather than investigating novel antimicrobial agents as treatments for MDR bacteria, the research presented in this thesis focused on polyunsaturated fatty acids (PUFAs) as potential vectors for MDR bacteria treatment; the PUFAs were not hypothesized to be treatments themselves, but rather to induce phenotypic changes in the bacteria that influence survivability and virulence. The PUFAs used were linoleic acid (18:2), α-linolenic acid (18:3-α), γ-linolenic acid (18:3-γ), dihomo-γ-linolenic acid (20:3), arachidonic acid (20:4), eicosapentaenoic acid (20:5), and docosahexaenoic acid (22:6). The three MDR, Gram-negative bacteria experimented on in this research were *Acinetobacter baumannii* ATCC17978, *Klebsiella pneumoniae* ATCC13883, and *E. coli* MG1655. *A. baumannii* and *K. pneumoniae* are notorious MDR bacteria and members of the ESKAPE pathogens, a group of infectious bacteria largely responsible for the nosocomial outbreaks around the world; *E. coli* is a model organism that is mostly harmless to humans, but some strains of *E. coli* are infectious and have demonstrated resistance to common antibiotics.

Before some of the conclusions could be drawn about the phenotypic consequences of membrane remodeling following PUFA exposure to any of the three bacteria, confirmation that membrane remodeling had even occurred was necessary. This was achieved by extracting the lipids from bacterial samples that had been grown in the presence of one kind of PUFA or in the absence of PUFAs, which was the case of the control samples. The total lipid extracts were subjected to reversed-phase gradient elution ultra performance liquid chromatography/mass spectrometry analysis. The purpose of the UPLC/MS analysis was to simply show that phospholipid modifications had been made to at least one of the fatty acyl chains of the phospholipid species, not to quantify the degree of modification. The specific UPLC gradient that was used allowed for the formation of a distinct region in time where the phospholipid species eluted from the C8 column, typically between 6 and 9 minutes from sample injection. Within this phospholipid elution region, phosphatidylglycerol species were found to elute from the column sooner than phosphatidylethanolamine species due to their slightly more polar headgroups, effectively partitioning the phospholipid regions of the chromatograms into PG and PE regions. In Gram-negative bacteria, PE species are much more abundant than PG species, and 16:0 fatty acyl chains are the most common phospholipid constituents followed by 18:1 fatty acyl chains. Therefore, the most common PUFA-modified phospholipids were PE 16:0/X species, where X represents a polyunsaturated fatty acyl chain. Generally, given the two fatty acyl chains of a phospholipid, the shorter and more saturated of the two will be located at the sn-1 position[40]. In addition to this, the cone fragments generated from the sn-2 position ($R_2CO_2^-$) are generally of higher abundance than cone fragments generated from the sn-1 position ($R_1CO_2^-$)[41]. Consequently, signal

intensities of sn-2 cone fragments are greater than the signal intensities of sn-1 cone fragments, which is reflected by the peak height differences between the two signals in mass spectra. Using this knowledge, the PUFA chains on PUFA-modified phospholipids were identified as being at the sn-2 position since they formed the more intense peak signals. The chain positions could not be explicitly determined by m/z values alone.

The chromatograms and mass spectra of various *A. baumannii*, *K. pneumoniae,* and *E. coli* samples were presented in Figures 3.1-3.44. The chromatograms and mass spectra presented in Chapter 3 were not exhaustive; however, examination of all the chromatograms and mass spectra generated from the UPLC/MS analysis of the *A. baumannii* and *K. pneumoniae* samples showed successful phospholipid modification with each of the PUFAs they were exposed to during growth; *E. coli* demonstrated successful phospholipid modification with all PUFAs other than 22:6. XICs were generated to show that the three bacteria do not natively produce phospholipid species with PUFA chain constituents.

Double substitutions with exogenous PUFAs were observed in some *A. baumannii* samples, namely in the 18:2, 18:3-α, 18:3-γ, 20:3, and 20:4 samples. The double substitutions were found in PE species and have the form PE X/X, where X is a PUFA chain. The doubly substituted PE species in order of greatest abundance to least abundance were PE 18:2/18:2, PE 18:3-α/18:3-α, PE 18:3-γ/18:3-γ, PE 20:3/20:3, and PE 20:4/20:4. PE 18:3-α/18:3-α appeared to be approximately two times more abundant than PE 18:3-γ/18:3-γ, and PE 20:3/20:3 appeared to be approximately four times more abundant than PE 20:4/20:4. These estimates were made by comparing chromatogram peak areas and assumes that the true concentrations of all *A baumannii* samples were

actually equal to each other (in this case, 250 ppm). PE species doubly substituted with 20:5 and 22:6 were not found in the *A. baumannii* samples. While other bacteria are suspected to doubly substitute both PE and PG species, only the ability of *A. baumannii* to doubly substitute PE species was investigated in this research, leaving the investigation of doubly substituted PE and PG species in other bacteria open to future work.

In general, shorter, more saturated PUFAs were used to remodel the phospholipid membranes of each of the three bacteria more readily than longer chain PUFAs, which was evidenced by the decrease in phospholipid signal intensities going from 18:2-modified phospholipid species to 22:6-modified phospholipid species. No quantitation of the phospholipid species was performed for any of the samples, but this conclusion was made based on the signal intensities of the phospholipids relative to one another. While the comparison of phospholipid signal intensities is a natural step to take for a set of mass spectra generated from samples originating from the same bacteria, comparisons were also able to be made between each of the three bacteria since the lipid extraction procedure was conserved across the three bacteria and the total lipid extracts were raised to similar concentrations. The concentrations of the total lipid extracts of *A. baumannii*, *K. pneumoniae*, and *E. coli* were 250 µg/mL, 400 µg/mL, and 400 µg/mL respectively. Moreover, after comparing the mass spectra of the samples grown in the absence of PUFAs (the control samples) to each other, the signal intensities of identical phospholipid species were greater in the *A. baumannii* control sample than both the *K. pneumoniae* and *E. coli* control samples, despite the *A. baumannii* total lipid extract being less concentrated. For example, the signal intensities of PE 16:0/18:1 in the mass spectra of the *A, baumannii, K. pneumoniae,* and *E. coli* control samples were 1.48 X 10^7, 7.20 X

10^6, and 4.64 X 10^5, respectively. This general trend of decreasing signal intensity among the three bacteria was also observed for the PUFA-modified phospholipid species, possibly implying that either *A. baumannii* has a greater number of phospholipids to begin with or a greater propensity for membrane remodeling than *K. pneumoniae* or *E. coli*. Likewise, it is possible that *K. pneumoniae* has a greater propensity for membrane remodeling than *E. coli*.

The suspicion that the trend for decreasing membrane remodeling capability with PUFAs among the three bacteria follows the sequence *A. baumannii*, *K. pneumoniae*, and *E. coli* was supported after investigating the nature of membrane remodeling. Membrane remodeling in *E. coli* relies on a long-chain fatty acid transporter (FadL), a long-chain fatty acyl-CoA synthetase (FadD), and acyltransferases (PlsB/C/X/Y)[6,26,42]. *A. baumannii* and *K. pneumoniae* have been shown to possess several homologs to these enzymes, with *A. baumannii* having more homologs than *K. pneumoniae*[6,26]. Since *A. baumannii* and *K. pneumoniae* possess a greater number of homologs for enzymes involved in the acquisition and incorporation of exogenous PUFAs, it follows that they should have a greater propensity for membrane remodeling than *E. coli*, which can be inferred from the results of the UPLC/MS analysis. The greater number of FadL, FadD, and acyltransferase homologs in *A. baumannii* and *K. pneumoniae* may also explain why they were able to remodel their membranes with 22:6, but *E. coli* was not.

The results of the motility, permeability, biofilm formation, and antimicrobial peptide susceptibility assays performed on *E. coli* were presented in Figures 3.45-3.50. Although similar assays were performed on *A. baumannii* and *K. pneumoniae*, the results of these assays were not presented in this thesis. However, the results are discussed here in

conjunction with the *E. coli* assay results. Student's t-test was used to statistically assess the results of the assays.

Motility is an important phenotype for virulence and survivability in some Gram-negative bacteria. Therefore, the motilities of *A. baumannii* and *E. coli* in the presence and absence of PUFAs were assessed using motility plates. The motility of *K. pneumoniae* was not assessed because *K. pneumoniae* is not motile. The twitching motility of *A. baumannii* was significantly ($p < 0.01$) reduced in the presence of each of the seven PUFAs compared to the control sample. Interestingly, only 20:3, 20:4, and 20:5 significantly reduced motility in *E. coli* compared to the control sample. These results suggest that *A. baumannii* and *E. coli* have drastically different chemotactic responses to PUFAs and may also imply that *A. baumannii* is more sensitive to PUFAs than *E. coli*. Furthermore, PUFAs may serve as effective motility retardants for *A. baumannii*.

Cell membrane permeability is an essential characteristic vital to the survival of all bacteria since it influences what passes into and out of the cell. Permeability assays with the hydrophobic compound crystal violet (CV) were performed on *A. baumannii*, *K. pneumoniae*, and *E. coli* after growing the three bacteria in the presence or absence of PUFAs. Since the PUFAs used in this experiment were *cis*-isomers, it was hypothesized that as the degree of unsaturation increased, cell membrane permeability would increase accordingly. Surprisingly, exposure to each of the seven PUFAs decreased membrane permeability to CV compared to the control sample in *A. baumannii*; 18:3-α, 20:4, 20:5, and 22:6 decreased permeability significantly ($p < 0.002$) in *A. baumannii*. However, increased membrane permeability to CV was observed in all but the 18:2 and 18:3-α PUFA-exposed *K. pneumoniae* samples compared to the control sample; 20:4 and 22:6

significantly increased membrane permeability to CV in *K. pneumoniae*. Likewise, the 20:4 and 22:6 samples showed significantly increased membrane permeability to CV in *E. coli*. It is interesting to note that 22:6 and 20:4 increased membrane permeability in *K. pneumoniae* the greatest and second greatest, respectively, but in *E.* coli, 20:4 and 22:6 increased membrane permeability the greatest and second greatest, respectively. The reason for this flip between the two bacteria is not clear. Additional permeability assays with ethidium bromide (EtBr) were performed on *K. pneumoniae* and *E. coli*. All PUFAs except for 18:2 significantly ($p < 0.002$) decreased the membrane permeability of *K. pneumoniae* to EtBr, and all PUFAs except for 20:3 significantly decreased the membrane permeability of *E. coli* to EtBr. Clearly, PUFAs can be used to manipulate the membrane permeabilities of *A. baumannii*, *K. pneumoniae*, and *E. coli* to various molecules, giving them tremendous utility in dealing with these MDR bacteria.

Biofilm formation is an important phenotype for bacterial survival and virulence. Biofilm formation assays were performed on *A. baumannii*, *K. pneumoniae*, and *E. coli* samples in the presence and absence of PUFAs. In M9 minimal medium, 18:3-γ, 20:4, 20:5, and 22:6 significantly ($p < 0.002$) increased biofilm formation in *A. baumannii* compared to the control sample while 18:2 significantly lowered biofilm formation. In M9 minimal medium supplemented with casamino acids, 20:4 and 22:6 significantly ($p < 0.002$) increased biofilm formation in *K. pneumoniae* compared to the control sample while 18:2 and 20:3 significantly lowered biofilm formation. The biofilm increase caused by 22:6 in *K. pneumoniae* was drastic, as the control sample showed approximately OD_{600} 0.3 and the 22:6 sample showed approximately OD_{600} 1.0. In M9 minimal medium supplemented with casamino acids, 18:3-α, 18:3-γ, 20:4, and 22:6 all significantly increased biofilm

formation in *E. coli*. Interestingly, the influence of the PUFAs on biofilm formation may not be directly related to the ability of the bacteria to assimilate the PUFAs into their cell membranes, since 22:6 was shown to significantly increase biofilm formation in *E. coli* despite the inability of *E. coli* to remodel its membrane with 22:6. Nevertheless, PUFAs can be used to manipulate biofilm formation in these MDR, Gram-negative bacteria.

Susceptibility to certain antimicrobial agents is clearly an important factor for the virulence and survivability of bacteria. Therefore, antimicrobial peptide susceptibility assays were performed on *A. baumannii*, *K. pneumoniae*, and *E. coli* in the presence and absence of PUFAs to determine the effect that the PUFAs have on the minimum inhibitory concentrations (MICs) of the antimicrobial agents. Two of the antimicrobial agents used in these assays were the cationic antimicrobial peptides (cAMPs) polymyxin B and colistin. All PUFAs increased the susceptibility of *A. baumannii* to polymyxin B at a concentration of 12.8 µg/mL compared to the control sample, with 18:2, 18:3-α, and 20:5 significantly (two-fold MIC) increasing susceptibility at that concentration; 20:4 significantly increased susceptibility to polymyxin B at a concentration of 6.4 µg/mL. All PUFAs increased the susceptibility of *A. baumannii* to colistin at concentrations of 3.2 µg/mL, 6.4 µg/mL, and 12.8 µg/mL compared to the control sample. Notably, all PUFAs other than 22:6 and 20:3 significantly increased colistin susceptibility at concentrations of 3.2 µg/mL and 6.4 µg/mL; 20:3 significantly increased colistin susceptibility at a concentration of 12.8 µg/mL along with those PUFAs. The exogenous PUFAs 18:3-α, 18:3-γ, and 20:5 significantly increased the susceptibility of *K. pneumoniae* to polymyxin B at a concentration of 12.8 µg/mL compared to the control sample; 18:2 significantly increased polymyxin B susceptibility at a concentration of 25.6 µg/mL along with those

PUFAs. All PUFAs except for 20:3 significantly increased the susceptibility of *K. pneumoniae* to colistin at a concentration of 32 µg/mL compared to the control sample; 20:3 significantly increased susceptibility at a concentration of 64 µg/mL along with those PUFAs. Interestingly, 20:4 and 22:6 significantly decreased the susceptibility of *E. coli* to both polymyxin B and colistin at most concentrations tested compared to the control sample. The PUFA 20:5 significantly increased the susceptibility of *E. coli* to polymyxin B at a concentration of 2 µg/mL; 20:3 significantly decreased susceptibility at a concentration of 4 µg/mL. The PUFA 18:2 significantly increased the susceptibility of *E. coli* to colistin at a concentration of 0.8 µg/mL compared to the control; 20:3 significantly decreased susceptibility at a concentration of 1.6 µg/mL. Most PUFAs tended to increase the susceptibility of *A. baumannii* and *K. pneumoniae* to polymyxin B and colistin at the various concentrations tested, but PUFA-exposed *E. coli* cells demonstrated more variability in their susceptibility to these cAMPs. *E. coli* was shown to be incapable of remodeling its cell membrane with 22:6, yet 22:6 caused a significant decrease in susceptibility of *E. coli* to polymyxin B and colistin at most concentrations tested. Significant decreases in the susceptibility of either *A. baumannii* or *K. pneumoniae* to polymyxin B or colistin caused by 22:6 were not observed at any of the concentrations tested, suggesting that 22:6 as a membrane constituent increases the efficiency of cAMPs, but as a free fatty acid serves to impede the efficiency of cAMPs. Additional antimicrobial assays were performed on *A. baumannii* and *K. pneumoniae* using the β-lactam imipenem. No significant deviations in susceptibility compared to the control samples were observed in any of the PUFA-exposed *A. baumannii* or *K. pneumoniae* samples. Polymyxin B and colistin operate by different mechanisms of

action compared to β-lactam antibiotics such as imipenem. Polymyxin B and colistin directly interact with the cell membrane when attacking Gram-negative bacteria, whereas imipenem does not. Therefore, the efficiency of polymyxin B and colistin were expected to be affected by membrane remodeling, and imipenem was expected to be largely unaffected by membrane remodeling. The results of the assays affirm this hypothesis.

In conclusion, the multi-drug resistant, Gram-negative bacteria *Acinetobacter baumannii*, *Klebsiella pneumoniae*, and *E. coli* were shown to be able to remodel their cell membranes with exogenously supplied polyunsaturated fatty acids. These PUFAs profoundly altered phenotypes important to virulence and survivability, such as motility, biofilm formation, membrane permeability, and susceptibility to antimicrobial agents. Therefore, PUFAs may be utilized in the future as tools for treating these MDR, Gram-negative bacteria as well as many others.

There are many potential topics to consider for the future work of this research project. The most obvious is the extension of this research to other multi-drug resistant bacteria. Another possible endeavor for future work could be further optimization of the mobile phase and gradient used in the UPLC/MS analysis. The UPLC conditions used in this research allowed for chromatographic separation of 18:3-α and 18:3-γ; the separation time was approximately 0.1 minutes. Perhaps the chromatographic separation of ω-3 and ω-6 PUFAs like 18:3-α and 18:3-γ could be investigated in the future. In addition to this, the mass spectrometric technique of multiple reaction monitoring (MRM) could be employed to fragment parent phospholipid ions via collision with inert argon gas to aid in the identification of unknown phospholipid peaks. An investigation into the modification of large lipids like cardiolipins with exogenous PUFAs could yield interesting results.

Assays designed to investigate the roles of various enzymes produced by MDR bacteria that are involved in the recognition, retrieval, and assimilation of PUFAs into the cell membrane could be utilized in future work. Finally, the anomalous observations presented in section 4.2 could be investigated further in the future.

4.2 Anomalous Observations

Although Gram-negative bacteria were thought to not natively produce phospholipid species with polyunsaturated fatty acyl chains, PE 16:0/16:3 species were found in the 18:3-α, 20:3, and 20:4 *A. baumannii* samples. In addition to this, strange high m/z peaks were found in all bacterial samples subjected to UPLC/MS analysis. It is suspected that these peaks may be related to phospholipid dimers, but this suspicion has not yet been validated. The average mass spectrum of a 7.23 minute peak in the 20:4 *A. baumannii* sample chromatogram is presented in Figure 4.1 to show both of these anomalies. It displays the 684.5 m/z peak, which corresponds to the $[M-H]^-$ ion of PE 16:0/16:3, as confirmed by LIPID MAPS and the 16:0 and 16:3 cone fragments that correspond to the 255.5 m/z and 249.5 m/z peaks respectively. The high m/z peaks in the 1100-1500 m/z range are displayed as well. The 1370.0 m/z peak is most notable.

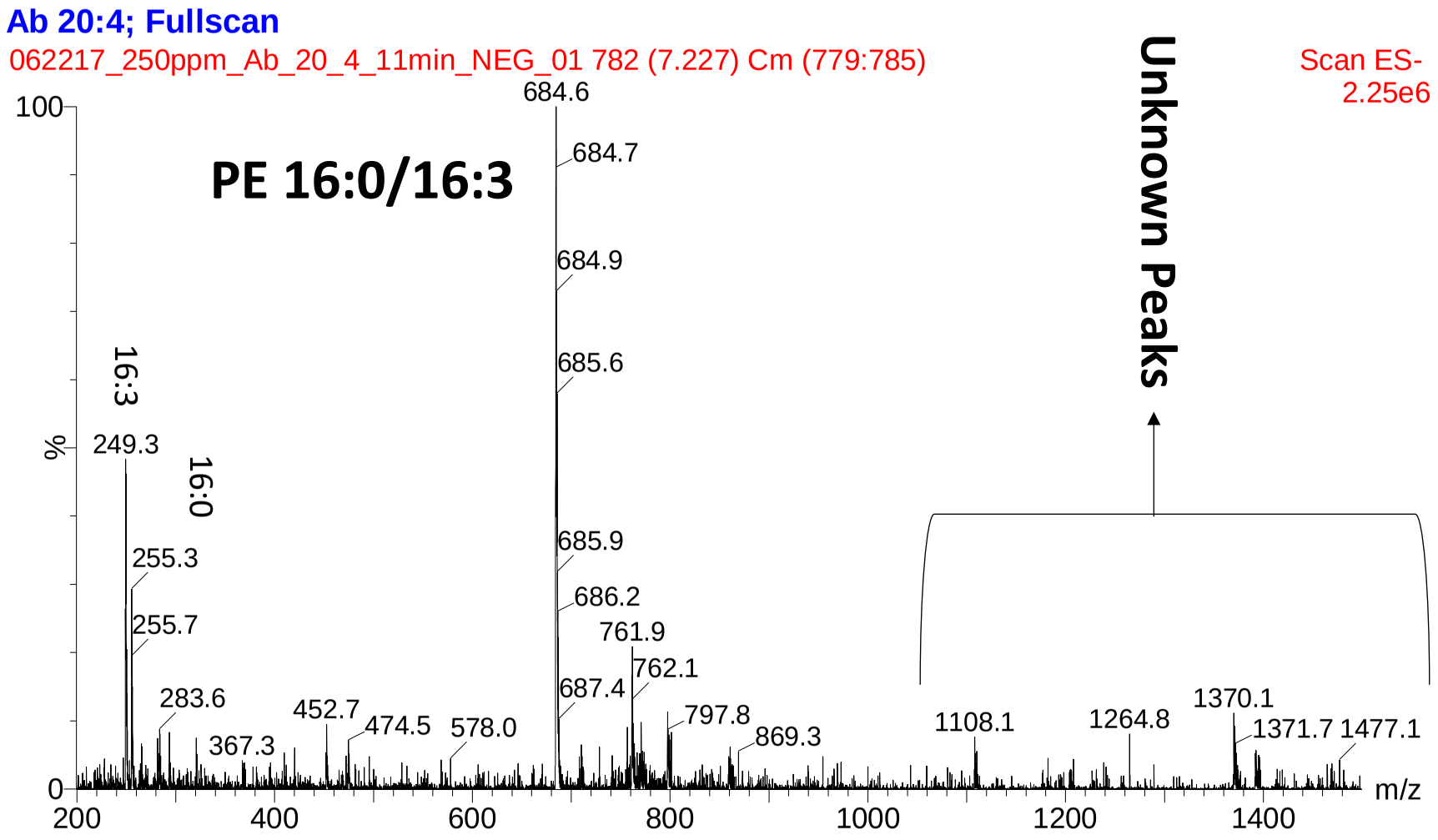

Figure 4.1: Anomalous PE 16:0/16:3 peak and high m/z peaks

BIBLIOGRAPHY

(1) Ahmed, M.; Williams, N.; Clegg, P.; van Velkinburgh, J.; Baptiste, K.; Bennett, M. Analysis of Risk Factors Associated With Antibiotic-Resistant *Escherichia coli*. *Microb.. Drug Resist.* **2012**, *18*, 161-168.

(2) Micek, S.; Wunderink, R.; Kollef, M.; Chen, C.; Rello, J.; Chastre, J.; Antonelli, M.; Welte, T.; Clair, B.; Ostermann, H.; Calbo, E.; Torres, A.; Menichetti, F.; Schramm, G.; Menon, V. An international multicenter retrospective study of *Pseudomonas aeruginosa* nosocomial pneumonia: impact of multidrug resistance. *Crit. Care* **2015**, *19*, 219.

(3) Santajit, S.; Indrawattana, N. Mechanisms of antimicrobial resistance in ESKAPE pathogens. *BioMed Res. Int.* **2016**, *2016*, 1-8.

(4) Giles, D.; Hankins, J.; Guan, Z.; Trent, M. Remodeling of the *Vibrio cholerae* membrane by incorporation of exogenous fatty acids from host and aquatic environments. *Mol. Microbiol.* **2010**, *79*, 716-728.

(5) Black, P. N. The FadL gene product of *Escherichia coli* is an outer membrane protein required for uptake of long-chain fatty acids and involved in sensitivity to bacteriophage T2. *J. Bacteriol.* **1988**, *170*, 2850-2854.

(6) Eder, A.; Munir, S.; Hobby, C.; Anderson, D.; Herndon, J.; Siv, A.; Symes, S.; Giles, D. Exogenous polyunsaturated fatty acids (PUFAs) alter phospholipid composition, membrane permeability, biofilm formation and motility in *Acinetobacter baumannii*. *Microbiol.* **2017**, *163*, 1626-1636.

(7) Liaw, S.; Lai, H.; Wang, W. Modulation of swarming and virulence by fatty acids through the RsbA protein in proteus mirabilis. *Infect. Immun.* **2004**, *72*, 6836-6845.

(8) Lai, H.; Soo, P.; Wei, J.; Yi, W.; Liaw, S. The RssAB two-component signal transduction system in serratia marcescens regulates swarming motility and cell envelope architecture in response to exogenous saturated fatty acids. *J. Bacteriol.* **2005**, *187*, 3407-3414.

(9) Davies, D.; Marques, C. A fatty acid messenger is responsible for inducing dispersion in microbial biofilms. *J. Bacteriol.* **2008**, *191*, 1393-1403.

(10) Giamarellos-Bourboulis, E.; Grecka, P.; Dionyssiou-Asteriou, A.; Giamarellou, H. *In vitro* influence of polyunsaturated fatty acids on nosocomial *Pseudomonas aeruginosa*: a preliminary report. *Int. J. Antimicrob. Agents* **1995**, *6*, 47-50.

(11) Weber, F.; Isken, S.; de Bont, J. Cis/trans isomerization of fatty acids as a defence mechanism of *Pseudomonas putida* strains to toxic concentrations of toluene. *Microbiol.* **1994**, *140*, 2013-2017.

(12) Singer, S.; Nicolson, G. The Fluid Mosaic Model of the Structure of Cell Membranes. *Science* **1972**, *175*, 720-731.

(13) Randle, C.; Albro, P.; Dittmer, J. The phosphoglyceride composition of Gram-negative bacteria and the changes in composition during growth. *Biochim. Biophys. Acta, Lipids Lipid Metab.* **1969**, *187*, 214-220.

(14) Silhavy, T.; Kahne, D.; Walker, S. The Bacterial Cell Envelope. *Cold Spring Harb. Perspect. Biol.* **2010**, *2*, a000414-a000414.

(15) Kamio, Y.; Nikaido, H. Outer membrane of *Salmonella typhimurium*: Accessibility of phospholipid head groups to phospholipase C and cyanogen bromide activated dextran in the external medium. *Biochem.* **1976**, *15*, 2561-2570.

(16) de Duve, C.; Wattiaux, R. Functions of lysosomes. *Annu. Rev. Physiol.* **1966**, *28*, 435-492.

(17) Perez, F.; Hujer, A.; Hujer, K.; Decker, B.; Rather, P.; Bonomo, R. Global challenge of multidrug-resistant *Acinetobacter baumannii*. *Antimicrob. Agents Chemother.* **2007**, *51*, 3471-3484.

(18) Dijkshoorn, L.; Nemec, A.; Seifert, H. An increasing threat in hospitals: multidrug-resistant *Acinetobacter baumannii*. *Nat. Rev. Microbiol.* **2007**, *5*, 939-951.

(19) Peleg, A.; Seifert, H.; Paterson, D. *Acinetobacter baumannii*: Emergence of a successful pathogen. *Clin. Microb. Rev.* **2008**, *21*, 538-582.

(20) Maragakis, L.; Perl, T. Antimicrobial resistance: *Acinetobacter baumannii*: Epidemiology, antimicrobial resistance, and treatment options. *Clin. Infect. Dis.* **2008**, *46*, 1254-1263.

(21) Guerrero, D.; Perez, F.; Conger, N.; Solomkin, J.; Adams, M.; Rather, P.; Bonomo, R. *Acinetobacter baumannii*-associated skin and soft tissue infections: recognizing a broadening spectrum of disease. *Surg. Infect.* **2010**, *11*, 49-57.

(22) Rice, L. Challenges in identifying new antimicrobial agents effective for treating infections with *Acinetobacter baumannii* and *Pseudomonas aeruginosa*. *Clin. Infect. Dis.* **2006**, *43*, S100-S105.

(23) Thomson, J.; Bonomo, R. The threat of antibiotic resistance in Gram-negative pathogenic bacteria: β-lactams in peril! *Curr. Opin. Microbiol.* **2005**, *8*, 518-524.

(24) Arroyo, L.; Herrera, C.; Fernandez, L.; Hankins, J.; Trent, M.; Hancock, R. The *pmrCAB* operon mediates polymyxin resistance in *Acinetobacter baumannii* ATCC 17978 and clinical isolates through phosphoethanolamine modification of Lipid A. *Antimicrob. Agents Chemother.* **2011**, *55*, 3743-3751.

(25) Gaddy, J.; Actis, L. Regulation of *Acinetobacter baumannii* biofilm formation. *Future Microbiol.* **2009**, *4*, 273-278.

(26) Hobby, C.; Herndon, J.; Morrow, C.; Peters, R.; Symes, S.; Giles, D. Exogenous fatty acids alter phospholipid composition, membrane permeability, capacity for biofilm formation and antimicrobial peptide susceptibility in *Klebsiella pneumoniae*. *MicrobiologyOpen* **2018**, [in press].

(27) Hsu, C.; Pan, Y.; Liu, J.; Chen, C.; Lin, T.; Wang, J. *Klebsiella pneumoniae* translocates across the intestinal epithelium via Rho GTPase- And Phosphatidylinositol 3-Kinase/Akt-Dependent Cell Invasion. *Infect. Immun.* **2014**, *83*, 769-779.

(28) Endimiani, A.; DePasquale, J.; Forero, S.; Perez, F.; Hujer, A.; Roberts-Pollack, D.; Fiorella, P.; Pickens, N.; Kitchel, B.; Casiano-Colon, A.; Tenover, F.; Bonomo, R. Emergence of bla_{KPC}-containing *Klebsiella pneumoniae* in a long-term acute care hospital: A new challenge to our healthcare system. *J. Antimicrob. Chemother.* **2009**, *64*, 1102-1110.

(29) Di Martino, P.; Cafferini, N.; Joly, B.; Darfeuille-Michaud, A. *Klebsiella pneumoniae* type 3 pili facilitate adherence and biofilm formation on abiotic surfaces. *Res. Microbiol.* **2003**, *154*, 9-16.

(30) Anderl, J.; Franklin, M.; Stewart, P. Role of antibiotic penetration limitation in *Klebsiella pneumoniae* biofilm resistance to ampicillin and ciprofloxacin. *Antimicrob. Agents Chemother.* **2000**, *44*, 1818-1824.

(31) Blount, Z. The unexhausted potential of *E. Coli*. *eLife* **2015**, *4*, e05826.

(32) Kaper, J.; Nataro, J.; Mobley, H. Pathogenic *Escherichia coli*. *Nat. Rev. Microbiol.* **2004**, *2*, 123-140.

(33) Belanger, L.; Garenaux, A.; Harel, J.; Boulianne, M.; Nadeau, E.; Dozois, C. *Escherichia coli* from animal reservoirs as a potential source of human extraintestinal pathogenic *E. coli*. *FEMS Immunol. Med. Microbiol.* **2011**, *62*, 1-10.

(34) Sahm, D.; Thornsberry, C.; Mayfield, D.; Jones, M.; Karlowsky, J. Multidrug-resistant urinary tract isolates of *Escherichia coli*: prevalence and patient demographics in the United States in 2000. *Antimicrob. Agents Chemother.* **2001**, *45*, 1402-1406.

(35) Colpan, A.; Johnston, B.; Porter, S.; Clabots, C.; Anway, R.; Thao, L.; Kuskowski, M.; Tchesnokova, V.; Sokurenko, E.; Johnson, J.; Allen, B.; Baracco, G.; Bedimo, R.; Bessesen, M.; Bonomo, R.; Brecher, S.; Brown, S.; Castellino, L.; Desai, A.; Fernau, F.; Fisher, M.; Fleckenstein, J.; Fleming, C.; Fries, N.; Kan, V.; Kauffman, C.; Klutts, S.; Ohl, M.; Russo, T.; Swiatlo, A.; Swiatlo, E. *Escherichia coli* Sequence Type 131 (ST131) Subclone *H*30 as an Emergent Multidrug-Resistant Pathogen Among US Veterans. *Clin. Infect. Dis.* **2013**, *57*, 1256-1265.

(36) Bligh, E. G.; Dyer, W. J. A rapid method of total lipid extraction and purification. *Can. J. Biochem. Phys.* **1959**, *37*, 911-917.

(37) Chen, R.; Lv, R.; Xiao, L.; Wang, M.; Du, Z.; Tan, Y.; Cui, Y.; Yan, Y.; Luo, Y.; Yang, R.; Song, Y. A1S_2811, a CheA/Y-like hybrid two-component regulator from *Acinetobacter baumannii* ATCC17978, is involved in surface motility and biofilm formation in this bacterium. *MicrobiologyOpen* **2017**, *6*, e00510.

(38) O'Toole, G. Microtiter dish biofilm formation assay. *J. Vis. Exp.* **2011**, *47*, 2437.

(39) LIPID MAPS Lipidomics Gateway : Home http://www.lipidmaps.org/ (accessed Jan 17, 2018).

(40) Uhl, O.; Glaser, C.; Demmelmair, H.; Koletzko, B. Reversed phase LC/MS/MS method for targeted quantification of glycerophospholipid molecular species in plasma. *J. Chromatogr. B* **2011**, *879*, 3556-3564.

(41) Hsu, F.; Turk, J. Studies on phosphatidylglycerol with triple quadrupole tandem mass spectrometry with electrospray ionization: fragmentation processes and structural characterization. *J. Am. Soc. Mass Spectrom.* **2001**, *12*, 1036-1043.

(42) Nunn, W.; Simons, R. Transport of long-chain fatty acids by *Escherichia coli*: mapping and characterization of mutants in the FadL gene. *Proc. Natl. Acad. Sci. U.S.A.* **1978**, *75*, 3377-3381.

(43) Bacterial Cell wall: Structure, Composition and Types - http://www.onlinebiologynotes.com/bacterial-cell-wall-structure-composition-types/ (accessed Apr 10, 2018).